CHARACTERIZATION OF CYB5D2 AND ITS HEME BINDING FUNCTIONS

CHARACTERIZATION OF CYB5D2 AND ITS HEME BINDING ASSOCIATED FUNCTIONS

By ANTHONY BRUCE, B.Sc., M.Sc.

A Thesis Submitted to the School of Graduate Studies

in Partial Fulfillment of the Requirements for the Degree

Doctor of Philosophy

McMaster University

DOCTOR OF PHILOSOPHY (2013) McMaster University

Medical Sciences Hamilton, Ontario, Canada

TITLE: Characterization of CYB5D2 and its heme binding associated functions

AUTHOR: Anthony Bruce, B.Sc. (University of Western Ontario), M.Sc. (York University)

SUPERVISOR: Dr. Damu Tang

NUMBER OF PAGES: xxi, 192

ABSTRACT

Cytochrome b5 heme binding domain 2 (CYB5D2) is a heme binding protein that was initially identified for its ability to attenuate the function of the PTEN tumor suppressor gene. CYB5D2 sustains ectopic PTEN expression in U87 cells, and can also confer survival from serum starvation in NIH3T3 cells. An antibody was generated to the carboxyl terminus of CYB5D2 to detect endogenous protein expression. The highest expression of CYB5D2 protein is in neural cancer cell lines. CYB5D2 is weakly expressed in breast and kidney cancer cell lines, and moderately expressed in prostate cancer cell lines. To investigate the role of the heme binding domain in CYB5D2, a conserved aspartic acid (D86) within this domain was mutated to glycine, and this was characterized as being unable to bind heme. CYB5D2(D86G) displayed a loss of function compared to wild-type CYB5D2. To study the loss of expression of CYB5D2, stable CYB5D2 shRNA was achieved in HeLa and Huh7 cells. While ectopic CYB5D2 inhibited HeLa cell proliferation and growth in soft agar, CYB5D2(D86G) expression and CYB5D2 shRNA increased cell proliferation and soft agar growth. While ectopic CYB5D2 conferred survival from chemotherapeutic drugs in HeLa cells, CYB5D2(D86G) and CYB5D2 shRNA cells were susceptible to drug treatments. CYB5D2 inhibits SREBP signalling, which requires its heme binding ability. Using cyclohexamide treatments, CYB5D2 stabilized ectopic Insig1, while CYB5D2(D86G) destabilized ectopic Insig1. CYB5D2 shRNA reduced endogeneous CYP51A1 (lanosterol demethylase) and Insig1 protein levels, and increased the susceptibility of HeLa cells to mevalonate treatments. Furthermore, CYB5D2 shRNA HeLa cells displayed reduced

CYP3A4 activity, a cytochrome P450 enzyme involved in drug metabolism. CYB5D2 binds to cytochrome P450 reductase (POR), while CYB5D2(D86G) cannot. CYB5D2 co-immunoprecipitates with endogenous POR under serum-free conditions in HeLa and Huh7 cells, while CYB5D2(D86G) cannot. Collectively, CYB5D2 is a POR interacting protein, which regulates CYP51A1 and CYP3A4 activity.

FOREWORD

This thesis is organized into eight chapters, of which the Results section comprises chapters 3 to 7. Special thanks to the following personnel for their experimental contributions: Dr. Lizhi He, Dr. Fengxiang Wei, Dr. Adrian Rybak, Dr. X. Feng, Dr. Yanyun Xie and Dr. Damu Tang. The cDNA for CYB5D2 was originally cloned by Lizhi He (Chapter 3). Dr. Fengxiang Wei generated GST-CYB5D2 ΔTM constructs and purified the GST-fusion proteins that were subsequently analyzed by absorbance spectrophotometry (Chapter 5). Furthermore, the colorimetric in-gel peroxidase assay used to assess heme binding was also performed by Dr. Fengxiang Wei (Chapter 5). Adrian Rybak contributed and assisted with soft agar assays, xenograft tumor formation assays, and cell viability assays used to evaluate chemotherapeutic drug survival (Chapter 5). Dr. X. Feng performed the Insig stabilization assay by CYB5D2 following cyclohexamide treatment (Chapter 6). CYB5D2 polymorphism mutants (R7P, R7G, Q167K) were generated by Dr. Damu Tang and Dr. Yanyun Xie (Chapter 6). Gross deletion mutants of CYB5D2 (ΔTM, ΔCYB5) have been previously published (Xie *et al*., 2010).

ACKNOWLEDGEMENTS

I would like to thank my supervisor, Dr. Damu Tang, for allowing me to work in his lab. Thank you to Justin He, X. Feng, Cathy Chen, Yanyun Xie and Dr. Fengxiang Wei for all your help. Thanks to Dr. Richard Austin for your interest, your questions and your generosity. Thanks to Steve Colgan and Sana Basserri. I would like to thank my wife, Laurie Lyng, for all your love and support, and the sacrifices that have allowed me to do my Ph.D. studies. I would like to thank my mother, Naty Bruce, for all your love and support. I would like to thank my mother-in-law, Sandra Clegg, for all her help that was required during my studies. Thanks to my daughters, Riley and Avery Bruce. Special thanks goes out to Adrian Rybak for his companionship, his empathy, extensive scientific discussion, his courage and for all his help.

TABLE OF CONTENTS

LIST OF FIGURES

LIST OF TABLES

LIST OF ABBREVIATIONS

239T	Human Embryonic Kidney cell line
ABS	Antley Bixler Syndrome
AKT/PKB	Protein Kinase B (serine/threonine specific kinase)
CYB5D2	Cytochrome B5 Heme Binding Domain 2
CYP P450	cytochrome P450
Dap1	Damage-resistance protein 1
DMEM	Dulbecco`s Modified Eagle Medium
DMSO	Dimethyl Sulfoxide
DNA	Deoxyribonucleic acid
ddH_20	double distilled water, (sterile filtered)
EDTA	ethylenediaminetetraacetic acid
ER	Endoplasmic Reticulum
ERG11p	yeast CYP51A1 lanosterol 14-alpha-demethylase
EV	Empty Vector (pcDNA3.0 or pLHCX)
FBS	Fetal Bovine Serum
GAPDH	Glyceraldehyde 3-phosphate dehydrogenase
GP	Gag-Pol viral plasmid
GST	Glutathione S-transferase
HeLa	cervical cancer cell line from (Henrietta Lacks) by G. Grey
HPCD	Hydroxypropyl-beta-cyclodextrin
HPR6	Human Progesterone Receptor 6 (PGRMC1)

Huh7	differentiated hapatocyte carcinoma, male, (Nakabayshi and Sato., 1982)
Insig	Insulin Induced Gene
IPTG	Isopropyl β-D-1-thiogalactopyranoside (inhibits lac repressor)
LB	Luria Broth, bacteria growth media (10g tryptone, 5g yeast extract, 10g NaCl/1 L)
LNCAP	prostate adenocarcinoma cells, androgen sensitive, adherent epithelial. 1977.
M	Moles
MCF7	breast cancer cell line Michigan Cancer Foundation 7, 1970
MMS	methyl methanesulfonate
NIH3T3	Immortalized mouse embryonic fibroblasts
ob/ob	leptin knockout mouse, fat mouse phenotype
P450	pigment 450 absorbance (heme group wavelength)
PAGE	Polyacrylamide Gel Electrophoresis
PBS	Phosphate Buffered Saline
PEI	Polyethylenimine
PGRMC1	Progesterone Receptor Membrane Component 1
POR	Cyotochrome P450 Reductase
PTEN	Phosphatase and Tensin homolog on chromosome 10
qPCR	quantitative Polymerase Chain Reaction (Real Time PCR)
RLU	relative luciferase unit
rpm	revolutions per minute

RNA	Ribonucleic acid
SREBP	Sterol Regulatory Element Binding Protein
SCAP	SREBP Cleavage Activating Protein
SDS	Sodium Dodecyl Sulfate
shRNA	short hairpin Ribonucleic acid
siRNA	short interfering Ribonucleic acid
TBS	Tris Buffered Saline
U87	human primary glioblastoma
VSV	Vesicular Stomatitis Virus

DECLARATION OF ACADEMIC ACHIEVEMENT

Manuscript in Preparation "Heme-Binding by CYB5D2 Regulates HeLa Cell Growth and Confers Survival from Chemotherapeutic Agents". **Anthony Bruce** and Adrian Rybak.

I Anthony Bruce have contributed to the following publications:

Xie Y, **Bruce A**, He L, Wei F, Tao L & Tang D CYB5D2 enhances HeLa cells survival of etoposide-induced cytotoxicity. *Biochem Cell Biol* **89** 341-350.

Li Y, He L, **Bruce A**, Parihar K, Ingram A, Liu L & Tang D 2006 p14ARF inhibits the growth of p53 deficient cells in a cell-specific manner. *Biochim Biophys Acta* **1763** 787-796.

Wu D, Chen B, Parihar K, He L, Fan C, Zhang J, Liu L, Gillis A, **Bruce A**, Kapoor A & Tang D 2006 ERK activity facilitates activation of the S-phase DNA damage checkpoint by modulating ATR function. *Oncogene* **25** 1153-1164.

Zhang J, Lahti JM, **Bruce A**, He L, Parihar K, Fan C, Grenet J, Liu L, Kidd VJ, Cormier S & Tang D 2006 Identification of an ataxia telangiectasia-mutated protein mediated surveillance system to regulate Bcl-2 overexpression. *Oncogene* **25** 5601-5611.

Chapter 1

Introduction

1.0 Heme and Hemoproteins

Iron is one of the most abundant metals on earth, and is essential for nearly all organisms. The redox potential of iron has a greater range (depending on the ligand environment) relative to other transition elements because it can donate and accept electrons relatively easily. Iron exists the divalent ferrous [(Fe+2)] and the trivalent ferric [(Fe+3)] iron, which is required for electron transfer and for binding to biological ligands. This ability makes iron an important cofactor for several hemoproteins and non-heme iron containing proteins (Pantopolous *et al*., 2012). Heme is a prosthetic group composed of an iron atom, surrounded by a protoporphrin ring moiety (4 pyroles), which are attached to the iron by four nitrogen atoms (Kaplan, 1977). There are five types of heme ligands, type a, type b, type c, type d and type d_1. Heme type b, (protoporphyrin IX) is the original basic structure that other hemes (a,c and d) are derived, and is the most common type heme (Woodard and Dailey. 2000). Heme biosynthesis requires several steps, beginning and ending in the mitochondria. Heme has numerous functions, with the main functions being related to oxygen and oxidative metabolism (Khan and Quigley. 2011).

Some hemoproteins function in respiration as cytochromes in the mitochondria. Two of these are cytochrome reductase and cytochrome *c* oxidase (complex IV), which function in electron transfer, in the electron transport chain. Some hemoproteins function as gas sensors detecting levels of O_2, CO and NO, relaying responses in signal transduction (Gilles-Gonzalez and Gonzalez. 2005). Some hemoproteins function as

catalases, peroxidases, nitric oxide synthases (NOS), guanyl cyclases, oxygen binding proteins and transporters (hemoglobins), and transcription factors (Tsiftsoglou *et al.*, 2006; Khan and Quigley. 2011).

P450 cytochromes are a large family of heme binding proteins that function as monooxygenases. They are involved in the metabolism of foreign compounds (xenobiotics), the biosynthesis and metabolism of steroids, the metabolism of sterols and the synthesis of bile acids from cholesterol (Miller. 2012). All P450 cytochromes receive electrons from cytochrome P450 reductase (POR), or to a lesser extent cytochrome b5 (Strobel *et al*., 1995). The major P450 cytochrome in sterol synthesis in CYP51A1 a lanosterol demethylase which removes the 14α-methyl group from lanosterol (Nelson *et al*., 1993).

1.1.0 CYB5D2 and PGRMC1

1.1.1 Identification of CYB5D2 in a screen for Novel Negative Regulators of the PTEN Tumor Supressor Gene

CYB5D2 (MGC3214) was initially identified in a screen for PTEN negative regulators by Dr. Justin He in 2001 (McMaster University). The prostate cancer cell line LNCAP (a PTEN-null cell line), was initially transfected with a cDNA library from normal prostate. Sixty hours post-transfection, a pBabe-PTEN packaged retrovirus was used to infect these LNCAP cells (that were pre-transfected with the cDNA library). Ectopic PTEN expression in LNCAP cells is lethal. Puromycin was then used to selectively destroy all non-infected PTEN pBabe expressing cells. CYBD2 was found in a cell that attenuated this lethal PTEN induced cell death in these LNCAP cells.

1.1.2 Structure of CYB5D2

The CYB5D2 gene resides on chromosome 17p13.2, and it encodes for the protein CYB5D2 of 264 amino acid residues. It has an amino terminal transmembrane domain, residues 7-29. Adjacent and COOH terminal to the transmembrane domain lies a cytochrome b5 heme binding domain (amino acids 38-133). These microsomal cytochrome b5 heme binding proteins belong to the family of membrane associated progesterone receptors (MAPRs). This family of cytochrome b5 heme binding proteins are represented by, progesterone receptor membrane component 1 (PGRMC1), the most characterized protein in this family. Two polymorphisms, an R7G and an R7P have been reported for CYB5D2 in colon cancer in Gene Ontology searches for consensus coding of sequences of human colorectal cancer (Sjoeblom *et al*., 2006). A third polymorphism, a glutamine Q167K to lysine, has also been reported for CYB5D2 from the NIH full length cDNA project Mammalian Gene Collection (MGC) (Ota *et al*., 2004, Gerrard *et al*., 2004). A putative secretion signal sequence lies at the amino terminus amino acids 1-22 (Kimura *et al*., 2010). Structural analysis further reveals a 43% amino acid homology between the heme binding domain of PGRMC1 and CYB5D2. The conservation of three key tyrosines Y73, Y79 and Y127 and one aspartic acid D86 in the heme binding domain of four cytochrome P450 Heme binding proteins: Human PGRMC1, yeast Dap1, Arabidopsis IJO3 and human CYB5D2, imply these residues are important in the heme binding pocket (Figure 5.1, panel A).

1.1.3 CYB5D2 is a Heme Binding Protein that Inhibits Neural Differentiation

The first published report on CYB5D2 characterized CYB5D2/Neuferricin as an extracellular heme-binding protein that promoted neurogenesis (Kimura *et al*., 2010). High Five cells were used to produce recombinant CYB5D2, which was seen to be efficiently secreted into the media. When recombinant CYB5D was added to Neuro2a cells it suppressed their survival. A heme binding defective mutant (Δ55-98 amino acids) was generated, which abolished this inhibition of Neuroa2a survival when this recombinant protein was ectopically added (Kimura *et al*., 2010). This recombinant mouse neuferricin demonstrated the ability to promote neurogenesis in primary cultured mouse neural precursor cells. In differentiating Neuro2a cells, siRNA knockdown of CYB5D2/Neuferricin promoted cell survival and proliferation, and suppressed neurite outgrowth. It is unclear if these affects are due to the loss of the secreted protein (as claimed by the authors) or due to the loss of the intracellular protein. Endogenous mouse CYB5D2 mRNA was shown to be expressed mainly in the brain in the embryo stage, and later on in the heart, adrenal gland, kidney and brain in the post natal stage (Kimura *et al*., 2010). This group is the first to show that CYB5D2 is a heme binding protein, and that endogenous CYB5D2 present in the media of Neura2a cells is heme bound.

1.1.4 CYB5D2 Confers Survival from Etoposide

The first report on intracellular CYB5D2 function demonstrated that CYB5D2 could enhance HeLa cell survival from etoposide (Xie *et al*., 2011). When CYB5D2 conferred survival from etoposide, it did not affect the ATM-dependant DNA damage response,

induced by etoposide. Additionally, CYB5D2 did not affect TNFα induced apoptosis. Moreover, CYB5D2 did affect UV induced cell death, nor did it affect the core apoptotic machinery (Xie *et al*., 2011). The ability of CYB5D2 to confer survival from etoposide required its transmembrane domain (and subsequent peri-nuclear localization) and it`s cytochrome b5 heme binding domain (amino acids 35-134).

1.1.5 Cytochrome B5 Heme Binding Proteins: Progesterone Receptor Membrane Component 1 (PGRMC1)

The most characterized cytochrome b5 heme binding domain containing protein is PGRMC1. PGRMC1 was initially found in 1996 by two different groups. Using a differential display for dioxin induced genes in rat liver, researchers identified a 25 kDa protein that was found to be expressed in liver, lung and kidney (Selmin, O., *et al*., 1996). Another group discovered a 20 amino acid fragment of PGRMC1 to be contained in a membrane-associated progesterone binding complex (Meyer, C., *et al*., 1996). Microsomes were purified from porcine liver cells to eventually identify the progesterone binding component. Eventually this same group cloned the full length cDNA from rat and called it membrane progesterone receptor (mPR) (Falkenstein E., *et al*., 1998). Eventually antibodies were generated to this protein, and researchers subsequently cloned the human homologue Hpr6.6 (human progesterone receptor) (Gerdes, D., 1998).

PGRMC1 is located in the ER, and has been shown to exist as a dimer at 56 kDa (disulfide linked homodimers) and a monomer at 28 kDa (Falkenstein *et al*., 2001). PGRMC1 directly binds to b type heme (Min *et al*., 2005), various pharmacological

compounds, associates with cytochrome P450 proteins (Min *et al*., 2005, Hughes *et al*., 2007; Szczesna-Skorupa and Kemper., 2011) and has been implicated in progesterone signalling. When purified, PGRMC1 is alone unable to bind progesterone as it seems to bind in a protein complex, with unknown proteins that in concert serve to bind progesterone (Cahill *et al*., 2007, Losel *et al*., 2007). When PGRMC1 is overexpressed, it increased progesterone binding in intact granulosa cells, while siRNA PGRMC1 decreased progesterone binding (Peluso JJ., *et. al*., 2003). Functionally, PGRMC1 is induced in a spectrum of cancers, where it promotes tumor survival and genotoxic drug resistance (Rohe *et al*., 2009). PGRMC-1 is considered to be an adaptor protein, which functionally serves to bind to other proteins in various cellular contexts (Cahill, M. 2007; Losel *et al*., 2008). Despite the cytochrome b5 heme binding domain being the only functional domain in PGRMC1, the majority of publications on PGRMC1 are on its role as a progesterone receptor (Cahill, M. 2007; Losel *et al*., 2008; Rohe *et al*., 2009).

1.1.6 PGRMC1 (Hpr6) Regulates the Susceptibility of Cancer Cells to Chemotherapeutic Drugs

In order to study the affect of PGRMC1 on survival from chemotherapeutic drugs, a heme binding defective mutant a D120G of PGRMC1 was overexpressed with an Adenovirus in MDA-MB-231 breast cancer cells and treated with doxorubicin and camptothecin (Crudden *et al*., 2006). Using MTT cell viability assays, this heme binding defective Ad-D120G-PGRMC1 conferred a greater susceptibility to doxorubicin and camptothecin treatments than an Ad-LacZ control (Crudden *et al*., 2006).

PGRMC1 was also found to regulate the viability of cisplatin in ovarian cancer cells (Peluso *et al*., 2008). Here, in the presence of progesterone, overexpression of PGRMC1 in Ovcar-3 cells reduced the effectiveness of cisplatin treatment. Additionally, PGRMC1 siRNA increased cisplatin effects and an antibody to PGRMC1 increased cisplatin induced cell death (Peluso, JJ., *et al*., 2008).

1.1.7 PGRMC1 is a Sigma 2 Receptor, Connections with Progesterone

Recently, researchers screened for the elusive sigma 2 receptor using a photoaffinity probe WC-21 and found PGRMC1 as a protein that directly cross-linked to WC-21 (Xu *et al*., 2011). The first report of progesterone binding to sigma receptors was more than twenty years ago (Su *et al*., 1988). Furthermore, progesterone has been shown to be a ligand for sigma receptors (Su., TP., 1991), and others have shown that sigma receptor ligands competed for progesterone binding in porcine liver microsomes (Meyer *et al*., 1998). Recently, progesterone was reported to act as an antagonist to sigma receptor agonists in Na^+ channel inhibition (Johannessen M., *et al*., 2011). Because PGRMC1 so strongly connects progesterone biology to sigma-2 receptor mechanisms, Dr. Rolf Craven has renamed the protein $S2R^{Pgrmc1}$ (Ahmed *et al*., 2012).

1.1.8 Yeast Dap1 is a Heme Binding Protein that Regulates Ergosterol Synthesis

Yeast Dap1p is a cytochrome b5 heme binding protein that belongs to the family of highly conserved membrane-associated progesterone receptor (MAPR) family (Hand *et al*., 2003), which include PGRMC1. Initial experiments demonstrated that genes

involved in the ionizing radiation response and treatment with methyl methane-sulfonate (MMS) were involved in sterol synthesis (Bennett *et al.*, 2003). Deletion of ERG3 (encodes C-5 sterol desaturase) lead to increased MMS sensitivity. Others have shown that Dap1p is required for growth in the presence of MMS (Hand *et al*., 2003). Deletion of Dap1p resulted in sensitivity to MMS, elongated telomeres, loss of mitochondrial function and partial arrest in sterol synthesis. Moreover, Dap1p conferred resistance to the antifungal compounds itraconazole and fluconazole (ERG11, lanosterol demethylase inhibitors) (Hand *et al.*, 2003). Specifically, Dap1p mutant cells have decreased levels of ergosterol (the yeast version of cholesterol), but increased levels of the ergosterol intermediates squalene and lanosterol (Hand *et al.*, 2003). Later that year, it was confirmed that Dap1p was a indeed a *bona fide* heme binding protein, subsequently mutating conserved aspartic acid D91 to a glycine in Dap1p, rendering it unable to bind heme (Mallory *et al*, 2005). This heme binding defective Dap1p(D91G) was unable to confer survival from MMS, but this sensitivity to MMS could be bypassed by exogenous addition of heme (Mallory *et al*., 2005). Additionally, overexpressing ERG11 (lanosterol demethylase) in Dap1p mutant yeast suppressed this sensitivity to ERG11 inhibitors itraconazole and fluconazole (Mallory *et al*., 2005). Furthermore, protein expression of endogenous ERG11 required Dap1p protein expression. These experiments confirm that ERG11, the lanosterol demthylase is downstream of Dap1p. It is important to note that Dap1p also increased the metabolism of squalene and episterol, implicating Dap1p in activating Erg1/squalene epoxidase and Erg2/sterol-C5 desaturase (Craven *et al*., 2007, Hand *et al*., 2003, Mallory *et al*., 2005). Squalene epoxidase

requires cytchrome P450 reductase (POR) for its activity (Ono *et al*., 1980), however the mechanism of how Dap1p activates Erg3/sterol C-5 desaturase is unknown (Ahmed *et al*., 2012).

1.1.9 PGRMC1 Modulates Cytochrome P450 enzymes

The first physical association of Dap1p with yeast P450 cytochrome enzymes used TAP tagged Dap1p chromatography to show an interaction between endogenous ERG11 and Dap1p and between endogenous ERG5 and Dap1p (Hughes *et al.*,2007). These two interactions with Dap1p were subsequently confirmed with ectopic co-immunoprecipitations. A Y138F heme binding defective mutant of Dap1p, was used to show reduced ergosterol levels, and higher lanosterol levels and dienol and trienol levels, reflecting defects in ERG11 and ERG5 function (Hughes *et al*., 2007).

Turning to the mammalian PGRMC1, mass spec analysis was used on shRNA PGRMC1 knockdown in 293T cells, revealing an increase in lanosterol levels, three fold higher than shRNA control 293T cells (Hughes *et al*., 2007). This suggests that PGRMC1 was required specifically for the demethylation of lanosterol by the ERG11 homolog CYP5A1 (lanosterol demethylase) (Hughes *et al*., 2007). To detect a physical interaction, these researchers co-transfected PGRMC1 and CYP5A1 into 293T cells and performed co-immunoprecipitation experiments. PGRMC1 was able to co-immunoprecipitate with CYP5A1 (lanosterol demethylase), as well as with three other P450 cytochromes, CYP7A1 (bile synthesis), CYP21A2 (progesterone 21-hydroxylase), and CYP3A4 (drug metabolism) (Hughes *et al*., 2007).

This corroborates previous connections between PGRMC1 and the P450 system, which showed that the activity of CYP21A2 is enhanced in cells upon overexpression of PGRMC1 (Min *et al*., 2005). A clinical consequence of a PGRMC1 H165R missense mutation was observed in premature ovarian failure (Mansouri *et al*., 2008). Here the binding between PGRMC1 and CYP21A2 was abolished by this HI65R mutation (Mansouri *et al*., 2008).

The ability of PGRMC1 to affect the P45O CYP19 (aromatase) enzyme in breast cancer cells was examined. CYP19/aromatase is the major enzyme that converts androsteenedione and testosterone into estrogen (Miki *et al*., 2007, Bulun *et al*., 2005). Using PGRMC1 shRNA MCF7 and control shRNA MCF7 cells, CYP19 activity was significantly reduced in PGRMC1 knockdown cells, while expression of CYP19 was unchanged between control and PGRMC1 knockdown cells (Ahmed *et al*., 2012). Adding recombinant PGRMC1 ectopically to MCF7 cells had little effect on CYP19 activity at a 1:1 molar ratio but did affect activity at a 10:1 molar ratio (Ahmed *et al*., 2012). This relationship was examined further with co-immunoprecipitation experiments using ectopic PGRMC1 and ectopic CYP19. Using HEK 293T cells that were transfected with both plasmids, CYP19 was found to co-immunoprecipitate with PGRMC1, but only weakly co-immunoprecipitated with a D120G heme binding defective PGRMC1. This experiment shows that heme binding of PGRMC1 is required for its association with CYP19 (Ahmed *et al*., 2012).

1.2.0 SREBP transcription factors and their Regulation

1.2.1 PGRMC1 interacts with SCAP and INSIG1.

Work done in 2005 demonstrated that PGRMC1 could be found in a protein complex with SCAP and Insig1 (Suchanek *et al*., 2005). Using a novel photo-activatable amino acid cross linking method, researchers identified a protein complex of PGRMC1, SCAP and Insig1 in COS cells. This implies that PGRMC1 might reside in a protein complex with the sterol regulatory SCAP and Insig1 proteins to somehow modulate sterol signalling.

1.2.2 Sterol regulation of the SREBP transcription factors

Cholesterol is a critical component of mammalian cell membranes providing structure and membrane permeability (Brown and London. 1998; Schroeder *et al.*, 2001). In membranes, cholesterol plays a role in forming microdomains such as lipid rafts, and caveolae (Lajoie and Nabi. 2010; Staubach and Hanisch. 2011). Besides its function in cell membranes, cholesterol is a central precursor of steroid hormones, oxysterols and bile acids (Rezen *et al.*, 2010; Mclean *et al.*, 2012). Cholesterol homeostasis is regulated by the ER-resident transcription factors called Sterol Regulatory Element Binding Proteins SREBP (Horton and Shimomura 1999; Rawson 2003; Eberle *et al.*, 2004; McPherson and Gauthier, 2004). When processed into the nuclear amino terminal active form, SREBPs transcribe a specific set of genes involved in cholesterol metabolism and

fatty acid synthesis (Eberle *et al*. 2004). One target of SREBPs is the Low Density Lipoprotein Receptor (LDL Receptor) (Yokoyama *et al*., 1993). Other transcriptional targets of SREBPS are genes involved in fatty acid synthesis, triglyceride metabolism and phospholipid synthesis (McPherson and Gauthier, 2004). There are two genes for SREBPs, SREBP1 (which has two isoforms, 1a and 1c), and SREBP2 (Shimano H. 2001). For non-liver tissues, SREBP2 is the predominant isoform, and some of its transcriptional targets are genes that are involved in cholesterol metabolism ie HMG co-Reductase, and the LDL Receptor (Amemiya-Kudo *et al*., 2002). SREBP1c is the main liver SREBP isoform (and a different gene than SREBP2), and it is involved in transcribing genes involved in fatty acid and triglyceride metabolism ie fatty acid synthase (Horton *et al*., 2002).

SREBPs are retained in the ER by two proteins, SREBP cleavage activating protein (SCAP) and the insulin-induced gene product (Insig) (Nohturfft *et al*., 1998; Yabe *et al*., 2002). The abundance of sterol in the cell, regulates the proteolytic cleavage of SREBP (~120 kDa precursor) and activation of SREBPs through two proteins, SCAP and Insig (Brown and Goldstein. 1997; Brown and Goldstein 1999). When cholesterol levels are high, SREBPs are retained in the ER by SCAP (which has a sterol sensing domain) and Insig (Sakai *et al*., 1998; Espenshade *et al*. 1999). The binding of sterols to SCAP`s sterol sensing domain (SSD), causes a conformational change, which results in SCAP binding to Insig. This results in the SREBP/SCAP complex being retained in the ER (Brown *et al*., 2002, Yabe *et al*., 2002). When cholesterol levels are low, SCAP dissociates from Insig and escorts the full length SREBP precursors to the Golgi

apparatus. In the Golgi, the full length SREBP precursors are cleaved by site 1 and site 2 proteases to generate the mature protein (Sakai *et al*., 1998; Espenshade *et al*., 1999). Now the mature form of SREBP, an NH2-terminal processed fragment of SREBP containing the bHLH domain, translocates to the nucleus to transcribe genes involved in cholesterol and fatty acid synthesis (McPherson and Gauthier. 2004; Ye and DeBose-Boyd. 2011). A schematic model in figure 1.1 outlines this process.

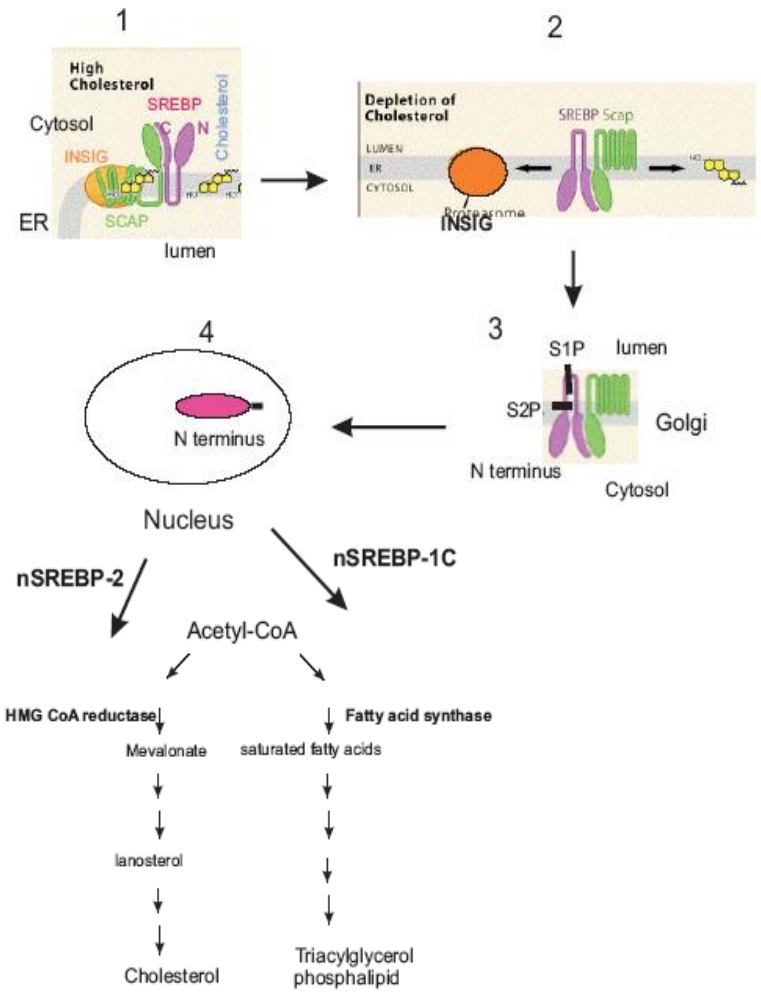

Figure 1.1 Schematic Model of SREBP signalling. 1. When sterols are high, SREBP and SCAP are retained in the ER by Insig1. 2. When sterols are low, SREBP and SCAP dissociate from Insig1, leave the ER and translocate to the Golgi. 3. In the Golgi, SREBP gets cleaved by two site directed proteases into the amino terminal active form. 4. This mature NH2 form of SREBP now translocates to the nucleus to transcribe genes for cholesterol metabolism. Figure from Rawson, R.B., 2003. The SREBP Pathway. Insight from Insigs and Insects. *Nat Rev Mol Cell Biol* 4.631-640.

1.2.3 SREBP Activation Regulated by AKT/PKB Signalling

When growth factors and serum stimulate cells to grow, they activate their respective cognate receptor tyrosine kinases (RTK), which in turn activate the PI3Kinase signalling pathway (Toker and Cantley. 1997; Franke *et al*., 1997). This is a key signal transduction pathway linking receptors and oncogenes to proliferation, and numerous cellular functions, and representing one of the most activated pathways in cancer (Luo *et al*., 2003; Engelman *et al*., 2006). PI3Kinase consists of two subunits, a p85 subunit which interacts with activated RTKs, and a catalytic subunit p110 which now activated, converts phosphatidylinositol-4,5-bisphosphate (Ptdlns(4,5)P_2) to phosphatidylinositol-3,4,5-triphosphate (Ptdlns(3,4,5)P_3) at the membrane (Tolias and Cantley. 1999). This (Ptdlns(3,4,5)$P_{3)}$ now serves as a docking site for pleckstrin homology domain containing proteins such as AKT, which now get recruited to the membrane to become activated (Stokoe *et al*., 1997; Stephens *et al*., 1998). The PTEN tumor suppressor is a lipid phosphatase that antagonizes PI3Kinase signalling by dephosphorylating (Ptdlns(3,4,5)P_3) to (Ptdlns(4,5)P_2) (Maehama and Dixon. 1998; Cantley and Neel. 1999; Maehama and Dixon. 1999). AKT/PKB phosphorylates numerous substrates ie GSK3β, FOXO family of transcription factors, proteins involved protein synthesis, cell survival, proliferation and metabolism, and mTOR (mammalian target of Rapamycin) a protein involved in regulating translation, and in the monitoring of cellular energy status (Manning and Cantley. 2003). Initial research uncovered that SREBP proteins were regulated targets of PKB and PI3Kinase signalling (Fleischmann and Lynedjian. 2000).

Using insulin stimulated rat hepatocytes, researchers demonstrated that SREBP1 mRNA levels were dependant on PKB and PI3Kinase. Others have also demonstrated this connection as well (Porstman *et al*., 2005; Yellaturu *et al*., 2009; Porstmann *et al*., 2009). Using inhibitors of PI3Kinase, Wortmanin and LY294002, ligand stimulated (VEGF, PDGF) activation of SREBP-1 was blocked, implicating this pathway in SREBP1 activation (Demoulin *et al*., 2004; Zhou *et al*., 2004; Hegarty *et al*., 2005). Moreover, PI3Kinase/Akt has been shown to be involved in the ER to Golgi transport of SCAP and SREBP2 (Du X., *et al*., 2006). More recently it has been demonstrated that this insulin stimulated SREBP lipogenesis pathway in primary rat hepatocytes was dependant on mTOR, PKB and PI3Kinase, (Li *et al*., 2010).

1.3.0 Insig interaction with SCAP and HMG CoA Reductase: a central role in sterol regulation

1.3.1 HMG CoA Reductase

HMG CoA reductase is a highly conserved, membrane bound enzyme in the ER. It catalyzes a rate-limiting step in sterol synthesis, the production of mevalonate, and is involved in isoprenoid biosynthesis (Goldstein and Brown. 1990; Burg and Espenshade. 2011). HMG CoA reductase is embedded in the ER membrane by its eight membrane spanning regions in its NH2 terminus (Roitelman *et al*., 1992). This region has been shown to mediate sterol regulated binding to Insig1 (Sever *et al*., 2003). Enzymatically, HMG-CoA reductase catalyzes the reduction of 3-hydroxy-3-methylglutaryl-CoA to mevalonate (Brown and Goldstein. 1980; Liscum *et al*., 1985)). This step is an

irreversible step, near the beginning of the pathway in the biosynthesis of cholesterol from acetyl-CoA. Mammalian HMG-CoA reductase enzymatic activity is regulated by AMP kinase which phosphorylates HMG-CoA reductase at a conserved serine 872 inhibiting it`s activity (Clarke *et al*., 1990, Istvan *et al*., 2000). As previously mentioned, HMG-CoA reductase is a transcriptional target of SREBPs.

1.3.2 Degradation of HMG CoA Reductase through Insig1

HMG-CoA reductase protein degradation is regulated by its association with Insig. In mice lacking Insig, liver HMG-CoA reductase was reported to be 85 fold higher than in control mice (Engelking *et al*., 2005). Insig regulates HMG-CoA reductase degradation by a sterol-responsive feedback inhibition system. When sterols induce HMG CoA reductase to bind to Insig, in results in the ubiquitination and degradation of HMG CoA reductase (Skalnik *et al*., 1988; Ravid *et al*., 2000). In high sterol conditions, Insig binds to the NH2 terminal region of HMG-CoA reductase and recruits enzymes that target ubiquitin to HMG-CoA reductase (Burg and Espenshade. 2011). When sterols are low, Insig1 and HMG-CoA reductase dissociate and HMG-CoA reductase is stable. This action required a tetrapeptide sequence YIYF, located in the second transmembrane segment of HMG CoA reductase. When this YIYF sequence was mutated to alanines, HMG CoA reductase (mutant) was unable to bind Insigs, and was refractory to rapid degradation (Sever *et al*., 2003).

Evidence demonstrating that degradation of HMG CoA reductase was dependant on Insig1 and Insig2 came from experiments transfecting (overexpressing) HMG CoA

reductase in chinese hamster ovary (CHO) cells. When HMG CoA reductase was overexpressed using a CMV promoter plasmid, it was refractory to sterol mediated degradation (Sever *et al*., 2003). Re-establishment of this regulated degradation of overexpressed HMG CoA reductase was restored by co-overexpressing Insig1 or Insig2 (Sever *et al*., 2003). This re-established sterol induced HMG CoA reductase degradation was associated with the binding of HMG CoA reductase to Insig1 as demonstrated by co-immunoprecipitation (Sever *et al*., 2003). Moreover, siRNA dual knockdown of Insig1 and Insig2 ablated the sterol mediated ubiquitination of HMG CoA reductase (Sever *et al*., 2003). Lastly, in mutant cells lacking Insig1, sterols fail to induce sterol mediated ubiquitination and degradation of HMG CoA reductase (Sever *et al*., 2004).

1.3.3 Lanosterol, an intermediate in the synthesis of cholesterol, promotes the Insig-mediated degradation of HMG CoA Reductase

Initial studies using a mammalian cell line with a mutant lanosterol 14 alpha-methyl demethylase, implicated lanosterol as a key intermediate molecule in sterol synthesis (Chen *et al*., 1988). Subsequent studies implicated lanosterol in the regulation of HMG CoA reductase levels (Frye *et al*., 1994, Leonard *et al*., 1994; Trzaskos *et al*., 1995). Eventually it was demonstrated that lanosterol was the sterol intermediate that promoted the Insig mediated degradation of HMG CoA reductase (Song *et al*., 2005). Using SV-589 transformed human fibroblasts cells, lanosterol and 24,25-Dihydrolanosterol, and 25-Hydroxycholesterol was added individually and HMG CoA reductase

immunoprecipitations were probed for ubiquitination and protein levels. This was done using a previously established permeabilized cell system that supported the ubiquitination of HMG CoA-reductase, stimulated by the in vitro addition of sterols (Song and DeBose-Boyd, 2004). Here, 25-Hydroxycholesterol, lanosterol, and 24,25-dihydrolanosterol were able to promote the ubiquitination of HMG CoA reductase in a dose dependant manner, whereas cholesterol only modestly stimulated HMG CoA reductase ubiquitination (being 10 fold less potent than lanosterol and 24,25-dihydrolanosterol) (Song *et al*., 2005). Further studies testing zymosterol, zymostenol, demosterol and 7-dehydroxycholesterol demonstrated these sterol moieties could not promote HMG CoA reductase ubiquitination implicating the C4 and/or C14 methylation of lanosterol and 24,25- dihydrolanosterol as being required for ubiquitination of HMG CoA reductase, (Song *et al*., 2005).

1.3.4 Gp78 is a membrane ubiquitin ligase, associated with Insig1 (and couples lanosterol-regulated ubiquitination to degradation of HMG CoA reductase)

In order to identify proteins that could be interacting with the sterol mediated HMG CoA reductase-Insig complex, mass spec technology was used to find proteins that co-immunoprecipitated (affinity purification) with this HMG CoA reductase-Insig complex (Song *et al*., 2005). Here gp78 a membrane bound ubiquitin ligase, was found to bind Insig-1. Knockdown of gp78 by RNA interference (RNAi) prevented the lanosterol dependant ubiquitination and degradation of endogenous HMG CoA reductase (Song *et al*., 2005). Subsequently, experiments overexpressing gp78`s membrane domain abrogated lanosterol induced Insig mediated ubiquitination of HMG CoA reductase.

This likely occurs because the membrane domain of gp78 competes with the endogenous full-length gp78 for Insig1 binding (Debose-Boyd. 2008).

Another protein, Valosin-containing protein (VCP), an ATPase, was found to bind to gp78, and eventually was demonstrated to be required for HMG CoA reductase degradation (Song *et al.*, 2005).

1.3.5 SCAP and HMG CoA Reductase bind to the same region on Insig1

As mentioned previously, the HMG CoA reductase YIYF tetrapeptide motif was found to be responsible for sterol (lanosterol) mediated Insig binding (Sever *et al*., 2003). SCAP, another Insig binding protein also contains this YIYF motif in its second transmembrane domain, and it also has been shown to mediate sterol dependant formation of SCAP-Insig complexes (Yang *et al.*, 2002; Yabe *et al*., 2002). When the sterol sensing domain of SCAP was overexpressed in cells, it blocked Insig mediated sterol (lanosterol) induced HMG CoA reductase degradation (Yang *et al.,* 2002). Mutating SCAP`s sterol sensing domain YIYF motif, abolished this inhibition. When a conserved aspartic acid 205 in Insig1 was mutated to alanine, it abolished Insig`s ability to bind to SCAP, as well as HMG CoA reductase, demonstrating that SCAP and HMG Co reductase both bind to Insig1 at the same site (Gong *et al*., 2006). Therefore, this strongly suggests that HMG CoA reductase and SCAP bind to Insigs on the same site, and that HMG CoA reductase and SCAP compete for Insigs (De-Bose Boyd. 2008).

1.3.6 Sterol regulated ubiquitination and degradation of Insig1 by gp78

Early reports on Insig1 degradation came from the lab of Jin Ye in 2004. Using thapsigargin (an ER stress inducer), and hypotonic cell stress culture conditions, researchers demonstrated that Insig1 becomes degraded and subsequently SREBP becomes activated in each of these stress conditions (Lee and Ye. 2004). These two cellular stresses bypass the sterol regulation of Insig1 degradation. Researchers in the lab of Drs. Brown and Goldstein demonstrated that Insig1 gets ubiquitinated in sterol depeleted cells where it is rapidly degraded by proteasomes (Gong *et al.*, 2006). When sterols are low, this SCAP/SREBP complex dissociates from Insig1, which now gets ubiquitinated on lysines 156, and 158 and is degraded in proteosomes (Gong *et al*., 2006). Eventually, this sterol regulated degradation of Insig1 was determined to be mediated by the membrane bound ubiquitin ligase gp78 (Lee *et al*., 2006). These researchers demonstrated that when sterols induce SCAP to bind Insig1, gp78 becomes displaced, and is unable to ubiquitinate Insig-1, consequently stabilizing the Insig-1 protein (Lee *et al*., 2006). This blocked the release of SCAP-SREBP from the ER, and subsequently inhibited SREBP maturation (Lee *et al*., 2006; De-Bose Boyd, 2008). While the release of SCAP/SREBP from Insig1 does not require ubiquitination, Insig1 degradation post SCAP/SREBP dissociation establishes a requirement for synthesis of new Insig1 for feedback inhibition (Gong *et al*. 2006). As mentioned previously, sterol deprivation causes SCAP/SREBP to translocate to the Golgi, where SREBP gets cleaved by two site directed proteases, S1P and S2P, generating an NH2 terminal nuclear fragment. This N-terminal SREBP fragment then translocates to the nucleus to transcribe genes to

synthesize more cholesterol, one of these transcriptional targets being Insig-1 (Gong *et al*., 2006). When this newly generated Insig1 and cholesterol converge on SCAP, SCAP/SREBP bind to Insig-1, preventing ubiquitination (Gong *et al*., 2006). This process is called "convergent feedback inhibition" whereby the newly synthesized Insig-1/SCAP/SREBP complex accumulates in the ER, awaiting regulation by sterol deprivation once again (Gong *et al*., 2006).

Experiments using domain swapping mutations on Insig1 demonstrated that serine 149, which lies NH2 terminal to the ubiquitination sites (lysines 156, and 158) regulates the accelerated degradation by ubiquitin of Insig1 (Lee *et al*., 2006). Insig2 stability was demonstrated to be regulated by serine 106, which lies COOH terminal to the ubiquitination site of glutamine 214 on Insig2 (Lee *et al*., 2006).

1.4.0 A connection between PGRMC1 and cytochrome P450 reductase (POR)

1.4.1 PGRMC1 Heme binding defective mutants

In accordance with containing a cyt-b5 domain, PGRMC1 binds to heme and the association with heme contributes to PGRMC1 function (Crudden *et al*., 2006). Experiments using UV-visible absorption and electron paramagnetic resonance (ESR) spectra demonstrated that PGRMC1 could bind to b-type heme (Min *et al*., 2005). This group also demonstrated that PGRMC1`s hydrophobic heme binding pocket was affected by mutating two conserved tyrosines in PGRMC1 Y107, Y113 , and the amino acid residues between D99 and K102 (Min *et al*., 2005). These homologous tyrosines 107 and 113 in PGRMC1, are conserved in CYB5D2, at tyrosine 73 and tyrosine 79 (Results

Section Figure 5.1). Further characterization of the heme binding in yeast Dap1 used site directed mutagenesis to ablate heme binding when Y138 was mutated in Dap1 (Ghosh *et al*., 2005). This tyrosine, is homologous to Y165 in PGRMC1, and to tyrosine 127 in CYB5D2 (Figure 5.1). When a highly conserved aspartatic acid 120 to glycine (D120G) was mutated in HPR6 (PGRMC1) this generated a heme binding defective PGRMC1 (Crudden *et al.,* 2005). When this PGRMC1(D120G) mutant was overexpressed by an adenovirus in a MCF7 cell line, it rendered these cells more susceptible to the chemotherapeutic drugs doxorubicin and camptothecin (Crudden *et al*., 2005). This aspartic acid in PGRMC1 D120 mutated for loss of heme binding is conserved in CYB5D2, D86.

1.4.2 Cytochrome P450 enzymes

Cytochrome P450 enzymes are part of a large family of monooxygenases that catalyze the oxidation of organic substances. They function in the metabolism of foreign xenobiotic compounds, the biosynthesis and metabolism of steroids and in facilitating steps in sterol synthesis and homeostasis (Fluck and Pandey. 2010). They are well conserved throughout evolution, with over 50 different cytochrome P450 enzymes in humans, and many more (over 500) in plants (Omura. 2013). In humans, cytochrome P450 enzymes are expressed throughout the body, with the highest concentration of expression in the liver, and steroidogenic tissues (Miller. 2012). Cytochrome P450 enzymes can be located in the mitochondria or in the endoplasmic reticulum (ER) microsomes. The mitochondrial forms are mostly involved in steroid metabolism while

the ER forms are mostly involved in xenobiotic metabolism and sterol metabolism (Szczesna-Skorupa and Kemper, 2008). Cytochrome P450 enzymes catalyze a reaction whereby one oxygen molecule atom is incorporated into a monooxygenoase and one oxygen molecule is incorporated into water (Black and Coon, 1987). In this reaction, two electrons are consumed, which then get donated from NADPH to cytochrome P450 enzyme redox partners (Strobel *et al.*, 1995).

In the majority of tissues, there are significantly more cytochrome P450 enzymes than there is cytochrome P450 reductase (POR) protein. Thus cytochrome P450 enzymes interact with POR in a transient manner, instead of forming stable protein complexes (Szczesna-Skorupa and Kemper, 2010). Cytochrome P450 enzymes can form homo or hetero oligomeric structures (Backes and Kelley. 2003). A single POR molecule can bind to these oligomeric complexes of P450 enzymes (Szczesna-Skorupa and Kemper, 2010).

Cytochrome P450 enzymes have been shown to be targeted to the ER through a signal recognition particle mediated delivery to the sec61 complex (High *et al*., 1991; Oliver, J., *et al*., 1995). How Cytochrome P450 enzymes are retained in the ER is still unclear (Szczesna-Skorupa and Kemper, 2008). Certain experimental evidence showing that inhibiting heme synthesis in cos1 cells resulted in higher cytosolic levels of overexpressed CYP1A1, implicates a heme binding protein responsible for ER retention (Meyer *et al*., 2002). Also addition of hematin to cell-free reactions enhanced CYP1A1 activity in kidney and brain extracts. On this basis, Dap1p/PGRMC1 is a candidate for

an ER retention receptor for cytochrome P450 enzymes (Szczesna-Skorupa and Kemper, 2008).

1.4.3 PGRMC1 inhibits the activity of drug-metabolizing cytochrome P450s and binds to cytochrome P450 reductase (POR)

The first protein interaction between PGRMC1 and cytochrome P450 reductase (POR) was demonstrated by Byron Kemper`s group (Szczesna-Skorupa and Kemper, 2010). These experiments also showed that PGRMC1 could interact with CYP2C2 and CYP2C8 as well as CYP3A4. Experiments using PROMEGA`s P450 Glo luciferase assays to detect activity of CYP2C2, CYP2C8 and CYP3A4, determined that PGRMC1 in dose dependant transfections, led to the slight inhibition of the activities of these three P450 enzymes (Szczesna-Skorupa and Kemper, 2010). This PGRMC1 inhibition of these P450 cytochromes could be overcome with increased expression of POR. A different result was seen with CYP51A1 whereby shRNA knockdown of PGRMC1 in 293T cells resulted in an increase in lanosterol levels, indicating CYP51A1 was inhibited by a PGRMC1 shRNA knockdown (Szczesna-Skorupa and Kemper, 2010), corroborating previously reported results (Hughes *et al*, 2007).

Recently, it was reported that PGRMC1 negatively regulated the human drug-metabolizing activities of P450 enzymes CYP3A4, CYP2C9 through direct interaction, in liver cells (Oda *et al*., 2011). Using HEPG2 cells, and an adenoviral expression system, PGRMC1 inhibited the activity of CYP3A4 and CYP2C9, with minimal effect on CYP2E1 activity. These results were subsequently confirmed in human hepatocytes (Oda *et al*., 2011).

1.4.4 Cytochrome P450 enzymes and drug metabolism

Cytochrome P450 enzymes are responsible for the metabolism of therapeutic drugs, many exogenous and endogenous compounds. The CYP families classified as CYP 1-3 (grouped by pairwise amino acid sequence identity between family members) function in the metabolism of human drugs and xenobiotic compounds (Sim and Ingelman-Sundberg. 2010). Other CYP family members (CYP 4, 11, 17, 19, and 21) function in metabolising endogenous compounds such as fatty acids, steroids, eicosanoids, bile acids and vitamins (Ingelman-Sundberg. 2005). The six major drug metabolising enzyme families are CYP1A2, CYP2C9, CYP2C19, CYP2D6, CYP2E1 and CYP3A4, which collectively account for around 90% of all drug clearance and bioavailability (Singh *et al.*, 2011). CYP 3A4 accounts for nearly 50% of all drug metabolism (Pinto and Dolan. 2011). It is the most abundant CYP protein isoform expressed in human liver, and intestines, comprising almost 15-30% of the liver microsomal pool.

Additionally, CYP3A4 is a steroid hydroxylase, having an important role in the catabolism of several endogenous steroids ie testosterone, progesterone, cortisol and bile acids (Patki *et al.*, 2003, Bodin *et al.* 2005).

The CYP enzymes display extensive genetic polymorphic variability, with certain P450 enzymes conferring fast metabolising to poor metabolising drug affects. An example of this is seen in CYP2D6 which metabolizes the pro-drug tamoxifen in breast cancer treatment, which gets metabolized to active form 4-OH tamoxifen and endoxifen (Ingelman-Sundberg. 2005). CYP2D6 individual polymorphisms influence the effectiveness of the drug through the ability to metabolise the pro-drug.

Another drug example of a polymorphic P450 enzyme CYP2C9 affecting drug metabolism is with the anti-coagulant warfarin. Insufficient dosing in normal patients leads to clotting, stroke and heart attacks, while individuals who are slow metabolizers need longer time periods to achieve a stable dose and are vulnerable to serious bleeding (McClain *et al*., 2008; Lindh *et al*., 2009).

1.4.5 Roles and involvement of cytochrome P450 enzymes in cholesterol metabolism

Cholesterol is the precursor for the biosynthesis of steroid hormones, oxysterols, bile acids and vitamin D. In mammalian steroidogenesis, cholesterol is initially converted into pregnenolone, the precursor for all other steroid hormones ie progesterone, cortisol, aldosterone and testosterone (Miller and Bose. 2011). Cholesterol homeostasis is regulated through elimination pathways, where the oxysterols (oxidized derivatives of cholesterol) become significant intermediates in steroid and bile acid synthesis (Vaya *et al*., 2011). The increased polarity of oxysterols enhances their transport across membranes and the blood-brain barrier (Crosignani *et al*., 2011). Cholesterol conversion to bile acids to excrete cholesterol is necessary for its elimination. Additionally, bile acids are natural ligands for G protein coupled receptors and the nuclear transcription factor farnesoid X receptor (FXR) (Hylemon *et al*., 2009). Cholesterol is catabalized into bile acids by two major routes, the classic (neutral) pathway and the alternative (acidic) route (McClean *et al*., 2012). Primary bile acid formation in the classic neutral route requires CYP7A1 to make 7α-hydroxyxholesterol, then subsequent oxidations (Russel. 2003). In the alternative (acidic) pathway, CYP27A1 is required to generate 27-hydroxycholesterol and CYP7B1 to modify it (Norlin and Wikvall. 2007). In the brain,

bile acid synthesis by CYP46A1 converts cholesterol to (24S)-hydroxycholesterol which allows its permeablility across the blood brain barrier (Mast *et al*., 2010). (24S)-hydroxycholesterol (and other oxysterols) activate the liver X receptor (LXR) (Hylemon *et al*., 2009; Makishima *et al*., 1999). As previously discussed, CYP51A1 (sterol 14 alpha-demethylase) removes the 14 alpha-methyl group of lanosterol. This is the first rate limiting step after squalene in cholesterol biosynthesis. This 14 alpha-demethylation step was demonstrated to be dependent on addition of NADPH and cytochrome P450 reductase (Trazkos *et al*., 1984; Fischer *et al*., 1989). Some of the P450 cytochromes involved in bile acid synthesis, have dual roles in vitamin D synthesis (McClain *et al*., 2008).

Three cytochrome P450 hydroxylases are responsible for vitamin D synthesis and degradation: the liver D-25-hydroxylase (25-OHase), 25(OH)D-1alpha-hydroxylase CYP27B1 and CYP24A1 in the kidneys (Chen *et al*., 2012). The active form of vitamin D, 1 alpha, 25-dihydroxyvitamin D, interacts with the vitamin D receptor to induce anti-proliferative, anti-invasive, pro-apoptotic and pro-differentiation activities (Otto *et al*., 2003). Recently is has been shown that both CYP 27B1 and CYP24A1 are expressed in many tissues and cells, including the prostate, implicating their potential involvement in processing Vitamin D in prostate cancer (Flanagan *et al*., 2006; Chen *et al*., 2012).

1.4.6 Cytochrome P450 reductase (POR) mutations

A variety of POR mutations and polymorphisms have been linked to several characteristics in the heterogeneous disease Antley Bixler Syndrome (ABS) (Miller. 1986). ABS collectively comprises a group of heterogeneous disorders characterized by

skeletal, cardiac, and urogenital abnormalities (Miller. 2012). ABS has often been associated with mutations in fibroblast growth factor receptor 2 (FGFR2) and cytochrome P450 reductase (Chun *et al*., 1998; Miller. 2012). Recessive mutations in POR are often found in more disordered steroidgenesis type ABS, while a mainly skeletal phenotype lacking genital anomalies or disordered steroidgenesis correlate with a dominant mutations in a FGFR2 gene (Fluck and Pandey. 2011). Clinically, these ABS heterogeneous pathologies include brachycephaly, facial hypoplasia, bowed ulna or femur, synostosis of the radius, camptodactyly and cardiac and urogenital abnormalities (Miller *et al*., 2005). Severe POR mutations A287P and R457H have been shown to cause Antley-Bixler skeletal malformation syndrome (ABS) (Miller *et al*., 2004, Pandey *et al*., 2004, Fluck *et al*., 2004). The A287P mutation is the most common documented mutation in Caucasian patients (Fluck *et al*., 2004; Arlt *et al*., 2004)., while the R457H mutation is most often found in the Japanese population (Huang *et al*., 2005; Fukami *et al*., 2009). Infants with ABS had genital ambiguity, as a result of deficiencies of 17 alpha-hydroxylase and 21-hydroxylase, caused (indirectly) by combined deficiencies in the steroidogenic enzymes CYP17A1 and CYP21A2, and also by the sex steroid aromatase CYP19A1 (Fluck *et al*., 2004).

The skeletal malformations seen in many (but not all) in POR ABS patients are thought to caused by disruption of enzymes involved in sterol synthesis, specifically 14 alpha-lanosterol demethylase (CYP51A1) and squalene epoxidase, and disruption of retinoic acid metabolism catalyzed by CYP26 isozymes (Idkowiak *et al*., 2012).

Another POR genetic disorder which is caused by the deletion of 1.2 Mb from the POR gene is Williams syndrome. This deletion reduces the transcription of the POR gene, as a cis-regulatory element in lost, affecting expression of the POR transcript (Merla *et al*., 2006). Some patients with Williams syndrome display characteristics of POR deficiency, ie radio-ulnar syntosis and other skeletal abnormalities (Charvat *et al*., 1991). Also, some individuals show modest defective cortisol synthesis, and defective androgen synthesis (Partsch *et al*., 1994).

1.4.7 Cytochrome P450 reductase (POR) knockout mice and POR^{Low} mice

POR knockout (-/-) mice with germline deletions of POR have been reported initially by two groups (Shen *et al*., 2002; Otto *et al*., 2003). The first POR -/- mouse was constructed by a targeted deletion of the translational start site and membrane-binding domain of POR (Shen *et al*., 2002). By mid-gestation, these POR -/- mice developed multipile embryonic defects including neural tube defects, eye, heart and limb abnormalities, an overall retardation of development and embryonic death at day 13.5 of gestation (Shen *et al*., 2002). The POR heterozygotes displayed limited embryonic lethality. A second POR -/- mice was generated by deleting exons 4 to 15, which contain the majority of the coding sequence of POR (Otto *et al*., 2003). This POR -/- mouse displayed inhibited vasculogenesis and hematopoiesis, as well as defects in the brain and limbs, as it died embryonically, in early to mid gestation (Otto *et al*., 2003).

In order to overcome the embryonic lethality of these POR -/- mice, a hypomorphic, reduced POR (low expressing) mouse was generated by the insertion of a neomycin cassette into the 15th intron of the genomic POR gene, and resulted in a global reduction in POR (74% to 95% decrease in POR expression) in all tissues examined (Wu *et al*., 2005). A decrease in overall body weight was observed in male adult POR*low* homozygote mice, with decreased weights of heart, lung and kidney (Wu *et al*., 2005). Adult female homozygous POR*low* mice had increased serum testosterone and progesterone and were infertile (Wu *et al.*, 2005). Both male and female adult POR *low* homozygous mice had decreased plasma cholesterol, with some mice displaying mild centrilobular hepatic lipidosis (Wu *et al*., 2005). Also, reductions in the systemic clearance of pentobarbital, as well as hepatic microsomal metabolism of testosterone and acetomenophin were observed (Wu *et al*., 2005).

1.4.8 Cytochrome P450 reductase (POR) and cholesterol

There are several lines of evidence that implicate cholesterol biosynthesis in POR deficient ABS. Firstly, cholesterol biosynthesis requires two major enzymes lanosterol 14alpha demethylase (CYP51A1) and a non-P450 enzyme squalene epoxidase (Ono and Bloch, 1975; Debeljak *et al*., 2003). Two studies have shown that in fibroblasts from an infant with ABS and POR deficiency, researchers detected reduced lanosterol demethylase activity (Fluck *et al*., 2004 and Kelley *et al*., 2002). Secondly, maternal ingestion of fluconazole, an antifungal agent that inhibits CYP51A1 activity is associated with ABS (Aleck and Bartley, 1997; Pursley *et al.*, 1996). Thirdly, Smith-Lemli-Opitz

syndrome, a cholesterol Sonic Hedge-Hog disorder is also associated with skeletal malformations (Miller *et al*., 2011). Moreover, cholesterol modification of hedgehog proteins is required for signalling in bone formation (Cooper *et al*., 2003). ABS phenotype is a result of POR mutations disrupting the metabolism of all-trans retinoic acid, as increased doses of maternally ingested retinoic acid partially rescued the phenotype of the POR -/- mouse (Otto *et al*., 2003).

CYP51A1 is a lanosterol 14 alpha-demethylase, and is the most conserved member or the CYP enzyme family as it is present in yeast, fungi and plants where it functionally is also conserved, participating in the synthesis of ergosterol (yeast and fungi) and sitosterol (plants) respectively (Stromstedt *et al*., 1996). In mammals, the lanosterol de-methylation reaction is essential for the biosynthesis of sterols. Because of its high amino acid conservation across kingdoms, CYP51A1 can by inhibited by the anti-fungal compounds fluconazole and itraconazole. While fluconazole has been used to treat meningitis, numerous reports of maternally ingested fluconazole resulted in babies born with ABS (Lee *et al*., 1992; Pursley *et al*., 1996). Some of these congenital anomalies seen included craniofacial, skeletal (thin, wavy ribs and ossification defects) and cardiac defects (Pursley., *et al*., 1996). Although serum concentrations are largely normal in individuals with ABS, lanosterol and dihydrolanosterol accumulate when cells from affected individuals are grown in cholesterol-depleted medium (Fukami *et al*., 2005).

Recently, a CYP51A1 (lanosterol 14 alpha-demthylase) -/- mouse was generated (Keber *et al*., 2011). These mice died at embryonic day 15, with marked accumulation of the two CYP51A1 substrates, lanosterol and 24,25-dihyrolanosterol. Cholesterol

precursors downstream of the CYP51A1 enzyme step were not detected, indicating a blockage of cholesterol synthesis at this step. Lethality was attributed to heart failure due to hypoplasia, and vascular defects, suggesting that CYP51A1 was involved in heart development and coronary vessel formation, with downstream defects detected in sonic hedgehog signalling and retinoic acid signalling pathways (Keber *et al*., 2011). This phenotype strongly resembles those of Antley-Bixler Syndrome (loss of cytochrome P450 reductase activity). This knockout confirms a genetic interaction of POR and CYP51A1, and further implicates CYP51A1 as the major substrate of POR in Antley-Bixler syndrome (Kerber *et al*., 2011).

1.4.9 Tissue specific liver knockouts of cytochrome P450 reductase (POR) in mice develop fatty liver

In the liver, the P450 system executes a major role in bile acid synthesis, as well as in the metabolic breakdown of xenobiotic chemicals. Several groups have generated liver specific mouse models with POR deleted in the mouse liver (Gu *et al*., 2003,Henderson *et al*., 2003, Weng *et al*., 2005).

These mice with conditional liver POR deletions developed fatty liver, characteristics similar to non-alcoholic fatty liver disease. These mice developed hepatic steatosis, which had accumulated triglycerides and cholesterol esters, and had around a 90% reduction in bile acid production, and increased lipid metabolism resulting in fatty liver. This severe hepatic lipidosis was characterized by the accumulation of diglycerides, triglycerides and monosaturated fatty acids, which eventually led to development of fibrosis and inflammation (Weng *et al*., 2005; Mutch *et al*., 2007).

Specifically, POR null liver mice had drastic increases in hepatic lipid content (diacylglycerols, triacylglycerols, phosphtidylcholine and cholesterol esters) and a specific enrichment in n-7 and n-9 monounsaturated fatty acids. In the liver, cholesterol is converted to bile acids by the cytochrome P450 enzymes CYP7A1 and CYP8B1, which could explain why bile acid reductions were lower in these livers (Mutch *et al*. 2007). Numerous groups continue to study this liver POR -/- mouse and the mechanisms for the observed fatty liver, with data pointing to lipids accumulating in the liver due to impaired secretion (Mutch *et al*., 2007, Finn *et al*., 2009., Porter *et al*., 2011).

In the experiments with the POR -/- liver mice, metabolic changes in drug metabolism were also measured (Henderson *et al*., 2003). Hepatic POR-/- mice had a dramatically reduced ability to metabolize the narcotic drug pentobarbital, as well as the analgesic acetaminophen (Henderson *et al*., 2003). This further demonstrates the predominant role of the cytochrome P450 liver enzymes in metabolic involvement in the pharmacology and toxicology of these compounds.

1.5 Hypothesis, Objectives and Summary of thesis work

1.5.1. Hypothesis

Initially we set out to determine how CYB5D2 attenuated the function of the PTEN tumour suppressor. We hypothesized that CYB5D2 was directly inhibiting PTEN. Alternatively, our null hypothesis addressed whether CYB5D2 conferred survival from the inhibition of the PI3Kinase signalling pathway. At the time these studies were initiated, CYB5D2 was classified as a "hypothetical protein". Therefore we needed to determine if CYB5D2 was a real *bona fide* protein, thus an antibody to detect the endogenous CYB5D2 protein was generated. During the development of a CYB5D2 antibody, CYB5D2 was observed to inhibit SREBP signalling in transient transfection assays. We therefore hypothesized that CYB5D2 inhibited SREBP signalling because it could co-immunoprecipitate with ectopic Insig1and stabilize it. Alternatively, in a corresponding null hypothesis, we addressed whether the heme binding of CYB5D2 was required for this inhibition of SREBP signalling. Subsequently, the requirement of heme binding of CYB5D2 to inhibit SREBP signalling was uncovered, using a CYB5D2(D86G) heme binding defective mutant. We attempted to determine why heme binding of CYB5D2 was required for inhibition of SREBP signalling. More specifically, we hypothesized that heme binding was required for CYB5D2 to function in the cytochrome P450 reductase and P450 cytochrome system, resulting in the regulation of sterol synthesis and Insig1 stability. We predicted that CYB5D2 would modulate CYP51A1 (lanosterol demethylase) like Dap1p and PGRMC1 did. Lastly, we questioned whether

other CYB5D2 functions were associated with heme binding, and loss of CYB5D2 expression.

1.5.2. Objectives

Aim 1. To determine whether CYB5D2 is a direct negative regulator of the PTEN tumor suppressor protein, or if CYB5D2 attenuated ectopic PTEN death through another mechanism.

Aim 2. Initially, CYB5D2 was uncharacterized and classified as a "hypothetical protein". Published reports of the protein were non-existent, and a commercially produced antibody was not available. Therefore a polyclonal antibody was generated to determine if the CYB5D2 gene encodes for a *bona fide* protein, and to determine where the endogenous CYB5D2 protein was expressed.

Aim 3. To examine how CYB5D2 modulates SREBP signalling. Specifically, we addressed if CYB5D2 inhibited SREBP signalling because of CYB5D2 binding and stabilization of the ectopic Insig1 protein, or was this due to CYB5D2`s ability to bind to heme? In order to address this question a heme binding defective mutant was generated and characterized.

Aim 4. To determine why heme binding of CYB5D2 was required to inhibit SREBP signalling. A D86G heme binding defective mutant of CYB5D2 was made that could not inhibit SREBP signalling, or stabilize ectopic Insig1. I next researched why heme binding of CYB5D2 was required to inhibit SREBP signalling.

Aim 5. To ascertain the role of heme binding in CYB5D2 functions. Using this CYB5D2(D86G) heme binding defective mutant, and a CYB5D2 shRNA, I examined the heme binding requirement in the functions of CYB5D2 in conferring survival from chemotherapeutic compounds, regulation of proliferation, stabilizing CYP51A1 and binding to cytochrome P450 reductase (POR).

1.5.3. Summary of thesis work

Initially we set out to examine how CYB5D2 prevented PTEN induced apoptosis in LNCAP prostate cancer cells. CYB5D2 also prevented ectopic PTEN from killing U87 glioma cells. In U87 cells stably expressing CYB5D2, the ability of PTEN to kill U87 cells was attenuated, and its ectopic expression was sustained. When CYB5D2 sustained ectopic PTEN expression, we observed reduced levels of phosphorylated serine 473 ATK/PKB, indicating that PTEN was expressing sufficiently in the inactivation of the PI3Kinase pathway. When these dual expressing CYB5D2 + PTEN U87 cells were cultured in reduced serum conditions, CYB5D2 could be immunoprecipitated as a 56 kDa dimer. CYB5D2 did not co-immunoprecipitate with PTEN in these conditions. CYB5D2 also conferred survival from serum starvation in NIH3T3 cells. While CYB5D2 could confer survival from serum starvation, CYB5D2 could not co-immunoprecipitate with PTEN in these NIH3T3 cells. Moreover, CYB5D2 serum starved NIH3T3 cells were more viable after three days of culturing without serum. When cultured in reduced serum, CYB5D2 could also be immunoprecipitated as a 56 kDa dimer. A schematic model summarizing this work is seen in figure 1.2.

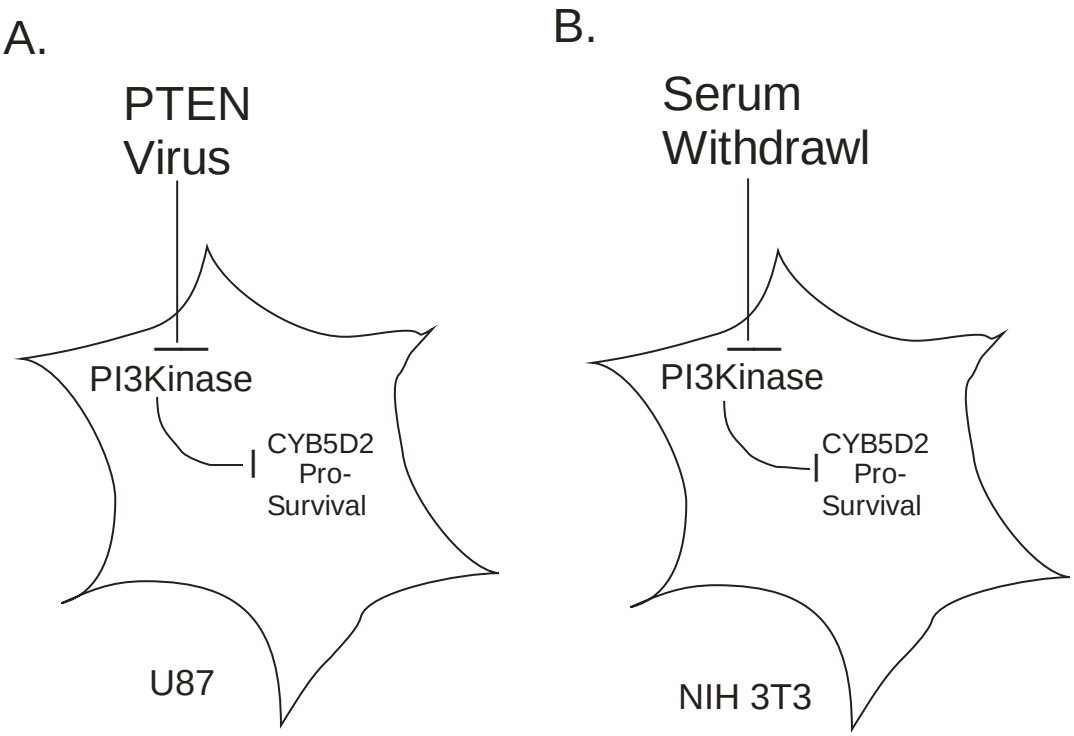

Figure 1.2 Schematic Model of Regulation for CYB5D2`s Pro-Survival Functions. A. A PTEN retrovirus serves to inactivate PI3Kinase in U87 cell, promoting cell death. CYB5D2 conferred survival from ectopic PTEN death. B. Serum withdrawl serves to inactivate PI3Kinase in NIH3T3 cells. CYB5D2 confers survival from serum starvation in NIH3T3 cells.

A polyclonal antibody to CYB5D2 was made to the COOH terminal of CYB5D2. Specificity of this antibody was confirmed with siRNA and shRNA knockdown methodologies. This antibody detected the presence of endogenous CYB5D2 in liver, kidney, breast, prostate and neural cancer cell lines. CYB5D2 protein was not detected in HEPG2 liver cells, but was detected in Huh7 liver cells.

In order to ascertain the role of the heme binding domain of CYB5D2, I generated a heme binding defective mutant. Examining the structure of the heme binding domain, three conserved tyrosines, Y73, Y79 and Y127 were individually mutated to alanine, along with a conserved aspartic acid D86 which was mutated to glycine. These CYB5D2 mutants were measured for heme binding. When these three conserved tyrosines were individually mutated to alanine, they still maintained the ability to bind to heme-agarose. The CYB5D2(D86G) mutant however, could not be precipitated by heme-agarose. When purified as a recombinant protein this CYB5D2(D86G) mutant could not be oxidized or reduced, like wild type recombinant CYB5D2 protein. Functionally, this CYB5D2(D86G) behaves in the opposite fashion to wild-type CYB5D2. CYB5D2 inhibited HeLa cell proliferation and growth in soft agar. Stable CYB5D2(D86G) HeLa cells and CYB5D2 shRNA HeLa cells demonstrate increased cell proliferation and growth in soft agar. CYB5D2 conferred survival from chemotherapeutic compounds (paclitaxel, cisplatin and doxorubicin) in HeLa cells. CYB5D2(D86G)-expressing HeLa cells and CYB5D2 shRNA HeLa cells have diminished survival responses from these chemotherapeutic drugs. Previously, the transmembrane domain of CYB5D2 was

responsible for the subsequent peri-nuclear localization of CYB5D2, and for its ability to confer survival from etoposide (Xie *et al*., 2011).

CYB5D2 inhibited 3xSREBP reporters in transient transfection assays in 293T cells. Moreover, when CYB5D2 and Insig1 were co-transfected into 293T cells, CYB5D2 co-immunoprecipitated with ectopic Insig. More significantly, CYB5D2 stabilized ectopic Insig1 levels, when both cDNAs were transfected into 293T cells and treated with cyclohexamide. CYB5D2 can inhibit the transcriptional activity of full length SREBP1c and SREBP2 in 3xSRE-Luciferase assays. CYB5D2 cannot inhibit the mature amino terminal form of SREBP1c and SREBP2 in 3xSRE Luciferase assays. The heme binding domain and the transmembrane domain of CYB5D2 were required for inhibition of 3xSRE-reporters, when transiently co-transfected into 293T cells. The CYB5D2(D86G) heme binding defective mutant could not inhibit 3xSRE-Luciferase reporters. This CYB5D2(D86G) mutant destabilized ectopic Insig1 with cyclohexamide treatments, even though it could still interact with ectopic Insig1. PGRMC1 can also stabilize ectopic Insig1, and can also inhibit a 3xSRE-reporter in transient transfection assays performed in 293T cells.

CYB5D2 can co-immunoprecipitate with cytchrome P450 reductase, (POR), when both CYB5D2 and POR were co-tansfected into 293T cells. When ectopic POR is co-transfected with ectopic CYB5D2, CYB5D2 is induced into a 56 kDa dimer form. In stable CYB5D2 Hela cells, ectopic CYB5D2 can immunoprecipitate with endogenous POR in serum free conditions. When CYB5D2(D86G) was stably expressed in HeLa cells, it was unable to co-immunoprecipitate with endogenous POR in 10% FBS or

serum-free culture conditions. HMG CoA reductase protein levels were higher in CYB5D2-expressing HeLa cells relative to control cells, and CYB5D2(D86G) cells. In stable CYB5D2 shRNA HeLa cells, CYP51A1 protein levels were significantly reduced. This would indicate that the function of endogenous CYB5D2 is to stabilize CYP51A1, similar to Dap1. Protein levels of endogenous Insig1 were also reduced in stable CYB5D2 shRNA HeLa cells. These CYB5D2 shRNA HeLa cells were more susceptible to increasing concentrations of mevalonate than shRNA HeLa cells. Lastly these CYB5D2 shRNA HeLa cells had a slight reduction in CYP3A4 activity compared to shRNA HeLa cells.

In stable CYB5D2-expressing Huh7 liver cells, ectopic CYB5D2 slightly increased cell proliferation (not significant statistically). Conversely, stable CYB5D2(D86G)-expressing Huh7 cells displayed decreased cell proliferation. Additionally, CYB5D2 shRNA Huh7 cells proliferated slower compared to shRNA control cells. This result is the opposite to that seen in HeLa cells for CYB5D2, CYB5D2(D86G) and CYB5D2 shRNA. In CYB5D2 shRNA Huh7 cells, reduced levels of Insig1 protein were observed. Ectopic CYB5D2 (in stable Huh7 cells) could co-immunoprecipitate with endogenous POR in serum reduced culture conditions. Ectopic CYB5D2(D86G) (in stable Huh7 cells) could not co-immunoprecipitate with endogenous POR. This result is the same as seen for CYB5D2 and endogenous POR in HeLa cells. Furthermore, CYB5D2 shRNA Huh7 cells could not form colonies in soft agar, unlike shRNA control Huh7 cells. Subcutaneous mouse xenograft tumours generated from CYB5D2 knockdown Huh7 cells displayed significantly reduced size compared to Huh7 shRNA control xenograft tumours.

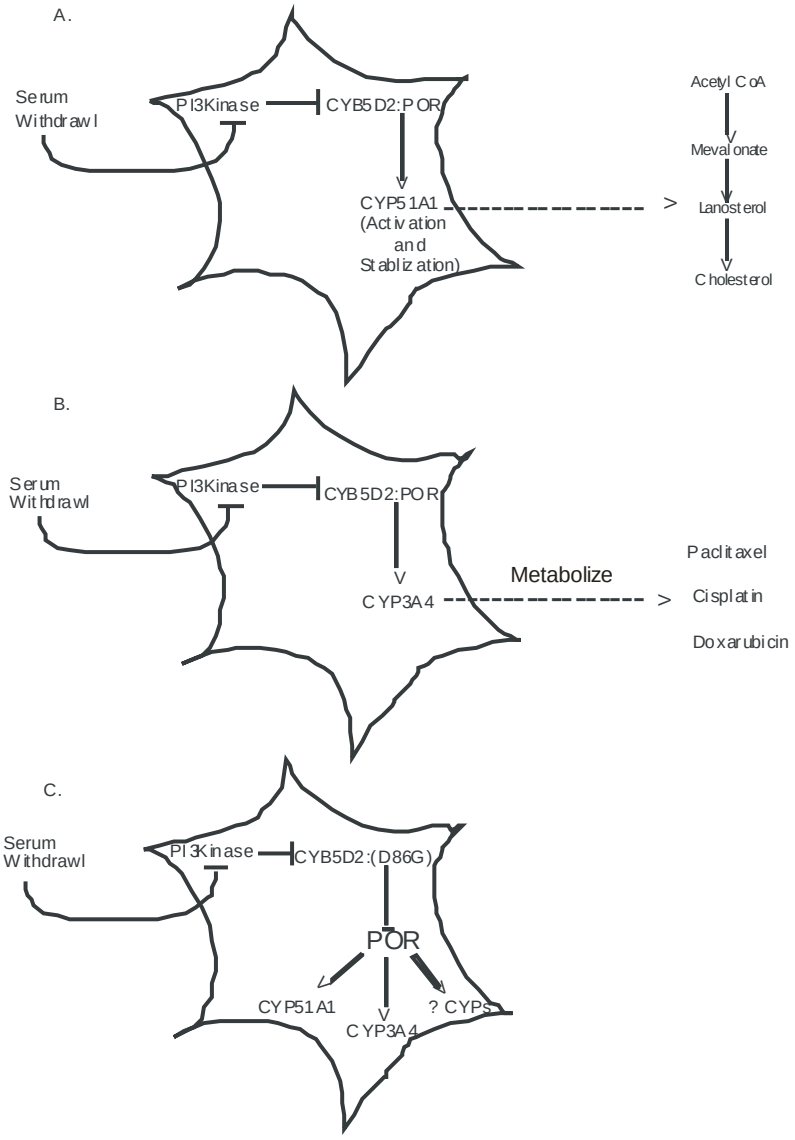

Figure 1.3 Schematic model of CYB5D2 function. A. Inactivation of PI3Kinase by serum withdrawl induces CYB5D2 into a complex with POR. CYB5D2 stabilizes CYP51A1, and activates it with POR. This results in the turnover of lanosterol levels. B. The CYB5D2/POR interaction activates the drug metabolizing cytochrome CYP3A4. C. A heme binding defective CYB5D2(D86G) cannot bind to POR, and acts like a dominant negative.

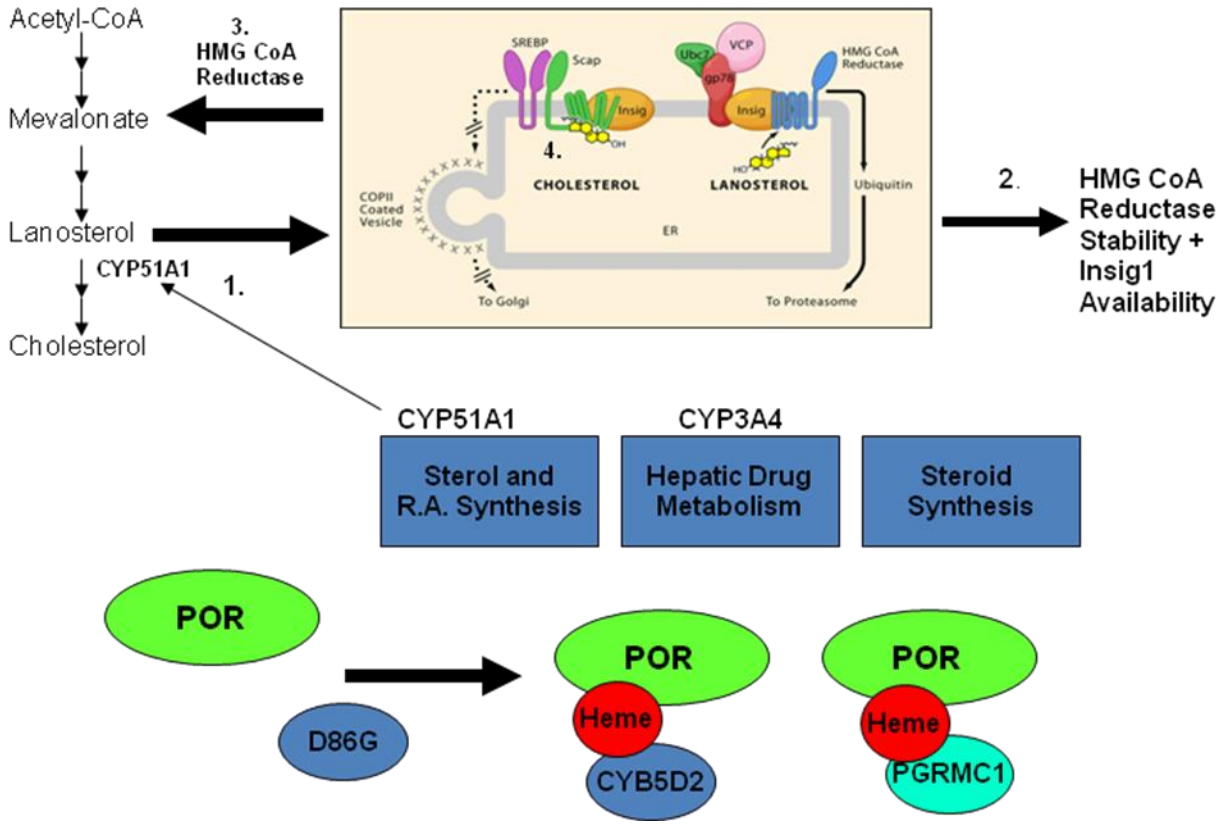

Figure 1.4 Overall schematic model of CYB5D2 . 1. CYB5D2 stabilizes CYP51A1(lanosterol demethylase) and activates it through cytochrome P450 reductase (POR). This facilitates the turnover of lanosterol, decreasing its levels, increasing the rate at this step in sterol synthesis. 2. Reduced lanosterol results in less HMG CoA reductase associated with Insig1, which means more Insig1 is available for SCAP. This also results in more stable HMG CoA reductase. 3. More stable HMG CoA reductase and CYP51A1 result in more cholesterol. 4. Increased cholesterol binds to SCAP which now binds to Insig1 resulting in the stabilization of Insig1 and inhibition of SREBP signalling. Inset from Goldstein, J., DeBose-Boyd, R., and Brown, M. Protein Sensors for Membrane Sterols. Cell. 2006. 124. 35-46.

Chapter 2. MATERIALS AND METHODS

2.1 Cloning of CYB5D2

The CYB5D2 cDNA was cloned from a cDNA library derived from normal prostate by Dr. Justin He in 2001 (McMaster University, Hamilton. Ontario. Canada). The cDNA was found in a screen of LNCAP prostate cancer cells, for its ability to confer survival from ectopic PTEN induced cell death. CYB5D2 was then cloned into pCDNA3.0 with an N-terminal Flag tag.

2.2 Plasmids and constructs

The cDNA for CYB5D2 was cloned with an N-terminal Flag tag into pcDNA3.0 (Invitrogen), and pLHCX. Empty vectors pcDNA3.0 and pLHCX were used as controls. PTEN was subcloned in the pcDNA3.0 plasmid, and pBabe retroviral plasmids. The CYB5D2(D86G), and all heme binding domain mutants (Y73A, Y79A, and Y127A) were mutated and re-inserted back into the pcDNA3.0 plasmid. The mutants with deletions in the transmembrane domain (ΔTM) and the entire cytochrome b5 heme binding domain (ΔCYB5, ~300bp deleted) were subcloned into the pcDNA3.0 plasmid, and described previously (Xie *et al*., 2010). The polymorphism mutants, R7G, R7P and Q167P were generated according to our site directed mutagenesis protocol (see site directed mutagenesis section) and cloned in the pcDNA3.0 plasmid.

For generation of GST fusion proteins, the PGEX4T.1 plasmid was used to generate GST fusion proteins.

SREBP1 plasmids were obtained from Dr. Joan Krepinsky (McMaster University, Hamilton. Ontario. Canada), who originally obtained the SREBP1c full length from Dr. Almut Shulze (London Research Institute, London. U.K.), and the SREBP1c mature nuclear form from Dr. Hitoshi Shimano (University of Tsukuba, Tsukuba. Japan). The PGRMC1 plasmid was obtained from Dr. Peter Espenshade (NIH Institute, Washington D.C. U.S.A.). The YFP-Cytochrome P450 plasmid was obtained from Dr. Byron Kemper (University of Illinois at Urbana-Champaign, Illinois, U.S.A.). The Insig1 plasmid (c-myc tagged) was obtained from Dr. Richard Austin (McMaster University, Hamilton. Ontario. Canada). The 3xSRE-GFP and the 3xSRE-Luciferase plasmid were also obtained from Dr. Richard Austin (McMaster University, Hamilton. Ontario. Canada). The full length SREBP2, and the nuclear N-terminal mature form were also obtained from Dr. Richard Austin (McMaster University, Hamilton. Ontario. Canada).

The 3xSRE-GFP and the 3xSRE-Luciferase constructs used in this thesis contain this SREBP responsive element from the LDL Receptor 5′-ATCACCCCAC-3` (Brown and Goldstein. 1997; Athanikar and Osborne 1997; Yokoyama *et al*., 1993).

2.3 Cesium Chloride/Ethidium Bromide (CsCl/EthBr) DNA preparation

All plasmids used in cell culture transfections were prepared according to our CsCl/EthBr protocol. Initially, an overnight starter culture of 3 ml Luria Broth (LB, 10 g tryptone, 5 g yeast extract, 10 g NaCl/1 Litre ddH_20) (usually with Ampicillin, 100 μg/ml) was inoculated with a single clone containing our plasmid of interest, and shaken overnight at 37˚C at 250 rpm. The next day, this starter culture was used to inoculate a

500 ml culture of LB media (ampicillin 100 μg/ml), shaking for several hours at 250 rpm, at 37˚C. These large scale inoculated cultures were then centrifuged at $5x10^3$ g for 15 minutes at 4˚C. Supernatant was decanted and pellets were then resuspended in 10 ml GTE solution (50 mM glucose, 25 mM Tris pH=8.0, 10 ml EDTA). To this solution 20 ml of 0.2N NaOH/1% SDS was added, inverted several times to mix, and incubated on ice for 5-10 minutes. Next 15 ml of a potasium acetate solution (3M K+, 5M Acetate pH=4.8) was added, and solutions were mixed by inverting several times, and then placed on ice for 20 minutes.

The supernatant was then centrifuged at 4˚C at $12x10^3$ g for 15 minutes. The supernatant was removed to new tubes and 0.67 X volume of isopropanol was added, mixed by inversion, then centrifuged at $2x10^4$ g for 15 minutes at 4˚C. The following pellet was then washed with 5 ml of 70% ethanol and centrifuged down at $6x10^4$ g for 5 minutes at 4˚C. The final pellet was air dried at room temperature and resuspended in 8.3 ml CsCl/TE (8.8 g of CsCl was added to 8 ml TE). This DNA CsCl/EthBr solution was added to a Beckman Quick-Seal tube with a pasteur pipette. Next, 800 μl of 1 mg/ml EthBr solution was added to these tube and then tubes were topped up with mineral oil to eliminate any bubbles. Tubes were then balanced by weight and then sealed with a heater from the Beckman Quick-Seal kit. Sealed tubes with the DNA and CsCl/EthBr in TE were then centrifuged (with red metal caps) in a Beckman Ultracentrifuge, in a Ti70 rotor at $6x10^4$ rpm for 24 hours.

Twenty four hours later, the DNA in the lower of two bands was removed with a 20 mm gauge needle. Ethidium Bromide was extracted with an equal volume of saturated

Butanol until all red color was removed. DNA was precipitated with 100% ethanol, and a final wash with 70% ethanol. DNA pellets were air dried in a sterile tissue culture laminar flow hood and resuspended in 1ml of sterile ddH20. DNA was quantified in a spectrophotometer.

2.4 Generation of a carboxyl terminal CYB5D2 polyclonal antibody

Two antibodies were made to the carboxyl terminal portion of CYB5D2. The carboxyl terminus of CYB5D2 (amino acids 171 to 264) was cloned in-frame into the GST fusion plasmid pGEX4T.1, that had been digested with the restriction enzymes *BamHI* and *XhoI*. This region does not include the heme binding domain.

BL21 *Rossetta* bacteria was transformed with pGET4T.1 containing the carboxyl terminus of CYB5D2 (aa 171-264) plasmid and cultured to an optical density of 1.0-1.2 at absorbance 595 nm. Isopropyl β-D-1-thiogalactopyranoside (IPTG) was added at a final concentration of 0.2 mM to induce expression of recombinant COOH-CYB5D2. IPTG induced cultures were shaken overnight at room temperature.

The following day, the culture was centrifuged at $4x10^4$ g for 15 minutes at 4˚C, and the pellet resuspended in 10 ml of MT-PBS-1 mM DTT. This resuspended pellet was sonicated at medium speed (5), "remote" setting, on ice, 20 times for 10 seconds, with a 20 second rest interval between each sonication. Triton X-100 (10%) was then added to a final concentration of 1%, and the solution centrifuged at $10x10^4$ g, for 20 minutes at 4˚C. The supernantant was then supplemented with 1 ml of reduced glutathione agarose, and

incubated on a nutator for 1 hour at 4˚C. This slurry was then washed with cold MT-PBS and then treated with 1 ml of 5 mM glutathione in several elutions, waiting 10 minutes for the second incubation of the second eluted fraction. Successful production of recombinant COOH-CYB5D2 was quantified with Bradford assays, and verified with SDS-PAGE gel and coomasie blue staining, and western blots.

To prepare glutathione agarose, 70 mg of dried powder was added to 7-10 mls of ddH_20, and incubated on a nutator at 4˚C overnight. This slurry was then washed with 10 mls of MTPBS –DTT (with DTT at a final concentration of 1 mM). This slurry was then resuspended in 1ml of MTPBS-DTT, and stored at 4˚C.

2.5 Injection of rabbits and purification of rabbit immunoglobulin (IgG) from serum.

An equal volume of complete Freund's adjuvant was mixed thoroughly with 300-400 μg of recombinant GST-COOH-CYB5D2. This was used by the Central Animal Facility at McMaster university to inject two large New Zealand White rabbits (8 to 10 weeks old), at several subcutaneous points. Rabbits were injected for over one year, with injections occurring every two months. Serum was extracted roughly one month after each injection, and immunoglobulins purified and tested for specificity. Western blots and immunoprecipitations were carried out to determine antibody specificity. The final bleeds were carried out after one year, and serum immunoglobulins purified with ammonium sulfate "salting out" precipitation and affinity purification. Affinity purification was performed using recombinant COOH-CYB5D2 that had the

transmembrane domain deleted. Deletion of the transmembrane domain resulted in significantly higher induction and expression of the recombinant protein in *E.-coli*. This COOH CYB5D2 was then coupled to CnBr Sepharose (CNBr)-activated-sepharose 4B (Sigma) to a final concentration of 9 mg recombinant protein/ml CNBr-sepharose 4B (CNBR) beads. Approximately, 15 mls of rabbit serum was initially eluted through a GST-coupled CNBR activated sepharose 4B column to exclude IgG against GST. The elution was then applied to a CYB5D2 coupled sepharose 4B column to affinity purify the anti-CYB5D2 antibody. The antibody specificity was confirmed, as signals could be specifically competed by addition of GST-CYB5D2 (1 mg/mL) but not GST (1 mg/mL) during western blotting analysis (Xie *et al.*, 2010).

2.6 Calcium Chloride Transfection Method

All DNA (CsCl prepared) was added to 450 μl sterile ddH_20. To this DNA/ddH_20, 50 μl of 2.5 M calcium chloride solution was added and mixed. This cocktail was then allowed to incubate at room temperature for 5 minutes. Then an equal volume of 2xHBSP (500 μl) was added while gently vortexing in a sterile tissue culture incubator This DNA cocktail was incubated at room temperature for 15-20 minutes. This DNA cocktail was then added to our 293T plates drop-wise. This transfection cocktail was incubated for 12 hours, and then the media replaced, and cultured for 48 hours.

2.7 Generating Stable cell lines of CYB5D2

All retroviral packaging was performed in 293T cells. Briefly, a 10 cm plate of sub-confluent (~70%) 293T cells were transfected via calcium phosphate transfection method.

All calcium phosphate transfections for retrovirus and shRNA lentivirus were done in 293T cells.

To package retrovirus, 10 μg of each retroviral packaging plasmids (VSV and GP), were co-transfected with 10 μg of pLHCX containing CYB5D2 cDNA. Twelve hours post-transfection, media was changed and replaced with fresh media. Viral conditioned media was then collected forty-eight hours later and centrifuged at 48 x10^4 g for 2 hours. After centrifugation, supernatant was immediately decanted into bleach, and the pellet resuspended with 1ml of media, and subsequently added to 1 x10 cm plate containing the cells of interest (HeLa, Huh7, NIH3T3 and U87 cells). These cells were incubated with the concentrated viral media for 3-4 hours with gentle agitation every 20 minutes. Afterwards, 9 ml of media was added to the plate and left overnight to incubate. The following day media was replaced with media containing antibiotics for successful selection (hygromycin at a concentration of 0.5 mg/ml for pLHCX constructs). Media containing corresponding hygromycin (0.5 mg/ml) was replaced every 2 or 3 days for two weeks to select for successful stable viral incorporation. All stable cell lines (HeLa, Huh7, NIH3T3 and U87) were confirmed by Western blot analysis.

2.8 Generating stable shRNA-mediated CYB5D2 knockdown cells

A pooled population of CYB5D2 shRNA lentiviral plasmids was purchased from Santa Cruz. These were packaged along with lentiviral packaging plasmids VSV, GP and Rev, by transfecting 10 μg of each plasmid into 1x10 cm plate of 293T cells via

calcium phosphate transfection. The same methodology for packaging retrovirus was then used to package the shRNA CYB5D2 knockdown virus to infect HeLa and Huh7 cells (see retrovirus production of stable cell lines). Puromycin (1μg/ml) was subsequently added to select for successful infection of CYB5D2 shRNA virus. Successful stable CYB5D2 shRNA was confirmed by western blot analysis using the CYB5D2 polyclonal antibody.

2.9 Construction of CYB5D2 Mutants through site-directed mutagenesis

All site directed mutants were made according to a slightly modified version of the Stratagene Quick Change site directed mutagenesis kit. Briefly primers were designed by the Primer X program, using overlapping primers with the designated mutation in both primers. Primers were then ordered from the McMaster Mobix facility. To start, 0.5 μl of a forward primer (2.5 *p*moles/μl), 0.5ul of a reverse primer (2.5 *p*moles/μl), 1.0 μl of dNTP mix (10 mM each), 1.25 μl 10xPfu buffer, 1μl (template DNA, 20 ng), 0.5 μl of PfuUltra HotStart (Invitrogen), and 8.25 μl sterile ddH20. This reaction was gently mixed and PCR was performed. Initially, a 5 minute denaturing step at 95˚C was performed, followed by 18 cycles (45 seconds denaturing at 95˚C, 45 seconds annealing at 60˚C, followed by 8 minutes extension at 68˚C). One final extension step for 10 minutes at 68˚C was performed. Conditions for each primer are listed in Table 2.

Amplified DNA was then extracted by phenol/chloroform and precipitated first with 100% ethanol, then 70% ethanol, lyophalyzed, then resuspended with 10 μl of sterile ddH20. The amplified PCR product was then digested with the *DpnI* restriction

endonuclease for 3-5 hours at 37˚C. Digested DNA was precipitated by phenol/chloroform, then transformed into XL-10 Gold competent cells, and plated at 37˚C overnight. The primers for each specific mutant are listed below, in Table 1.

Table 1. Site-directed mutants for CYB5D2 and their primer sequences

Q167K	Primer 1 Primer 2	AAAGAGAAGCAGACATTCCCGC CAGCTGTAGTTTGTTGGCCTCC
R7P	Primer 1 Primer 2	CCCAAGCTTATGTTGAGGTGCGGAGGCCCTGGGCTTTTGTTGGG GCTCTAGATTAGAGTGGAAGGGAGCATGTGATGG
R7G	Primer 1 Primer 2	CCCAAGCTTATGTTGAGGTGCGGAGGCGGTGGGCTTTTGTTGGG GCTCTAGATTAGAGTGGAAGGGAGCATGTGATGG
Y73A	Primer 1 Primer 2	GTCCTCCGGCCGGAGGCACTTTGAGCCTGGGTCCCACTATAG CTATAGTGGGACCCAGGCTCAAAGTGCCTCCGGCCGGAGGAC
Y79A	Primer 1 Primer 2	CTGGGTCCCACTTTAGCGGCTTCGC GACCCAGGGTGAAATCGCCGAAGCG
D86G	Primer 1 Primer 2	CTTCGCAGGCCGAGGAGCATCCAGAGCTTTC GAAAGCTCTCTGGATGCTCCTCGGCCTGCGAAG
Y127A	Primer 1 Primer 2	CATTCTATGAGAAGAATTTTGTGTGTGTTGGGAGGG CCCTCCCAACACACACAAAATTCTTCTCATAGAATG
GST/CYB5D2-GST/D86G	Primer 1 Primer 2	CGGGATCCGGTCCCCGCGCT GGAATTCTTAGAGTGGAAAGGAGCAT

Table 2. Site-directed mutants for CYB5D2 and their PCR conditions

Q167K	94^{O}C 1 minute, 59^{0}C 45 seconds, 72^{0}C 14 minutes, 35 cycles
R7P	94^{O}C 45 seconds, 64^{0}C 45 seconds, 72^{0}C 2 minutes, 35 cycles
R7G	94^{O}C 45 seconds, 64^{0}C 45 seconds, 72^{0}C 2 minutes, 35 cycles
Y73A	95^{O}C 50 seconds, 50^{0}C 50 seconds, 68^{0}C 7 minutes, 18 cycles
Y79A	95^{O}C 50 seconds, 60^{0}C 50 seconds, 68^{0}C 7 minutes, 18 cycles
D86G	95^{O}C 50 seconds, 60^{0}C 50 seconds, 68^{0}C 7 minutes, 18 cycles
Y127A	95^{O}C 50 seconds, 60^{0}C 50 seconds, 68^{0}C 7 minutes, 18 cycles
GST/CYB5D2-GST/D86G	94^{O}C 45 seconds, 56^{0}C 45 seconds, 72^{0}C 2 minutes, 35 cycles

2.10 Heme binding assays demonstrating D86G is heme binding defective

Heme agarose chromatography was performed on lysates prepared from 293T cells that were transfected with CYB5D2, and CYB5D2 heme binding domain mutants, Y73A, Y79A, D86G and Y127A. 10 μg of each plasmid were individually transfected into 293T cells via Calcium Phosphate. DMEM complete media was changed after 12 hours each transfection. After 48 hours, cells were scraped in cold 1xPBS, centrifuged at $5x10^4$ g for 5 minutes at 4˚C, then lysed in 1.0% Triton, 0.5 mM EDTA, 150 mM NaCl, and incubated for 20 minutes on ice. After lysis, cells were centrifuged for 5 minutes at $13x10^3$ g at 4˚C. After centrifugation, supernantant was transferred to a fresh tube and then 100 μl of this supernatant was added to 900 μl of co-immunoprecipitation buffer, and 20 μl of Hemin Agarose (Sigma) (washed three times with cold co-immunoprecipitation buffer). Subsequent lysates with heme-agarose were then placed on a shaker overnight at 4˚C. The following day, samples were washed with co-immunoprecipitation buffer, six times, and the final slurry resuspended in 20 μl 2xLamelli buffer. Samples were then boiled for 5 minutes and centrifuged down at $12x10^3$ g for 5 minutes at 4˚C. These heme-agarose precipitated samples were then run on a 12% SDS-PAGE gels and subsequent western blots performed, using 100 μg of the corresponding whole cell lysate for input. An M2 Flag antibody (Sigma) was used to probe these western blots.

2.11 In Gel Peroxidase assay

In order to produce higher amounts of recombinant GST-CYB5D2 and GST-D86G in BL21 *E. Coli*, the hydrophobic transmembrane domain, nucleotides 1-87, were deleted. Purified recombinant GST-CYB5D2 and GST-CYB5D2 (D86G) (200 μg) were resuspended in PBS. Solutions of protein were measured for absorbance by scanning from the wavelength 350 – 490 nm with an increment 1 nm using a spectrophotometer (Ultrospec2100).

Heme-bound GST-CYB5D2 was also assayed by peroxidase reaction staining following published conditions (Thomas *et al*., 1976; Kimura *et al*., 2008). Briefly, 10 μg of recombinant GST-CYB5D2 and GST-CYB5D2 (D86G) were individually incubated with heme (Sigma) (50 μM) at room temperature for 30 minutes, followed by separation by SDS-PAGE without addition of dithiothreitol (DTT). This SDS-PAGE gel was rinsed with TBST for 5 min, followed by developing signal using an ECL Western Blotting Kit (Amersham).

2.12 Oxidation and reduction of CYB5D2

In order to measure the oxidation and reduction of CYB5D2, the GST-fusion was removed from the purified recombinant CYB5D2 with thrombin. One mg of purified recombinant GST-CYB5D2 and GST-D86G was cleaved with thrombin overnight at room temperature. Cleaved recombinant CYB5D2 and D86G was separated from GST

using GST-Sepharose chromatography. Eluted purified CYB5D2 and D86G was then measured using a Bradford assay.

Absorbance differences between these two thrombin cleaved CYB5D2 and D86G were measured in oxidized and reduced states. Measurement of assays occurred in increment of 1nm using a spectrophotometer (Ultrospec2100). In a reaction containing 200 mM NaOH, 40% pyridine, and 0.6 mM $K_3Fe(CN)_6$, heme a and b will be release from a heme binding protein and it will become oxidised. While heme c will not be released from cytochrome c, the existence of the protein does not interfere with heme c oxidization (Berry and Trumpower 1987). Thrombin-cleaved recombinant CYB5D2 and CYB5D2(D86G) proteins were reduced by sodium dithionite treatment and scanned for their absorbance peaks within the indicated wavelength range.

2.13 Reporter Assays (Luciferase Assays)

All reporter assays were done in 293T cells that were seeded into 24 well Plates, and performed in quadruplicate. Cells were seeded at $5x10^3$cells per well, and transfected the next day with Polyethylenimine (PEI Sigma). Each well was transfected with 5 μg of 3xSRE-Luciferase and 2.5 μg of β- galactosidase (β- gal) plasmid, along with cDNAs of interest (varying amounts indicated in figure legends). All plasmids were purified by CsCl/EthBr method, and all reactions transfected with the same amount of DNA, topped up with pCDNA3.0 control plasmid.

PEI (Sigma) transfections were used for luciferase assays in 24 well plates in 500 μl of antibiotic free media. A DNA mixture (0.5μg of 3xSRE-Luciferase Reporter, 0.25 μg of β-gal and cDNA of interest) was mixed with 62.5 μl DMEM media, and vortexed gently.

Next 1 μl of PEI (2 mg/ml) was added to this mix, gently vortexed and incubated at room temperature for 5 minutes. This PEI/DNA cocktail was then added to the cells drop-wise and allowed to incubate for 4- 6 hours, when the transfection media was replaced with fresh media. Beta-gal and Luciferase assays were performed after 48 hours.

Luciferase assays were performed using the PROMEGA Luciferase Assay Substrate kit. Briefly, cells that were transfected in 24 well plates by PEI, were washed twice in 1xPBS, then 100 μl of 1x Passive Lysis Buffer (from the 5x Reagent, PROMEGA) was added, and incubated for 30 minutes with gentle shaking at room temperature. Samples were resuspended, and 25 μl used for a β-gal assay. The remainder (75 μl) of the resuspended sample was added to 25 μl of Luciferase reagent and samples read immediately in a 96 well white Luciferase plate (COSTAR), on a LUMIstar BMG LABTECH luminometer. Data was analysed with the corresponding BMG Labtechnologies, LUMIstar control program. All luciferase values were then divided by their corresponding β-galactosidase (β-gal) assay values, to obtain a normalized value.

Beta-galactosidase assays were performed by lysing each well of the 24 well plate with 100 μl 1xPassive Lysis Buffer (as mentioned above), then taking 25 μl of each sample for the beta-galactosidase assay. To each sample, 3 μl of 100xMg Buffer, 66 μl of ONPG (4mg/ml in N_2HPO4) made fresh, 211 μl of Sodium Phosphate Buffer (0.1M $NaHPO_4$ and 0.1M NaH_2PO_3) was added, pippetted up and down, and incubated at 37˚C, in clear 96 well plate, until yellow appeared in each sample. A blank of the reagent mix was used as a background control. Samples were read for 5, 10, 15 and 20 minutes, at an

OD of 420 nm on a uQuant BIOTEK Instruments Inc., plate reader. Only samples giving readings over 0.2 nm and under 0.8 nm absorbances were used.

2.14 Lysates for Western blot analyses and co-immunoprecipitations

Cell lysates for western blots were made as follows. Cells cultured in a 10 cm plate were washed twice with cold PBS buffer. Excess PBS was aspirated, and 1 ml of cold PBS was added to the plate. Cells were scraped with a rubber policeman, and centrifuged down at $6x10^3$ rpm for 5 minutes at 4˚C. The cell pellet was then resuspended in 500-1000 μl of cell lysis buffer. Cell lysis buffer consisted of 50 mM Tris pH 7.4-7.5, 150 mM NaCl, 5 mM EDTA, 1% Triton X-100, 10 μM sodium fluoride, 10 μM sodium orthovanadate, 1 mM PMSF, 2 μg/ml leupeptin, and 10 μg/ml aprotinin. Cells were resuspended in this lysis buffer and incubated on ice for 10 minutes. Cells were then centrifuged at $12x10^3$ g for 10 minutes. Bradford assays were then performed on the cell lysate supernatant. Cell lysates were then resuspended in Laemmli buffer (final concentration of 1% SDS, 10% glycerol, 5% β-mercaptoethanol, 0.002% bromophenol blue and 75 mM Tris HCL), boiled for 5 minutes, then centrifuged at $12x10^3$ g for 5 minutes, and stored at -80˚C.

Immunoprecipitations

Co-immunoprecipitation experiments were performed on cells that had been freshly lysed with our lysis buffer (see above). Cells cultured in 10 cm plates were washed and scraped in PBS. Cell were centrifuged at $6x10^3$ rpm for 5 minutes at 4˚C and then lysed in 500-1000 μl lysis buffer. After cells were lysed, and then centrifuged at $12x10^3$ gfor 5 minutes at 4˚C, an equal volume of 100 μl of lysate was added to 900 μl of co-

immunoprecipitation buffer (0.1% Triton X-100, 150 mM sodium chloride) solution. Protein A agarose was washed 2-3 times, and 20 μl of this slurry was added to these lysates in co-immunoprecipitation buffer. Roughly 1 μg of antibody of interest was also added, and the mixture incubated on a shaker for several hours at 4^{o}C. All immunoprecipitations were then washed with co-immunoprecipitation buffer at least 6-8 times, and the resulting slurry treated with an equal bed volume (20 μl to 25 μl) of 2xLaemmli buffer and boiled for five minutes. Boiled immunoprecipitations were then centrifuged down and stored at -80˚C. A list of all commercial antibodies used, their dilutions, species and company of production are listed in table 3 below.

Table 3. Antibodies used for Western blot analyses

ANTIBODY	COMPANY	SPECIES	DILUTION
HA 12CA5	SANTA CRUZ	Mouse monoclonal	1:1000
HA Y-11	SANTA CRUZ	rabbit polyclonal	1:200
PTEN (A2B1)	SANTA CRUZ	Mouse	1:1000
PTEN(138G6)	Cell signalling	Rabbit	1:1000
Insig1 N-19	SANTA CRUZ	goat polyclonal	1:200
HMG CoReductase H-3000	SANTA CRUZ	rabbit polyclonal	1:200
Cytochrome P450 Reductase (CYPOR) (F-2)	SANTA CRUZ	Mouse	1:1000
CYP51A1 13-431	Proteintech Group, Inc.	Rabbit polyclonal	1:1000
M2 Flag F3165	Sigma	Monoclonal	1:1000
c-myc (9E10), sc-40	SANTA CRUZ	Mouse monoclonal	1:1000
AKT C-20	SANTA CRUZ	Goat	1:1000
Phosphorylated serine 473 AKT 587F11	Cell signalling	Mouse monoclonal	1:1000
CyclinD1 H-295	SANTA CRUZ	rabbit polyclonal	1:200
CyclinE1 C-19	SANTA CRUZ	rabbit polyclonal	1:200
P27 (F-8)	SANTA CRUZ	Mouse monoclonal	1:200
P21 (C-19)	SANTA CRUZ	rabbit polyclonal	1:200
IKappaBα 9242	Cell Signaling	rabbit polyclonal	1:1000
GFP (FL) Sc-8334	SANTA CRUZ	Rabbit Polyclonal	1:1000
Phosphorylated ERK 1/2 (Thr202/Tyr 204)	Cell Signaling	Rabbit Polyclonal	1:1000
GRP78 (N-20)	SANTA CRUZ	Goat	1:200
SREBP2 2A4 ID2 hybridoma. . Cultures were grown in flasks and media and conditioned media was collected and IgG purified with Protein A agarose chromatography.	SANTA CRUZ	Mouse monoclonal	1:200
β-Actin C-11	SANTA CRUZ	Goat polyclonal	1:1000
SREBP1 K10	SANTA CRUZ	Rabbit	1:1000

2.15 RNA Extractions

RNA extractions were performed according to the manufacturer's protocol using Trizol reagent (Sigma). Briefly, a 10 cm plate containing cells of interest was washed 2x with PBS. Cells were then scraped with a rubber policeman in cold PBS, gently resuspended in 1ml PBS, and then centrifuged down at $2x10^3$ rpm for 5 minutes. Cell pellets were then lysed with 1-2 ml of Trizol Reagent (depending on cell confluency), pipetting up and down several times and then incubated at room temperature for 5 minutes. To separate phases, 0.2 ml of chloroform was added, and samples vigorously shaken by hand for 15 seconds, then incubated at room temperature for 2 to 3 minutes. Samples were centrifuged at $12x10^4$ g for 15 minutes at 4˚C. RNA from the top aqueous phase was removed and transferred to a fresh tube, where isopropyl alcohol (0.5 ml for every 1 ml of Trizol reagent) was added. Samples were gently mixed then centrifuged down at $12x10^3$ rpm for 10 minutes at 4˚C. All supernatant was removed and the RNA pellet was washed with 1 ml of 75% ethanol (for every 1 ml of Trizol reagent used). The RNA pellet was then centrifuged at $7.5x10^3$ g for 5 minutes at 4˚C. The RNA pellet was dried in a vacuum-dry spinner for 5 minutes and the final RNA pellet was resuspended in 20-30 μl of DEPC ddH20. All purified RNA was quantitated using a spectrophotometer 20 in a quartz cuvette.

Reverse transcription of RNA was performed in a 2 step procedure. Initially, 2 μg (2 μl) of Trizol purified RNA added in a mixture with 1 μg(1 μl) of Oligo dT (Invitrogen), 0.5 μl RNAase out (Invitrogen) (40U/μl) and 8.5 μl of DEPC ddH20. This cocktail was heated at 65˚C for 5minutes and then placed on ice for 2 minutes. To this reaction, 4 μl

of 5x First Strand Buffer (Invitrogen) , 2 μl of DTT (Invitrogen)(0.1M), 1μl of dNTP (Invitrogen)(10 mM), 0.5 μl of RNAase out, 0.5 μl of Superscript II Reverse Transcriptase (Invitrogen) was added. This cocktail was gently mixed and incubated at 42˚C for 50 minutes. In order to inactivate the reverse transcriptase enzyme, the reaction was incubated at 70˚C for 10 minutes.

2.16 Quantitative PCR (qPCR)

Quantitative PCR was performed on an Applied Biosystems 7500 Fast Real Time PCR system machine, using the 7500 Software v2.0.4. Primers for CYB5D2 were designed by the Genius program. Primer sequences are listed in table 4.

Table 4. Primers for qPCR.

PRIMER NAME	SEQUENCE
Human β-Actin Forward Human β-Actin Reverse	5` -ACC GAG CGC GGC TAC AG- 3` 5` -CTT AAT GTC ACG CAC GAT TTC C-3`
Human CYB5D2 Forward Human CYB5D2 Reverse	5` -GGT GGT CCA GGT CCC CAC GA-3` 5` -GGC CAG ATG CCG GAC AAC CC-3`
Human GAPDH Forward Human GAPDH Reverse	5-CCA CTC CTC CAC CTT TGA- 3` 5` -ACC CTG TTG CTG TAG CCA- 3`

Each Q-PCR reaction was performed in triplicate as follows. 9.5 μl of Nuclease Free water, 12.5 μl of SYBR Green, 0.5 μl of Forward primer (10 μM), 0.5 μl of Reverse primer (10 μM) and 2.0 μl of cDNA (one fourth diluted from RT-PCR reaction), for a total of 25 μl. All reactions were done as master mixes, thoroughly mixed and individual reactions loaded into 96 well ABI Prism plates (96 well Opitcal Reaction Plate). Beta-Actin and GAPDH were used as internal controls. A total of 35 cycles was selected, and

Rox selected as the detector. Samples were performed in triplicate, and the averages for each CT value calculated, along with the standard deviation of each value. The CT value was defined by the number of cycles each sample took for the end of the exponential phase of the reaction to reach threshold. The differences in two samples of the PCR reaction was used to calculate the delta delta CT, which represents the fold change in gene expression. Briefly, this calculation goes as $2^{-[delta][delta]Ct}$ method, where [delta][delta]Ct = [delta]Ct, sample - [delta]Ct reference. Final fold change values for each sample were normalized relative to a value of 1 for control.

2.17 Soft agar assays

Soft agar assays were performed in 6 cm plates, seeding $50x10^4$ cells per plate. Initially a bottom layer (4 mls) was poured, comprising 2 mls of 1.5% agar in ddH20, and 2 mls of 2xDMEM. This was allowed to solidify in a sterile tissue culture hood for 30-60 minutes. Next $5x10^4$ cells were added to pre-warmed top agar (2 mls 0.75% Agar and 2 mls 2xDMEM), and seeded on top of the solidified bottom layer. Assays were then cultured for several weeks in a sterile CO_2 incubator at 37˚C incubator, and 1ml DMEM media (10% FBS, 1% P/S) was added every two or three days to maintain the semi-solid media conditions.

After 5-6 weeks, hundreds of black and white contrast images were taken, in phase contrast setting 2x, at 5x and 10x magnification, for quantitation using the Image Pro Plus program. Images were then counted and measured using this program.

2.18 Tumour xenograft formation

Stable CYB5D2 shRNA and control shRNA Huh7cells (10^5 cells per cell line) were resuspended in DMEM/Matrigel mixture (1:1 volume), followed by implantation of 0.1 ml of this mixture subcutaneously (s.c.) into the flanks of 10-week-old male NOD/SCID mice (The Jackson Laboratory). A total of five mice were injected per cell line. Mice were inspected for tumour appearance, by observation and palpation, and tumor growth was measured weekly using a caliper. Tumour volume was determined using the standard formula: $L \times W2 \times 0.52$, where L and W are the longest and shortest diameters, respectively. All animal work was carried out according to experimental protocols approved by the McMaster University Animal Research Ethics Board, Animal Utilization Protocol 13-08-31.

2.19 Cell viability assay

Using a Roche Cell Proliferation Kit 1 (MTT) assay, cells were seeded in clear 96 well dishes at $5x10^4$ cells per well, with 100 μl volume of media. 24 hours after seeding, 10 μl of MTT labeling reagent (final concentration was 0.5 mg/ml) was added to each well, and samples were incubated at 37˚C for 4 hours. Next, 100 μl of solubilization solution was added and samples were incubated overnight in a chamber. Absorbance readings were carried out on SPECTRAmax Plus 384 spectrophotometer (Molecular Devices), and OD 575 values were subtracted from background (OD 690) values. Treated samples were then normalized against non-treated samples. All values were done in triplicate.

2.20 Growth curves (Evaluation of cell proliferation)

All cells (U87, NIH3T3, Huh7 and Hela) were culutured in DMEM (10%FBS, 1% P/S or 2% FBS, 1% P/S) on 12 well plates, in a sterile CO2 incubator at 37˚C. Cells were trypsonized then counted on a heamocytometer. All cells were counted using Typan Blue, to counter stain and exclude for dead cells (blue). Media was replaced every second day through the growth curve. Cells were counted for several days, or until cells started becoming confluent, with noticeable cell to cell contact. Each sample was counted 8x (four plates, 2x each), and averages plotted with standard deviation.

2.21 P450 CYP3A4 Activity assays

The P450-Glo CYP3A4 assay was obtained from PROMEGA. This assay was done in 12 well plates, where $5x10^4$ HeLa cells per well were seeded. HeLa cells were transfected with PEI (see above protocol) and all assays topped up with control pCDNA3.0. Media was changed 4 hours later, and 24 hours later P450 assays performed. Briefly, 50 μM Luciferin-IPA was added to each well, and all samples done in triplicate. Three hours later 100 μl of media was added to 100 μl Luciferase Detection Reagent, and 20 minutes later luciferase activity was measured on a LUMIstar luminometer (BMG LABTECH).

2.22 Mevalonate Treatment

Mevalonate was resuspended in DMSO, and added at the designated concentrations to DMEM supplemented with 0.5% Lipoprotein media. All cells, HeLa shRNA CYB5D2

and HeLa shRNA control cells were cultured in these treatments for 24 hours, and subsequently MTT cell viability assays were performed.

2.23 Immunofluorescence

Cells were seeded in chamber slides and fixed with 4% paraformaldehyde for 20 minutes. Cells were then washed with TBS 0.1% BSA. Cells were permeabolized with TBST (Triton 0.3%, 0.1% BSA). Primary antibody was added at a dilution of 1:200 to 1:300 overnight at 4˚C. The following day, primary antibody was removed and cells were washed with TBS. Secondary antibody was added for one hour at room temperature, then washed off. Cells were stained with Vectamount containing Dapi to stain for the nucleus.

2.24 Statistics

All values for cell proliferation were represented as mean, +/- standard error. When growth of a cell population was analyzed for differences from a control population, values were analyzed using the two sample independent student`s T test assuming unequal variance, n=4. Statistical significance was defined as $p > 0.05$ (*). When statistical significance was $p > 0.01$, double asterisks are indicated (**).

All luciferase assays were performed in triplicate, and pooled values were averaged, using standard deviation to measure the variance, n=3. Similarly statistical significance was analyzed using the two sample independent student`s T test. When statistical significance was defined as $p > 0.05$, a single asterisk is indicated (*), when significance was $p > 0.01$ double asterisks are indicated (**).

Chapter 3. CYB5D2 attenuates PTEN function, and confers survival from serum starvation

3.1 CYB5D2 confers survival from PTEN in U87 cells

As mentioned previously, CYB5D2 was identified in a screen for genes that conferred survival from ectopically expressed PTEN, in prostate LNCAP cells (PTEN deficient) by Dr. Justin He in 2001, (McMaster University, Hamilton. Ontario. Canada). The neural cancer cell line U87 is also a PTEN deficient cell line. Ectopic PTEN induces apoptosis in U87 cells (Beckner *et al.*, 2005). When CYB5D2 U87 cells were generated, they were able to confer survival from ectopic PTEN death (Figure 3.1). A control U87 cell line expressing the pLHCX virus was effectively killed by this PTEN retrovirus.

Interestingly, these CYB5D2 U87 cells could also sustain ectopic PTEN expression (Figure 3.1B). In these CYB5D2 stable U87 expressing cells (that were sustaining ectopic PTEN expression), a reduction in phosphorylated serine 473 AKT/PKB was observed using a phosphorylated serine/threonine 473 AKT/PKB antibody. This indicates that PTEN was still expressing sufficiently in de-activating the PI3Kinase pathway, as evidenced by this reduction in activated AKT/PKB signalling activation (Figure 3.1B).

Figure 3.1 Stable CYB5D2 U87 cells confer survival from ectopic PTEN and sustain its expression. A. U87 cells were constructed to stably express CYB5D2 and an EV(pLHCX) plasmid. A PTEN (pBabe) retrovirus was used to infect these stable U87 cells. Puromycin treatment was used to select for successful PTEN infection. B. Lysates of these cells were run on a 12% SDS-PAGE gel, and subsequent western blots performed. In CYB5D2 U87 cells that sustained ectopic PTEN, we see reduced levels of phosphorylated serine 473 AKT/PKB.

Figure 3.1

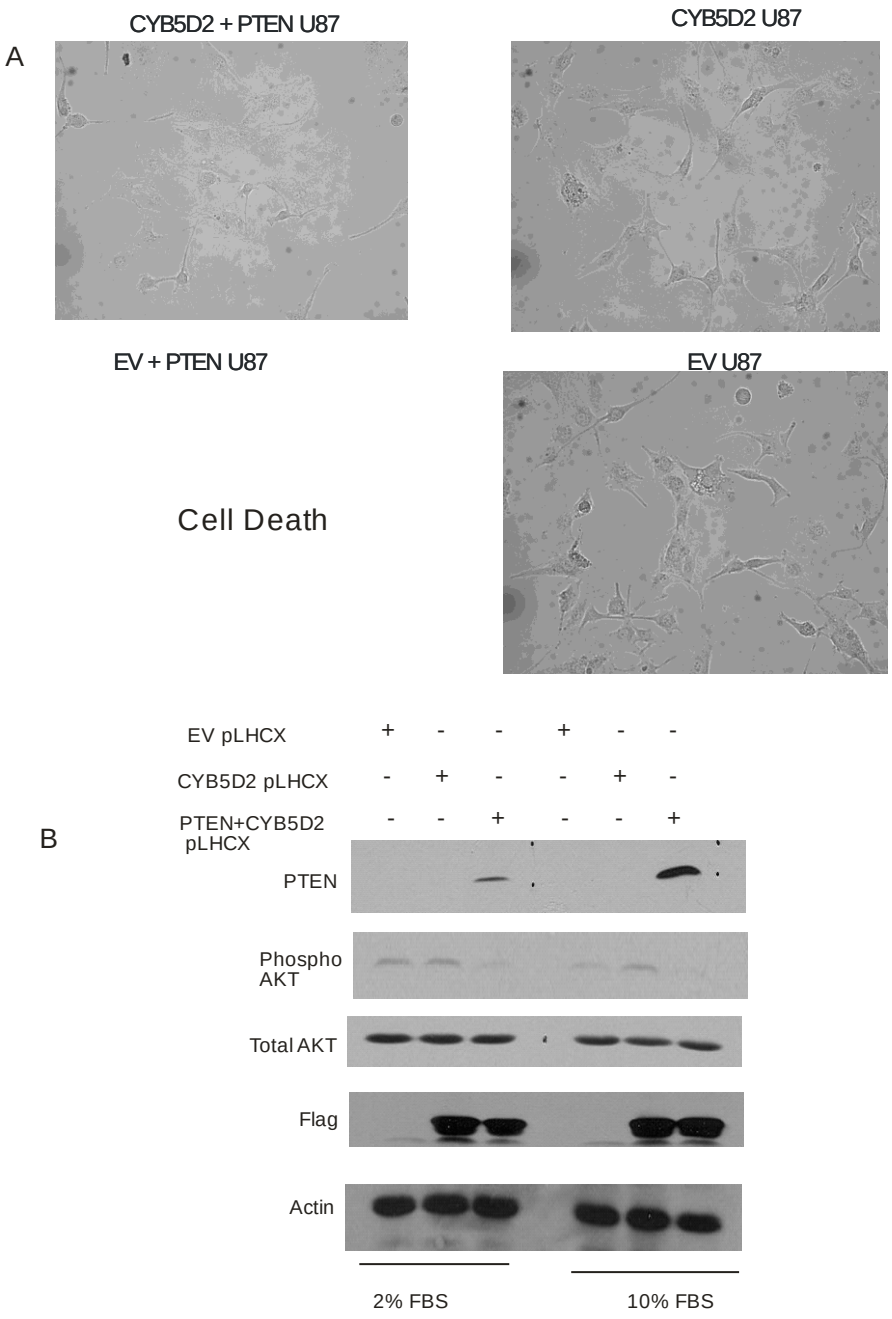
A
CYB5D2 + PTEN U87
CYB5D2 U87
EV + PTEN U87
EV U87
Cell Death
B
EV pLHCX + - - + - -
CYB5D2 pLHCX - + - - + -
PTEN+CYB5D2 pLHCX - - + - - +
PTEN
Phospho AKT
Total AKT
Flag
Actin
2% FBS
10% FBS

In order to examine if CYB5D2 was inhibiting PTEN function due to a protein association, co-immunoprecipitation experiments were performed using these dual stable (CYB5D2+PTEN) U87 cell lines. These U87 cells were cultured in 10% FBS and 2% FBS conditions for 24 hours. When CYB5D2 was immunoprecipitated with an M2 Flag antibody, ectopic PTEN could not be detected in a co-immunoprecipitation, in 10% FBS conditions, or in 2% FBS culture conditions (Figure 3.2). Similarly, when PTEN was immunoprecipitated, CYB5D2 could not be detected in co-immunoprecipitations, in either 10% FBS or 2% FBS culture conditions (Figure 3.2). This indicates that CYB5D2 and PTEN might not be associated in a protein interaction.

Interestingly, when ectopic CYB5D2 was immunoprecipitated in 2% FBS conditions (while sustaining PTEN expression) CYB5D2 appeared in a higher 56 kDa form, in addition to its 28 kDa form (Figure 3.2, asterisk *).

In order to measure how ectopic PTEN affected the proliferation of these CYB5D2 U87 cells, growth curves were performed in 10% FBS and 2% FBS conditions. These double stable CYB5D2 and ectopic PTEN U87 cells were also seen to proliferate slower than EV U87 cells and CYB5D2 stable U87 cells, when cultured in both 10% FBS and 2% FBS conditions (Figure 3.3). When CYB5D2 U87 cells were cultured in 2% FBS conditions, they displayed a reduction in proliferation, relative to EV U87 cells, but only at the highest cell densities seen in day 5 (Figure 3.3).

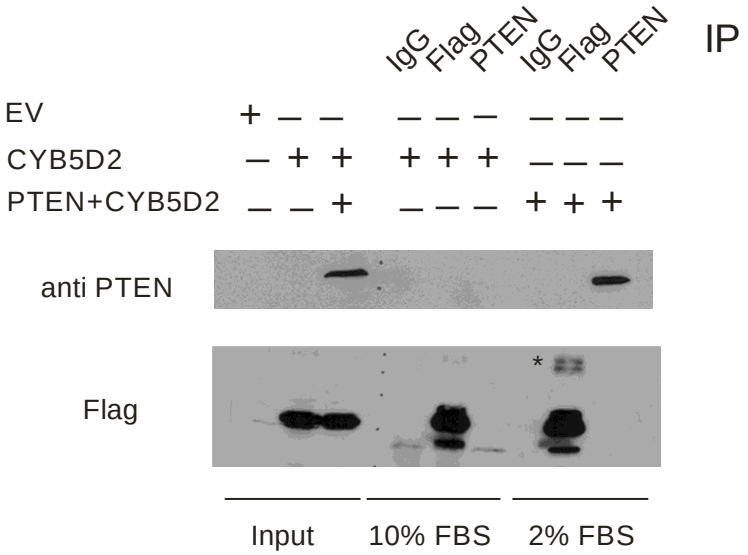

Figure 3.2 CYB5D2 sustains ectopic PTEN expression but does not co-immunoprecipitate with it. CYB5D2 and CYB5D2+PTEN U87 expressing cells were cultured in DMEM 10% FBS and 2% FBS serum (24 hours). CYB5D2 and PTEN were immunoprecipitated with 1μg of M2 Flag and PTEN monoclonal antibodies respectively. Immunoprecipitations were performed with 30 μl of protein G Sepharose at 4°C, followed by 6 washes in 0.1% triton co-immunoprecipitation buffer. Washed beads were then treated with Laemelli sample buffer and boiled, then run on 12.5% SDS PAGE gels. Western blots were probed with anti PTEN and M2 Flag antibodies. An asterisk indicates the appearance of the CYB5D2 56 kDa dimer that immunoprecipitates in the 2% FBS culture conditions.

■ **EV + CYB5D2**

▲**PTEN + CYB5D2**

♦ **EV**

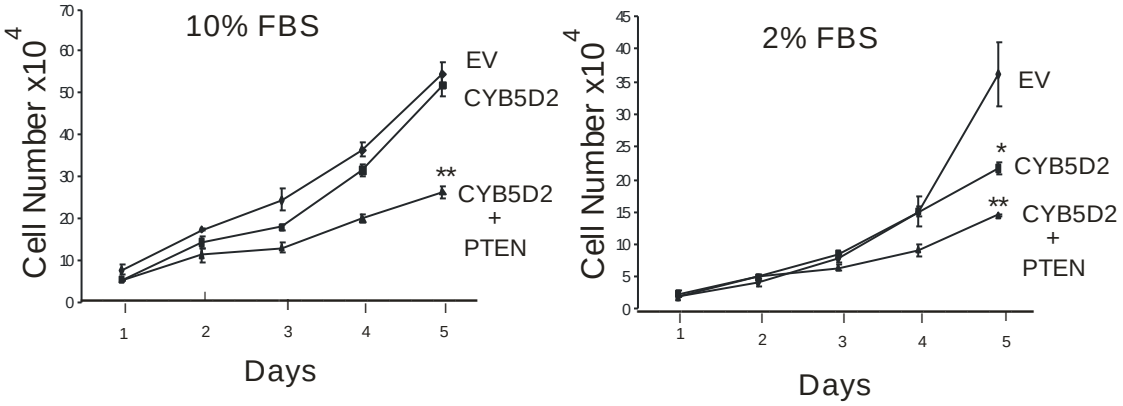

Figure 3.3 Growth Curve of CYB5D2 U87 with sustained PTEN expression.

CYB5D2 expressing U87, CYB5D2 + PTEN expressing U87 cells and control EV U87 cells were seeded in 6 well dishes (10^4 cells/well) and counted every 2 days for cell growth. Cells were cultured in both 10% FBS and 2% FBS, with serum being replaced every two or three days. All data points are presented as mean +/- standard error, n=4. A two tailed students T-test was used to analyse differences between cell lines and control EV U87 cell lines. A *p*-value <0.05 was considered statistically significant (*), *p*-value <0.01 was considered more statistically significant (**).

3.2 CYB5D2 confers survival from serum starvation in NIH3T3 cells

In order to study CYB5D2 in a non-transformed cell line, NIH3T3 cells were generated that stably express CYB5D2 and an EV (pLHCX). Using these NIH3T3 cells, cell viability was assessed in serum starved conditions. CYB5D2 NIH3T3 cells were able to survive better in serum starved conditions than EV cells (Figure 3.4). Bright Field microscopy was used to image adherent cells in conditions of prolonged serum starvation. After seeding the same number ($5x10^4$cells) of EV and CYB5D2 NIH3T3 cells in 6 cm plates, cells were serum starved up to 5 days. All floating cells were washed off. CYB5D2 NIH3T3 cells exhibited more attached cells, even after 5 days of serum starvation (Figure 3.4).

In order to better visualize this cellular adherence and viability, cells were fixed with 2% formaldehyde/2% glutaraldehyde and then stained at day 3 with 0.1% crystal violet. CYB5D2 NIH3T3 cells had significantly more adherent (viable cells) than the EV NIH3T3 cells (Figure 3.5 A). This was evident from day 3 to day 5 of serum starvation. To measure the non-adherent floating cells of these CYB5D2 and EV NIH3T3 cell lines that were serum starved at day three, floating cells were collected, centrifuged down for 5 minutes at $2x10^3$ rpm and stained with trypan blue (which stains for dead cells). The EV NIH3T3 cell line contained significantly more dead cells than the CYB5D2 NIH3T3, at day three (Figure 3.5 B).

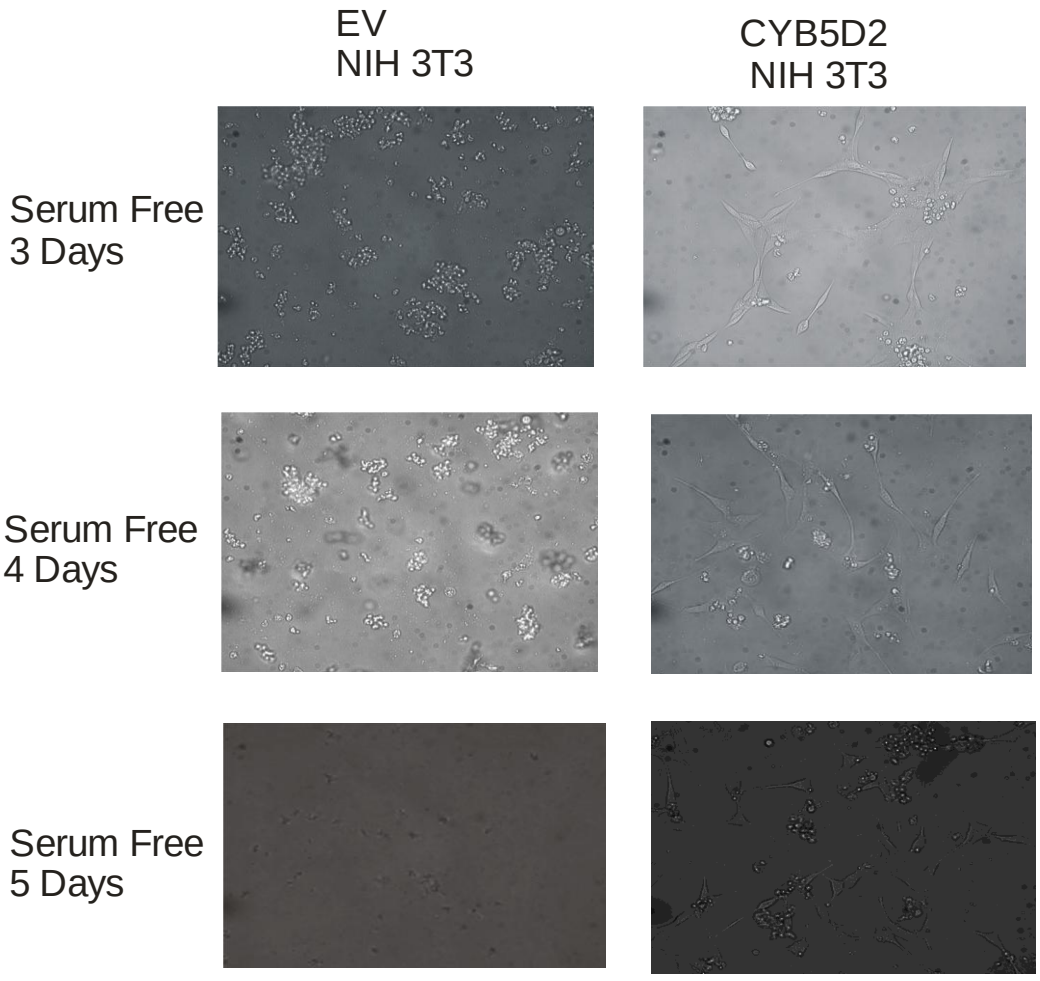

Figure 3.4 CYB5D2 confers survival from serum starvation in NIH3T3 cells. CYB5D2 and EV NIH3T3 cells were seeded at $5x10^4$ cells per 6 cm plate and then cultured in serum free DMEM. Photographs from day 3 to day 5, were taken at 20x magnification in bright field microscopy.

Figure 3.5 CYB5D2 NIH3T3 cells are more viable in serum starvation. CYB5D2 and EV NIH3T3 cells were seeded at $5x10^4$ cells per 6 cm plate and then cultured in serum free DMEM for five days. A. Cells were then fixed with 2% formaldehyde/ 2% glutaraldehyde and then stained at day 3, 4 and 5 with 0.1% crystal violet. B. CYB5D2 and EV NIH3T3 cells were seeded at $5x10^4$cells per 6 cm plate and serum starved for 5 days. At day 3 of serum starvation, cells that were floating were collected from the media, washed and stained with trypan blue and then counted. Values are presented as mean +/- standard error, n=4. A two tailed students T-test was used to analyse differences between CYB5D2 cell lines and control EV NIH3T3 cell lines. A p value <0.05 was considered statistically significant (*). A p value <0.01 was considered very statistically significant (**).

Figure 3.5

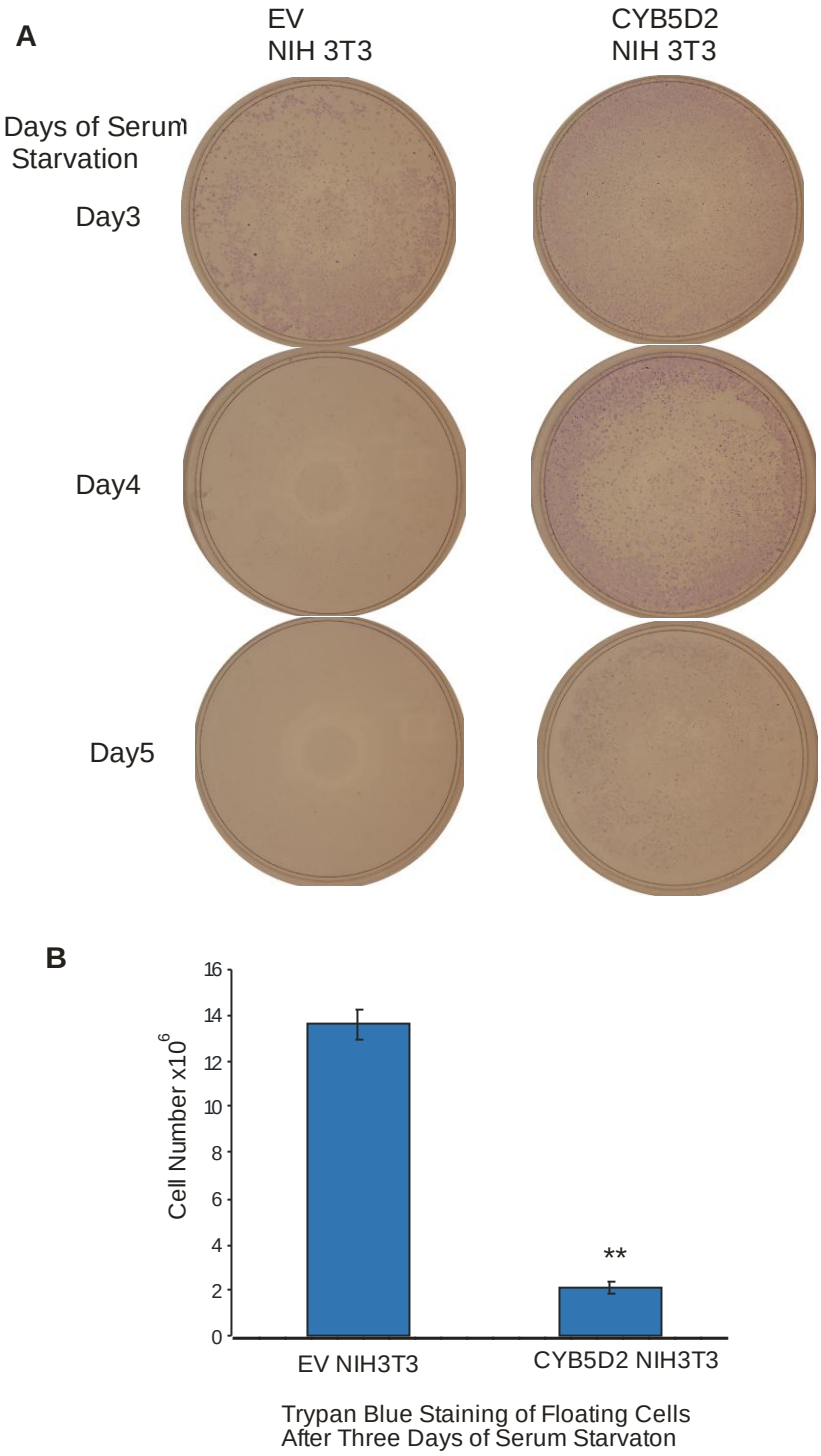
A
EV
NIH 3T3
CYB5D2
NIH 3T3
Days of Serum
Starvation
Day3
Day4
Day5
B
Cell Number x10^6
16
14
12
10
8
6
4
2
0
**
EV NIH3T3
CYB5D2 NIH3T3
Trypan Blue Staining of Floating Cells
After Three Days of Serum Starvaton

To ascertain whether the remaining attached cells were still viable after culturing under serum free conditions for 3 days, complete 10% FBS serum was added back to CYB5D2 NIH3T3 and EV NIH3T3 that had been cultured without serum for three days. These cells were then allowed to re-grow for two days after the re-addition of 10% FBS serum. After two days, a significant number of CYB5D2 NIH3T3 cells renewed proliferation and re-grew to confluence conditions when 10% FBS containing media was added back for 2 days. The EV NIH3T3 cells however, struggled to re-grow (images not shown). These NIH3T3 cells were then trypsonized and counted on a heamocytometer, staining with trypan blue to exclude for dead cells. CYB5D2 NIH3T3 cells significantly re-populated, compared to the EV NIH3T3 which struggled to re-grow (Figure 3.6).

In order to evaluate proliferation of these cells, growth curves were performed using CYB5D2 and EV NIH3T3 cells. Cells were cultured in 10% FBS and 2% FBS for several days. CYB5D2 NIH3T3 cells proliferated at a similar rate as the EV cells in 10% FBS conditions. However, when cultured in 2 % FBS conditions, CYB5D2 cells significantly impaired proliferation compared to the EV NIH3T3 cells (Figure 3.7).

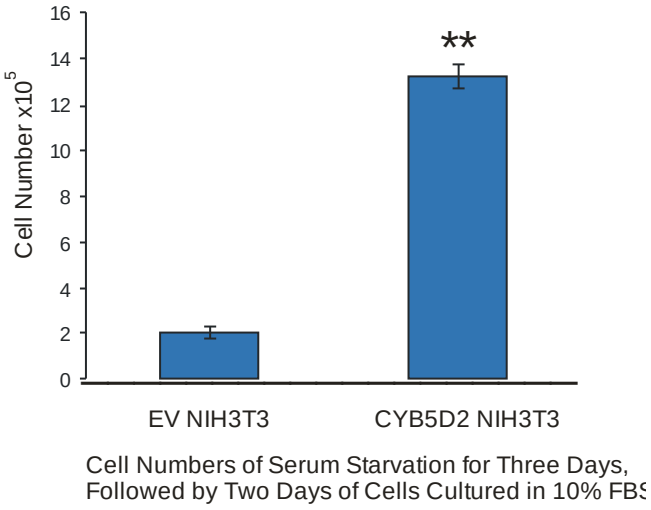

Figure 3.6 CYB5D2 NIH3T3 cells recovered from serum starvation better than EV NIH3T3 cells. A. CYB5D2 and EV NIH3T3 cells were seeded at $5x10^4$cells per 60 mm plate and then serum starved for 3 days. DMEM Media containing 10% FBS was then added back and the cells were counted after 2 days of culture in 10% FBS media. Cells were then counted on a heamocytometer, staining with trypan blue to exclude dead cells. Values are presented as mean +/- standard error, n=4. A two tailed students T-test was used to analyse differences between CYB5D2 cell lines and control EV NIH3T3 cell lines. A *p*-value <0.05 was considered statistically significant (*). A *p*-value <0.01 was considered very statistically significant (**).

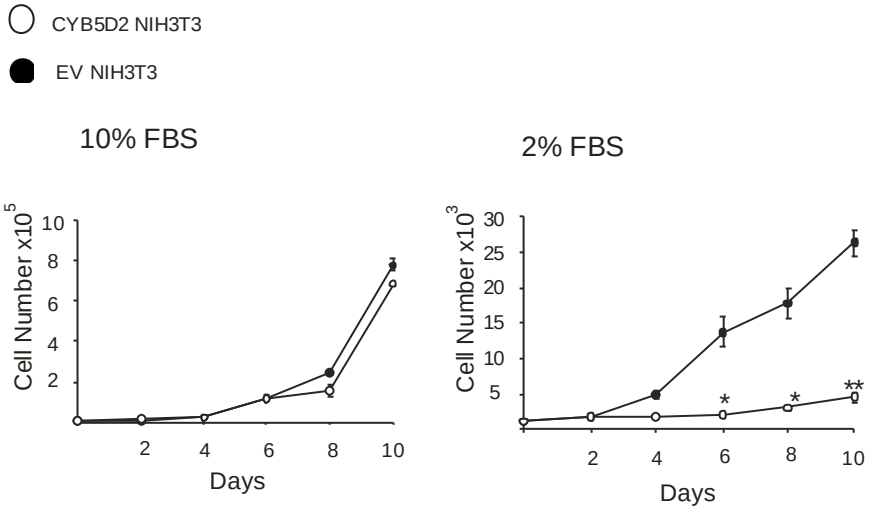

Figure 3.7 CYB5D2 NIH3T3 cells have impaired proliferation when cultured in reduced serum conditions. EV and CYB5D2 NIH3T3 cells, were seeded in 12 well plates, $10x10^3$cells per well. Cells were cultured in 10% FBS, and in 2% FBS conditions. Cells were counted every two days for 10 days. All data points are presented as mean +/- standard error, n=4. A two tailed students T-test was used to analyse differences between CYB5D2 cell lines and control EV NIH 3T3 cell lines. A *p*-value <0.05 was considered statistically significant (*), *p*-value <0.01 was considered more statistically significant (**).

It is unclear how CYB5D2 conferred survival from serum starvation here. Our overall objective was to determine whether CYB5D2 conferred survival from serum starvation by attenuating PTEN function. Therefore co-immunoprecipitations of CYB5D2 and PTEN were performed, to see if they were associated in a protein complex. This experiment was performed to detect an interaction between endogenous PTEN and ectopic CYB5D2, in different serum culture conditions. Immunoprecipitations were performed in these stable EV and CYB5D2 NIH3T3 cells in 10% and 2% FBS culture conditions. While the PTEN antibody could effectively immunoprecipitate endogenous PTEN (Figure 3.8 A and C), it could not co-immunoprecipitate ectopic CYB5D2 in either 10 % FBS or 2 % FBS culture conditions (Figure 3.8 B and D). In a reciprocal manner, when ectopic CYB5D2 was effectively immunoprecipitated with an M2 Flag antibody, endogenous PTEN could not be detected in co-immunoprecipitations (Figure 3.8 A and C). Whole cell lysates generated from these cells demonstrate that ectopic CYB5D2 protein is more abundant in the 2% serum conditions, as compared to the 10% FBS cultured conditions. Moreover, the appearance of the CYB5D2 56 kDa dimer, in immunoprecipitations performed in 2% FBS cultured conditions is observed (Figure 3.8 B, asterisk). This CYB5D2 56 kDa dimer is not present in immunoprecipitations performed in 10% FBS cultured conditions. This demonstrates that serum starvation induced ectopic CYB5D2 into this 56 kDa dimer form.

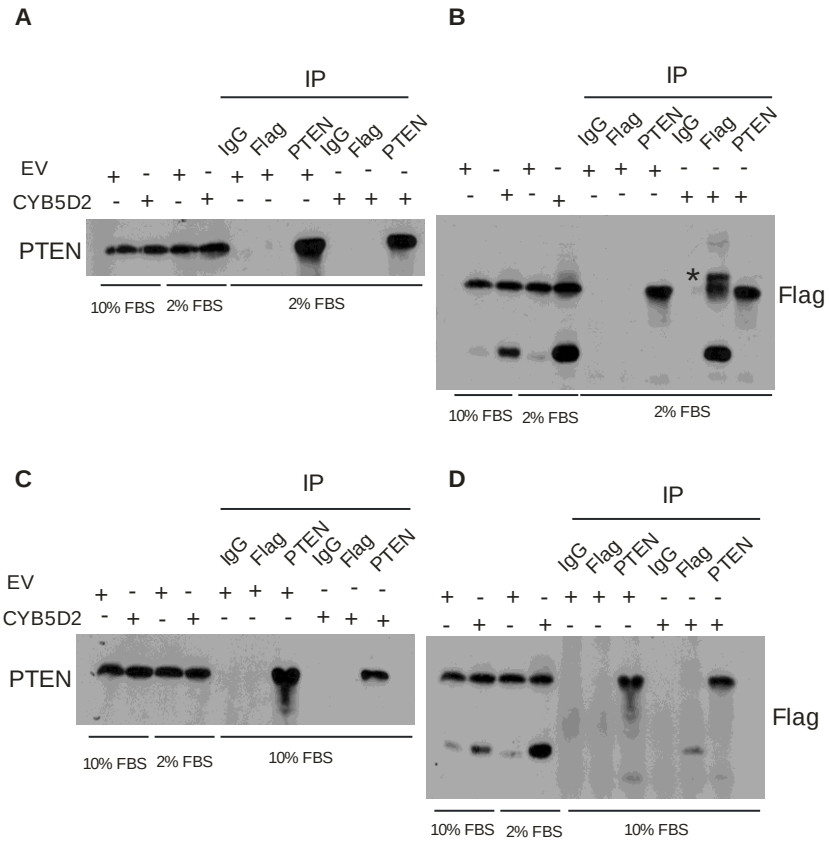

Figure 3.8 CYB5D2 does not co-immunoprecipitate with endogenous PTEN in NIH3T3 cells. EV and CYB5D2 NIH3T3 cells were cultured in 10% FBS and 2% FBS. Endogenous PTEN and ectopic CYB5D2 were then immunoprecipitated. A.C. Endogenous PTEN did not co-immunoprecipitate with CYB5D2, in either 10% FBS or in 2% serum culture conditions. B. D. Similarly, when endogenous PTEN was immunoprecipitated, CYB5D2 could not co-immunoprecipitate (A and C were re-probed with an M2 Flag antibody, to generate B and D western blots respectively). B. An asterisk is shown at the site that CYB5D2 immunoprecipitates as a 56 kDa dimer in 2% FBS culture conditions.

Chapter 4. Generation of a COOH-terminal Polyclonal Antibody to CYB5D2.

4.1 Generation of a COOH-terminal Polyclonal antibody to CYB5D2

At the time when I started to investigate CYB5D2, this protein was classified as "hypothetical", without any published reports of its existence. Furthermore, a commercial CYB5D2 antibody was not available. Therefore, it was essential to generate this reagent. A polyclonal COOH-terminal CYB5D2 antibody was then produced. This segment of the CYB5D2 gene encompassed amino acids 171-264, which was carboxy terminus to the cytochrome b5 heme binding domain (Figure 4.1). This segment did not contain any homology with any members of this cytochrome b5 heme binding family, thus was chosen to negate any cross reactivity with other proteins in this family. Subsequently this COOH terminus segment of CYB5D2 was cloned into the pGEX 4T.1 plasmid, in frame with a GST fusion gene. This segment is depicted in figure 4.1 as the underlined sequence. This COOH CYB5D2 fusion was then expressed in BL21 *E.coli* bacteria, and induced with IPTG to generate the expression of recombinant COOH-CYB5D2 protein.

```
1   MLRCGGRGLL LGLAVAAAAV MAARLMGWWG PRAGFRLFIP EELSRYRGGP
51  GDPGLYLALL GRVYDVSSGR RHYEPGSHYS GFAGRDASRA FVTGDCSEAG
101 LVDDVSDLSA AEMLTLHNWL SFYEKNYVCV GRVTGRFYGE DGLPTPALTQ
151 VEAAITRGLE ANKLQLQEKQ TFPPCNAEWS SARGSRLWCS QKSGGVSRDW
201 IGVPRKLYKP GAKEPRCVCV RTTGPPSGQM PDNPPHRNRG DLDHPNLAEY
251 TGCPPLAITC SFPL
```

Figure 4.1 Amino acid sequence of CYB5D2. The underlined sequence of CYB5D2 was used to generated the COOH terminal fragment for a polyclonal antibody (amino acids 171-264). The cytochrome b5 heme binding domain is outlined in red (amino acids 31-133). The transmembrane domain at the NH2 terminus is in green (amino acids 7-29). The CYB5D2 protein is 264 amino acids in total.

Recombinant COOH-CYB5D2 protein was then purified with GST-Sepharose affinity chromatography and run on a 12% SDS PAGE gel. A 10 minute incubation with 0.2 M glycine, was performed at the second eluted fraction to produce the highest elution quantity. Eluted fractions of recombinant purified CYB5D2 protein were subsequently run on a 12% SDS PAGE gel, and stained with coomasie blue. As seen in figure 4.2 A, the combined molecular weights making up the recombinant COOH- CYB5D2 are seen around the 46 kDa marker.

Because of the low visible yield seen in the coomasie blue stained SDS-PAGE gel, western blots were performed. The same eluted fractions of purified recombinant protein were run on a 12% SDS PAGE and then transferred to a nitrocellulose membrane, and western blots probed with an M2-Flag Sigma antibody. The same banding pattern from panel A is also seen in figure 4.2 B.

The COOH-CYB5D2 recombinant purified protein from more than one preparation were combined and used to immunize 2 rabbits (New Zealand White) and animals were boosted every 2 months for a year. Anti-CYB5D2 IgG was purified by ammonium sulphate precipitation and protein A agarose affinity chromatography purification.

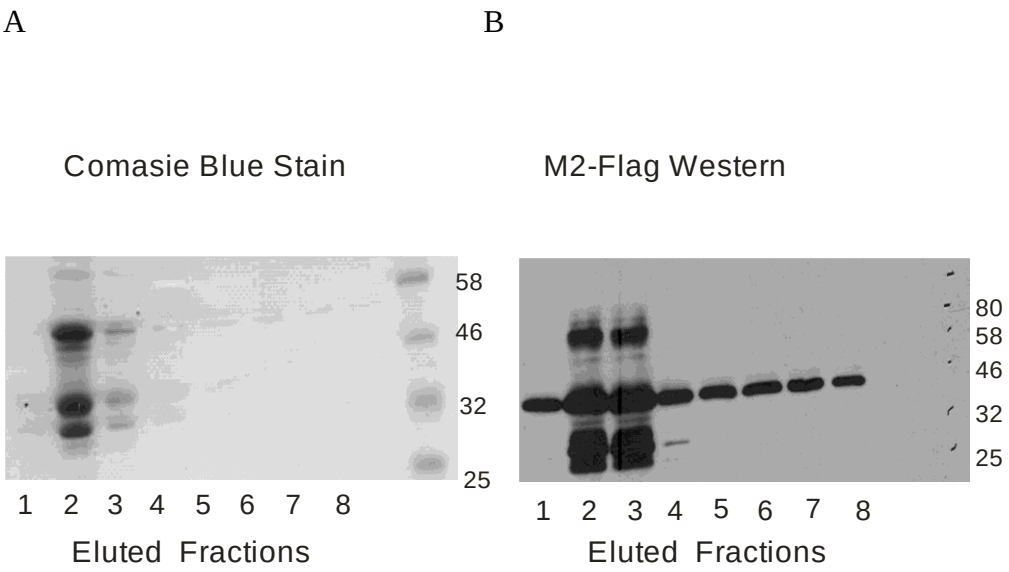

Figure 4.2 Generating a COOH-CYB5D2 recombinant fusion protein. A. COOH-CYB5D2 fusion protein was generated and recombinant protein induced in BL21 bacteria. The recombinant protein was then purified, and eluted fractions 1-8 were subsequently run on SDS-PAGE gels, then stained with coomasie blue (Figure 4.2 A). B. Eluted fractions of recombinant COOH-CYB5D2 protein 1-8 were also run on SDS-PAGE gels, transferred to western blots and probed for with an M2 Flag antibody.

The purified anti-CYB5D2 IgG was then used to examine CYB5D2 expression in a panel of various cell lines by western blot analysis (Figure 4.3). Cell lysates from various cell types were run on a 12% SDS PAGE gel, transferred to nitrocellulose membranes, and probed with this COOH-CYB5D2 antibody. Lysates from HEK 293T cells, HeLa, LNCAP, 1933, R32, ACHN, and A498 were used. As a positive control, HeLa cells stably over-expressing CYB5D2 were used. A doublet band around 56 kDa was predominantly seen in all cell lines tested (Figure 4.3, panel A). In order to re-confirm these results, the same lysates were run again with similar results (Figure 4.3, panel B). The predicted endogenous band for CYB5D2 around 27-28 kDa was not detected, except for the band in the positive control CYB5D2 HeLa cells around the 27-28 kDa region.

To explore the possibility that endogenous CYB5D2 protein in these cell lysates was not denatured and the lysis conditions might have caused the CYB5D2 to migrate as a 56 kDa dimer (and not the molecular weight at 28 kDa), 50 mM DTT was added to the laemelli sample buffer to increase the denaturing capacity of this buffer. Additionally, the final concentration of SDS was increased from 1% to 1.5%. Lysates were subsequently generated and treated with this more denaturing laemelli sample buffer. As seen in figure 4.4, a 27-28 kDa band now appeared in several samples. A predominant band in the high 40 kDa range also appeared in all lanes.

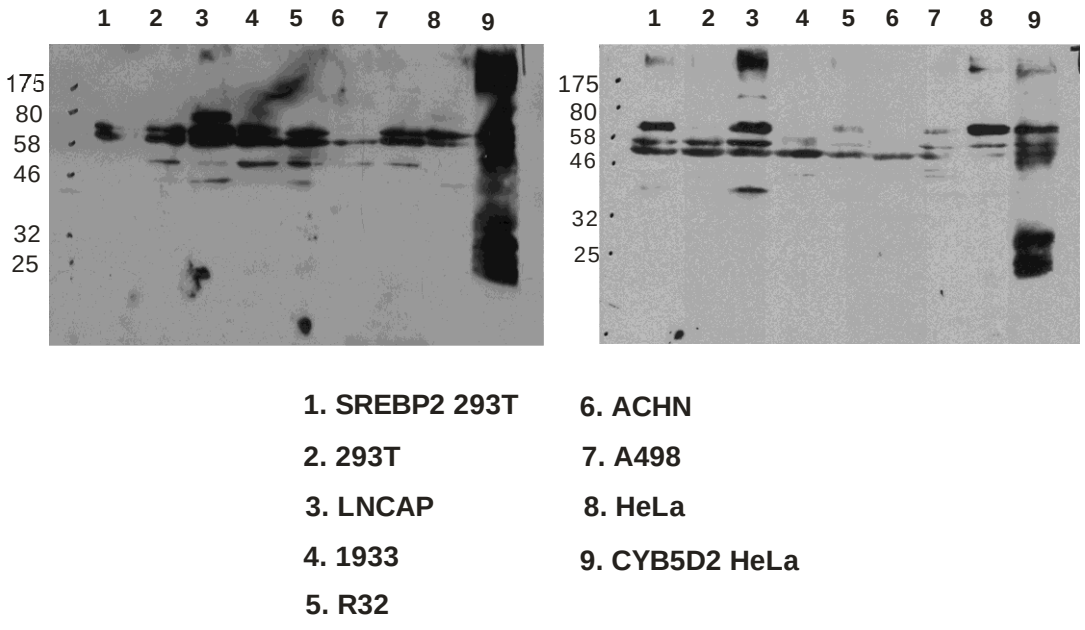

Figure 4.3 The COOH-CYB5D2 antibody detects an endogenous band that migrates as a doublet around 56-58 kDa. A control CYB5D2 Hela stable line was used. Lysates from 293T, 293T transfected with SREBP2, LNCAP, 1933, R32, ACHN, A498, Hela cells and a control CYB5D2 Hela cell were used.

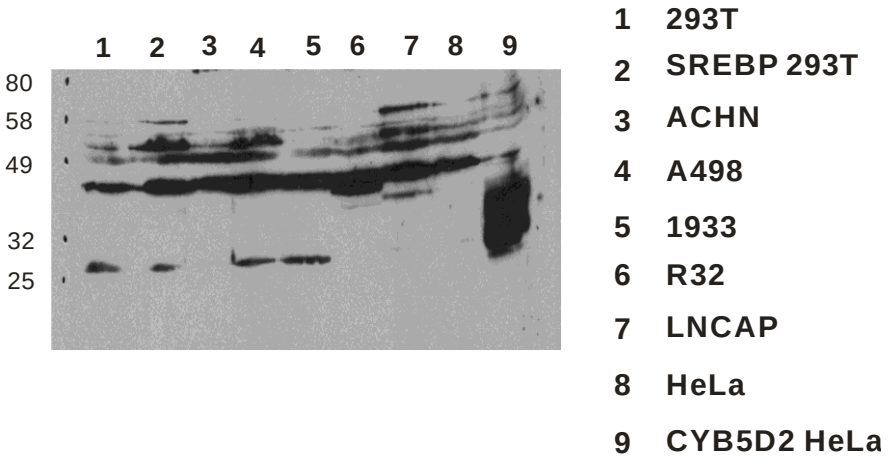

Figure 4.4 Increased denaturing conditions resolve CYB5D2 protein into a 28 kDa band. Lysates from various cell lines were made in a final 1.5 x SDS concentrated Lamelli sample buffer supplemented with 50 mM DTT. Lysates were run on a 12% SDS-PAGE gel then transferred to a western blot which was probed with the COOH-CYB5D2 antibody (1μg/ml). Endogenous CYB5D2 protein monomer bands appear at 28 kDa. CYB5D2 HeLa cells are used as a control.

To confirm the specificity of this COOH terminus CYB5D2 antibody, CYB5D2 siRNA knockdown technology was used to ablate CYB5D2 expression in 293T cells. Confirmation that endogenous CYB5D2 was successfully knocked down was sought at the level of RNA and protein. Subsequently, an siRNA oligo from Sigma, specifically designed to knockdown endogenous CYB5D2 was transfected into 293T cells with Lipofectamine 2000. Forty-Eight hours post transfection, whole cell lysates were made and run on SDS PAGE gels and western blots performed. The COOH-CYB5D2 antibody was then used to probe western blots. We observe that endogenous CYB5D2 was successfully knocked down, and this result was performed in duplicate (Figure 4.4 A). Subsequent knockdown of CYB5D2 mRNA was confirmed by real time PCR (Figure 4.4 B).

Using this COOH terminal CYB5D2 antibody, we sought to determine where the protein was expressed. Subsequently, whole cell lysates of cell lines from breast cancer, prostate cancer, kidney cancer, neural cancer cells and liver cancers, were analyzed by western blots and subsequently probed with the COOH-CYB5D2 antibody. As seen in figure 4.5 A, Huh7 liver cancer cells expressed CYB5D2, but HEPG2 cells did not. In three breast cancer cell lines examined, MDA MB-231, MCF7 and T47D panel B. CYB5D2 was weakly detected (Figure 4.5 panel B).

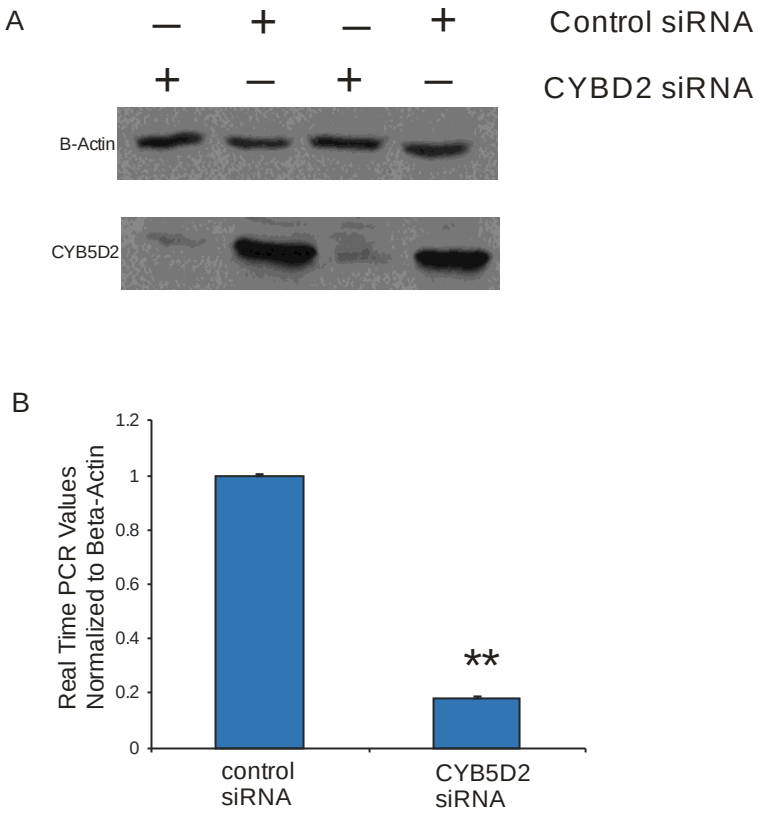

Figure 4.5 CYB5D2 siRNA knockdown confirms CYB5D2 antibody specificity. An siRNA oligo for CYB5D2 was purchased from Sigma. 293T cells were then transfected with Lipofectamine 2000 with this CYB5D2 siRNA and a control siRNA. A. Cell lysates were analyzed by western blot probed with the COOH-CYB5D2 antibody (1μg/μl). Beta-Actin was used as an internal control. B. RNA was extracted and reverse transcribed to cDNA. Real Time PCR reveals that CYB5D2 mRNA is reduced using this siRNA oligo for CYB5D2. Data represent mean +/- standard deviation, n=3. A two tailed student T-test was used to determine significance in differences in fold change. A *p*-value <0.01 was considered very statistically significant (**).

The kidney cell lines, 1933, R32, A498 and ACHN were probed with the COOH-CYB5D2 antibody (Figure 4.5 C). Expression of CYB5D2 protein was low in all kidney cell lines. Additionally, the prostate cancer cell lines DU145, LNCAP and PC3 were probed, expressing low to moderate levels of CYB5D2 protein (Figure 4.5 C). HeLa cell lysates were also run on this western blot as a relative control (Figure 4.5 C). Four neural cancer cell lines were examined next, LN229, U373, T98G and U87, for CYB5D2 protein expression (Figure 4.5 D). All neural cancer cell lines had high expression levels of CYB5D2 protein (Figure 4.5 D).

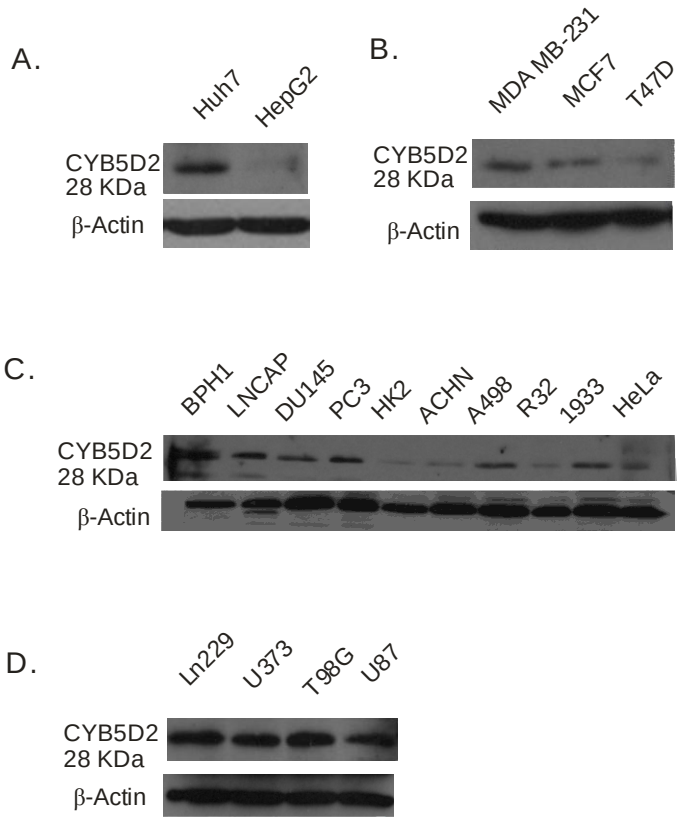

Figure 4.6 Expression of CYB5D2 protein in various cancer cell lines. The CYB5D2 COOH-terminus rabbit polyclonal (affinity purified) was used (1μg/ml) to probe these western blots. Beta-Actin was used to reprobe these western blots as an internal control**.** A. CYB5D2 protein is expressed in the liver cell line Huh7 but not HEPG2. B. CYB5D2 protein is weakly expressed in the breast cancer cell lines MDA MB-231, MCF7 and T47D. C. CYB5D2 protein is expressed weakly in the kidney cell lines of HK2, R32, A498, 1933 and ACHN, and moderately in the prostate cancer cell lines of BPH1, DU145 and LNCAP, and PC3. D. CYB5D2 protein is highly expressed in the neural cancer cell lines LN229, U373, T98G and U87. 50 μg of protein from each cell lines was run on a 12% SDS-PAGE.

Chapter 5. CYB5D2 binds to heme and a D86G heme binding defective mutant demonstrates loss of functions

CYB5D2/Neuferricin has been reported to bind heme (Kimura *et al*. 2010). Whether this association is mediated through specific residues in the cyt-b5 domain of CYB5D2 remains unclear. To identify these potential residues responsible for heme binding, we researched that Y107 and Y113 in human PGRMC1, as well as Y138 in Dap1 (the yeast homologue of PGRMC1), contribute to heme binding (Min *et al*. 2005; Ghosh *et al*. 2005). These three tyrosine residues are conserved in CYB5D2 as Y73, Y79, and Y127, respectively (Figure 5.1A). Additionally, D120 of PGRMC1 was recently reported to play a major role in heme binding (Crudden *et al*. 2006). This critical heme-binding D120 residue is conserved at D86 in CYB5D2 (Figure 5.1A). Collectively, this comparative structural analysis suggests that Y73, Y79, D86, and Y127 are conserved and potentially involved in CYB5D2-mediated heme association. As previously reported, all of these mutants were involved in affecting heme binding in either Dap1 in yeast or PGRMC1 in mammalian cells. Comparatively, these residue are conserved in yeast Dap1, human PGRMC1, Arabidopsis IJ03 and human CYB5D2 (Figure 5.1A). In order to generate a CYB5D2 mutant defective for heme binding, these three tyrosine residues were individually replaced with alanine (Y73A, Y79A, and Y127A), and the conserved aspartic acid D86 replaced with glycine (D86G). These mutants were confirmed by DNA sequencing through the McMaster MOBIX sequencing facility, McMaster University, Hamilton, Ontario, Canada. When transiently expressed in 293T cells, these mutants

were expressed at comparable levels to wild-type CYB5D2 in whole cell lysates (Figure 5.1B), suggesting that the overall configuration and folding was not significantly affected by the aforementioned substitutions.

Heme agarose was then used to affinity precipitate wild type CYB5D2 and these heme binding domain mutants. While CYB5D2, Y73A, Y79A, and Y127A were effectively precipitated by heme-agarose, the D86G mutant was not precipitated (Figure 5.1B, bottom panel). This result demonstrates that D86 is a critical residue responsible for CYB5D2-mediated association with heme.

5.1 D86 mediates a direct association of heme with CYB5D2

The above analysis of heme binding using transient expression of CYB5D2 in 293T cells, coupled with heme-agarose pull-down, does not exclude the possibility that D86 may mediate CYB5D2 to associate with a potential heme-binding protein. It could be possible that this putative CYB5D2 binding protein may thus be responsible for heme-agarose-mediated precipitation of CYB5D2. To exclude this possibility, we purified GST-CYB5D2 and GST-CYB5D2 (D86G) recombinant fusion proteins using BL-21 *E. coli*. To enhance the solubility of the fusion proteins, we have deleted the transmembrane domain (ΔTM). During the purification process, we noticed that GST-CYB5D2-bound glutathione displayed a dark brown color compared to GST-CYB5D2(D86G)-bound glutathione-agarose which had a light brown color (Figure 5.2A). This observation is consistent with those previously reported for recombinant Neuferricin (CYB5D2) and PGRMC1 (Kimura *et al*. 2010; Crudden *et al*. 2006).

Figure 5.1 The D86 residue of CYB5D2 contributes to CYB5D2-mediated heme binding. A. Alignment of a portion of the conserved cytochrome b5 heme-binding like (cyt-b5) domain of human CYB5D2 (aa. 33 to 133) with human PGRMC1 (aa. 73 to 170), Dap1 protein (*Saccharmyces cerevisiae*; aa. 44 to 144) and the putative steroid-binding protein 1J03 (*Arabidopsis thaliana*; aa. 5 to 100), as previously published in Cahill (2007). Identical residues are indicated with an astericks. Alignment was performed using the Clustal W Alignment Program**.** CYB5D2 shares 19.8% identity and 26.2% similarity with PGRMC1 as determined by the EMBOSS Alignment Program. The D86 residue of CYB5D2 and the conserved D120 residue in PGRMC1 are indicated, along with conserved tyrosine (Y73, Y79, Y127) residues previously implicated in PGRMC1-mediated heme binding. **B.** 293T cells were transiently transfected with empty vector (EV), CYB5D2, and the indicated CYB5D2 mutants. The expression of the ectopic proteins in whole cell lysates was examined by western blot (top panel), and the ectopic proteins were precipitated by heme-agarose (bottom panel). The D86G mutation rendered CY5D2 unable to bind heme agarose.

Figure 5.1

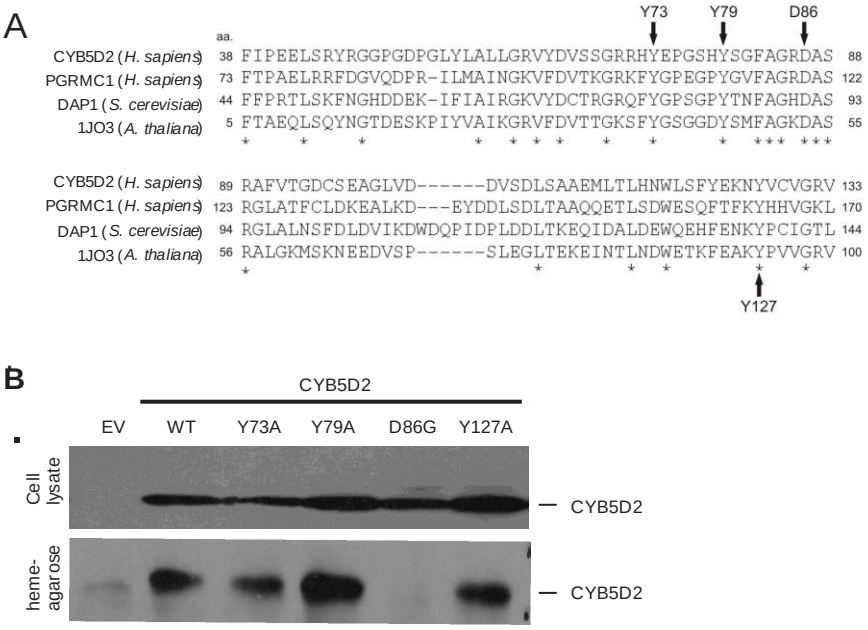
A
Y73
Y79
D86
aa.
CYB5D2 (H. sapiens) 38 FIPEELSRYRGGPGDPGLYLALLGRVYDVSSGRRHYEPGSHYSGFAGRDAS 88
PGRMC1 (H. sapiens) 73 FTPAELRRFDGVQDPR-ILMAINGKVFDVTKGRKFYGPEGPYGVFAGRDAS 122
DAP1 (S. cerevisiae) 44 FFPRTLSKFNGHDDEK-IFIAIRGKVYDCTRGRQFYGPSGPYTNFAGHDAS 93
1JO3 (A. thaliana) 5 FTAEQLSQYNGTDESKPIYVAIKGRVFDVTTGKSFYGSGGDYSMFAGKDAS 55
CYB5D2 (H. sapiens) 89 RAFVTGDCSEAGLVD------DVSDLSAAEMLTLHNWLSFYEKNYVCVGRV 133
PGRMC1 (H. sapiens) 123 RGLATFCLDKEALKD---EYDDLSDLTAAQQETLSDWESQFTFKYHHVGKL 170
DAP1 (S. cerevisiae) 94 RGLALNSFDLDVIKDWDQPIDPLDDLTKEQIDALDEWQEHFENKYPCIGTL 144
1JO3 (A. thaliana) 56 RALGKMSKNEEDVSP------SLEGLTEKEINTLNDWETKFEAKYPVVGRV 100
Y127
B
CYB5D2
EV
WT
Y73A
Y79A
D86G
Y127A
Cell lysate
CYB5D2
heme-agarose
CYB5D2

From the respective glutathione-agarose, GST-CYB5D2 and GST-CYB5D2(D86G) were subsequently eluted/purified with comparable levels of purity (Figure 5.2B). Heme-associated proteins possess a maximal absorbance at approximate 402 nm wavelength (Kimura *et al.*, 2010; Crudden *et al.*, 2006). In accordance with these reports, GST-CYB5D2, but not GST-CYB5D2(D86G), displayed a peak absorbance at approximately 402 nm (Figure 5.2C). This observation further confirms that GST-CYB5D2 associates with heme and that substitution of D86 with G substantially reduced the heme association.

To consolidate the above observation, we performed peroxidase reaction staining. When loaded with heme, heme-binding proteins were detected by peroxidase reaction staining (Thomas *et al.* 1976; Kimura *et al.* 2008; Kimura *et al*. 2010). While recombinant CYB5D2(D86G) was not detected by peroxidase reaction staining with and without heme loading, CYB5D2 was detected only under the heme-loaded condition (Figure 5.2D). In these reactions, heme was present in excess, as comparable amounts of free heme was observed among the reactions of CYB5D2 + heme, CYB5D2(D86G) + heme, and heme only (Figure 5.2D, middle panel). Therefore, the inability to detect CYB5D2(D86G) was not caused by an insufficient amount of heme being present. Taken together, the above observations reveal that D86 is directly responsible for CYB5D2 to bind heme.

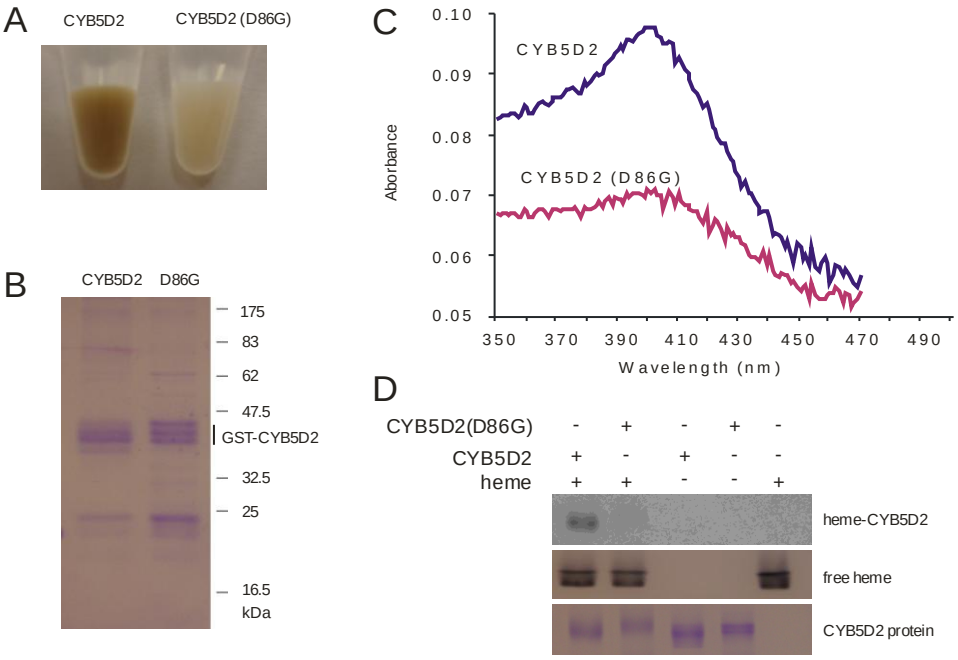

Figure 5.2 D86G substitution renders recombinant CYB5D2 incapable of binding heme. A. GST-CYB5D2 (CYB5D2)-bound and GST-CYB5D2(D86G)-bound glutathione-agarose. B. 10 μg of purified recombinant GST-CYB5D2 (CYB5D2) and GST-CYB5D2(D86G) (CYB5D2(D86G)) was separated by SDS-PAGE, followed by Coomassie blue staining. C. Recombinant GST-CYB5D2 and GST-CYB5D2(D86G) protein (200 μg protein in 1 ml of 1×TBST), referred to as CYB5D2 and CYB5D2(D86G) respectively, were scanned for their absorbance peaks within the indicated wavelength range. D. Recombinant GST-CYB5D2 (CYB5D2) and GST-CYB5D2(D86G) (200 μg) were analyzed by peroxidase reaction staining (see Materials and Methods for technical details). The recombinant proteins were also stained with Coomassie blue (bottom panel).

5.2 CYB5D2 binds to Heme b, and exists in both oxidized and reduced forms

The heme population consists of heme a, b, and c. While heme c covalently links to proteins (cytochrome c), both heme a and b attach to protein via non-covalent bonds (Nakamoto *et al*. 2000). In fact, cytochrome a, b, or c was named because of the existence of heme a, b, or c, respectively (Nakamoto *et al*. 2000). Among the three types of heme, heme b is the most common type (Nakamoto *et al*. 2000). Therefore, the existence of a cyt-b5 (heme-binding) motif suggests that CYB5D2 binds heme b. In a reaction containing 200 mM NaOH, 40% pyridine, and 0.6 mM $K_3Fe(CN)_6$, heme a and b will be released from a heme-binding protein and it will become oxidised. While heme c will not be released from cytochrome c, the existence of the protein does not interfere with heme c oxidization (Berry and Trumpower 1987). Oxidised heme a, b, and c display a specific spectrum of absorbance, with the peak absorbance for type a, b, and c being at 588 nm, 556 nm, and 550 nm, respectively (Berry and Trumpower 1987). To exclude the possibility that the presence of GST in the GST-CYB5D2 may have affected heme association, we cleaved off the GST portion by treating with thrombin (Figure 5.3A). When CYB5D2-associated heme is oxidized, its peak absorbance was observed at approximately 559 nm. Under the same conditions, CYB5D2(D86G) did not generate an absorbance peak (Figure 5.3B). Taken together, these observations thus suggest that CYB5D2 binds to type b heme.

To further characterize the association between CYB5D2 and heme, the properties of CYB5D2 under oxidized and reduced conditions have been examined. The GST-free CYB5D2 protein displayed peak absorbance at 402 nm (oxidized condition) which

shifted to 420 nm under reduced conditions (Figure 5.3C), the typical absorbance pattern for heme-associated proteins including CYB5D2/Neuferricin (Kimura *et al*., 2010). The GST-free CYB5D2(D86G) recombinant protein could not be oxidized, or reduced (Figure 5.3B). Taken together, the above observations reveal that D86 is directly responsible for CYB5D2 to bind heme.

5.3 Heme-binding contributes to CYB5D2-mediated regulation of HeLa cell proliferation and anchorage-independent growth

Neuferricin/CYB5D2 promotes neuron differentiation via inhibiting cell proliferation (Kimura *et al*., 2010). Initially, HeLa cells were infected with empty vector (EV), CYB5D2, or heme-binding defective CYB5D2(D86G) retrovirus (Figure 5.4A and B). Using dual immunofluorescence, CYB5D2 and D86G co-localized with GRP78, and ER marker, in HeLa cells (Figure 5.4 A). Subsequent western blots confirm stable expression of CYB5D2 and D86G in HeLa cells (Figure 5.4 B). To examine the impact of heme-association of CYB5D2 on cell proliferation, growth curves were conducted. In comparison to EV control cells, ectopic CYB5D2 significantly reduced HeLa cell proliferation (Figure 5.4 C). However, this inhibition of HeLa cell proliferation is cell density dependent, as seeding at densities $<10^4$ cells/well in a 12 well-plate does not result in a significant difference in cell growth between CYB5D2-expressing cells and EV control cells. Moreover, the concept that ectopic CYB5D2 reduces HeLa cell proliferation was strengthened by the observation that ectopic expression of the heme-

binding defective mutant CYB5D2(D86G) increased proliferation (Figure 5.4B). The impact of ectopic CYB5D2(D86G) on HeLa cell proliferation is likely not due to the induction of the unfolded protein response (UPR), as neither CYB5D2 nor CYB5D2(D86G) overexpression affected GRP78 expression (Figure 5.4B), an ER stress marker (Kim *et al.*, 1987; Normington *et al.*, 1989; Gething and Sambrook, 1992). Furthermore, ectopic CYB5D2 was not detected in the media of these CYB5D2 HeLa cells, therefore it was not detected as being secreted in these cells.

To address whether heme-binding by CYB5D2 contributes to HeLa cell anchorage-independent growth, CYB5D2 and CYB5D2(D86G)-expressing HeLa cells were seeded in soft agar-containing serum-supplemented media. CYB5D2 expression reduced HeLa cell anchorage-independent growth in soft agar, while CYB5D2(D86G) increased colony growth (colony number and size) compared to EV cells (Figure 5.4D, E). Taken together, this demonstrates that heme-binding by CYB5D2 is necessary in inhibiting HeLa cell proliferation and survival under anchorage-independent conditions.

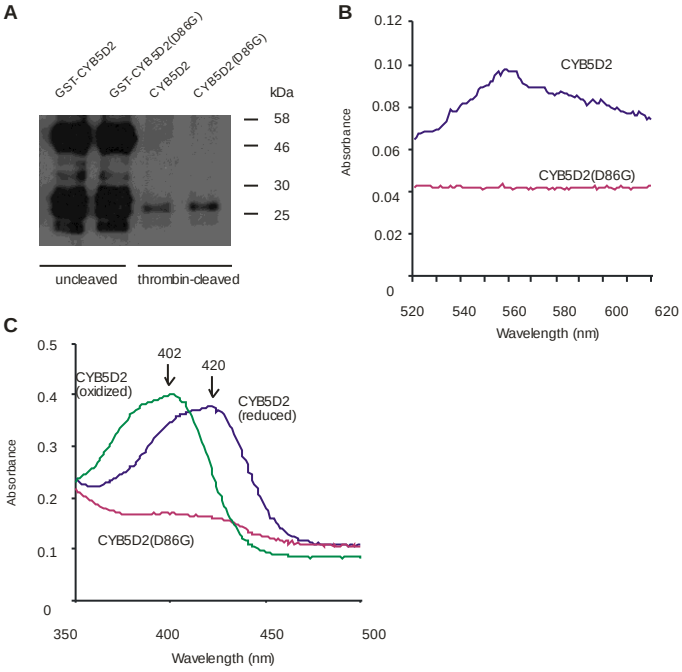

Figure 5.3 CYB5D2 binds to type *b* heme, and exists in both oxidized and reduced forms. A. 10 μg of purified recombinant GST-CYB5D2 and GST-CYB5D2(D86G) were thrombin-cleaved, and the uncleaved and cleaved (CYB5D2 and CYB5D2(D86G), respectively) proteins were separated by SDS-PAGE followed by Western blot analysis for CYB5D2 using anti-CYB5D2 antibody. B. Recombinant CYB5D2 and CYB5D2(D86G) protein (2 μM), were oxidised by $K_3Fe(CN)_6$, followed by scan with the indicated range of wavelength using a spectrophotometer. The peak absorbance for CYB5D2 was observed at approximately 559 nm. C. Thrombin-cleaved recombinant CYB5D2 and CYB5D2(D86G) proteins were reduced by sodium dithionite treatment and scanned for their absorbance peaks within the indicated wavelength range. The maximum absorbance peaks for the oxidized and reduced forms of human CYB5D2 were 402 nm and 420 nm, respectively.

Figure 5.4 CYB5D2 regulates adherent cell proliferation and colony growth of HeLa cells in a heme-association dependent manner. A HeLa cells were infected with pLHCX (empty vector: EV), pLHCX/CYB5D2, or and pLHCX/CYB5D2(D86G) retrovirus as indicated to generate stable cell lines. Co-localization with GRP78, an ER protein is demonstrated for both CYB5D2 and CYB5D2(D86G) in stable HeLa cell lines. B. The expression of ectopic CYB5D2 and CYB5D2(D86G) proteins is shown. The expression of GRP78 and β-actin were also determined. C. Cell proliferation of HeLa cells following ectopic expression of CYB5D2 and CYB5D2(D86G). The indicated cell lines were seeded at 10^4 cell/well in a 12-well plate. Cell numbers were determined daily for a period of 6 days. Experiments were conducted in quadruplicate, with triplicate replicates in each experiment. Cell numbers determined at each time point are presented as mean ± SD. $^{**}p < 0.01$ (two-tailed independent Student's *t*-test). D. Anchorage-independent growth. Representative images of soft agar plates (top panels) and phase contrast images of colonies at 50x magnification (bottom panels). Scale bar is equal to 200 μm. D and E. Mean number and diameter of colonies in 10 random fields. $^{**}p < 0.01$ (two-tailed independent Student's *t*-test).

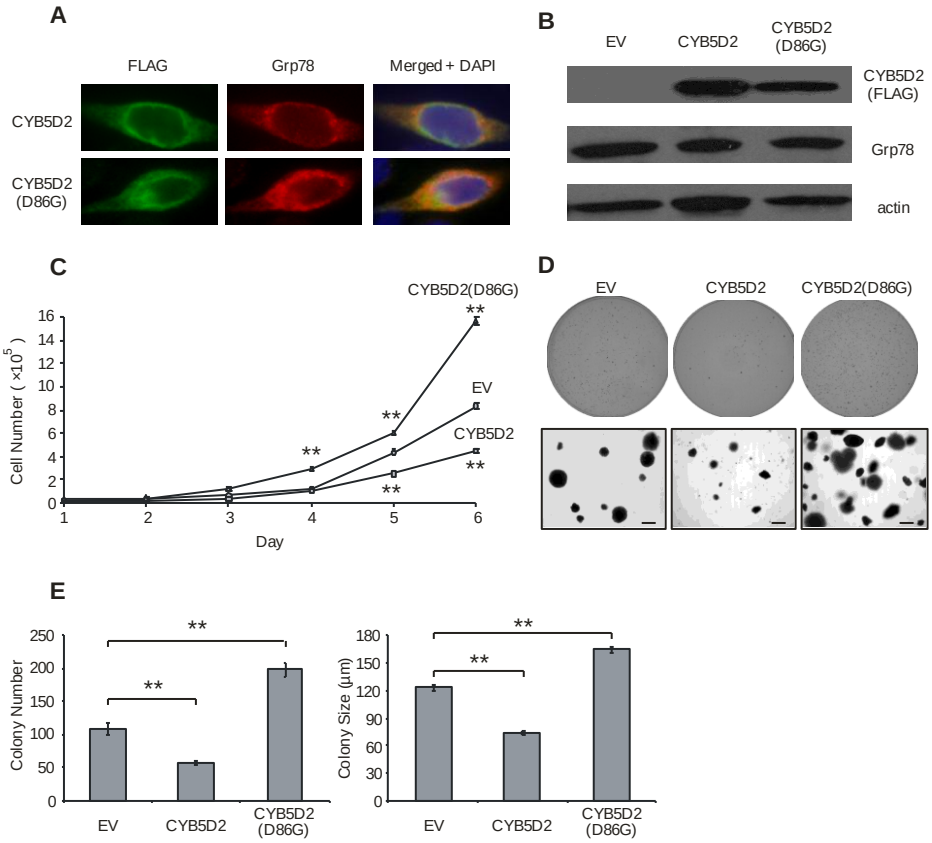
A
FLAG
Grp78
Merged + DAPI
CYB5D2
CYB5D2 (D86G)
B
EV
CYB5D2
CYB5D2 (D86G)
CYB5D2 (FLAG)
Grp78
actin
C
CYB5D2(D86G)
EV
CYB5D2
Cell Number (×10^5)
Day
D
EV
CYB5D2
CYB5D2(D86G)
E
Colony Number
Colony Size (μm)
EV
CYB5D2
CYB5D2 (D86G)

To further investigate the effects of CYB5D2 on HeLa cell proliferation, shRNA CYB5D2 HeLa cells were generated using shRNA lentivrus technologies for CYB5D2 (Santa Cruz, see Materials and Methods) (Figure 5.5A). In comparison to shRNA HeLa treated cells, CYB5D2 shRNA enhanced HeLa cell proliferation (Figure 5.5B). In addition, knockdown of CYB5D2 in HeLa cells increased their anchorage-independent growth, in terms of colony number and size, compared to shRNA HeLa treated cells (Figure 5.5C, D). Collectively, these results reveal that the heme-binding activity of CYB5D2 is required for CYB5D2 to inhibit HeLa cell growth under anchorage-dependent and independent conditions, which results in a loss of function of CYB5D2 similar to the shRNA CYB5D2.

As an effect on proliferation of these stable HeLa cell lines was observed, we examined whether various cell cycle regulators or signalling pathways were affected. Whole cell lysates were prepared from EV, CYB5D2 and D86G HeLa cell lines, as well as shRNA control and shRNA CYB5D2 HeLa cells. As seen in figure 5.6 panel A, phosphorylated serine 473 AKT/PKB levels were unchanged between these cell lines (top panel). Next IkB-α protein levels were also examined and also observed to be unchanged. Cell cycle regulators CyclinD1, CDK inhibitors p27 and p21 were also found to be unchanged.

Similar to what has been previously published, no significant differences were seen in ERK1/2 phosphorylation levels, relative to total ERK levels, (Figure 5.6 B) (Kimura *et al*, 2010).

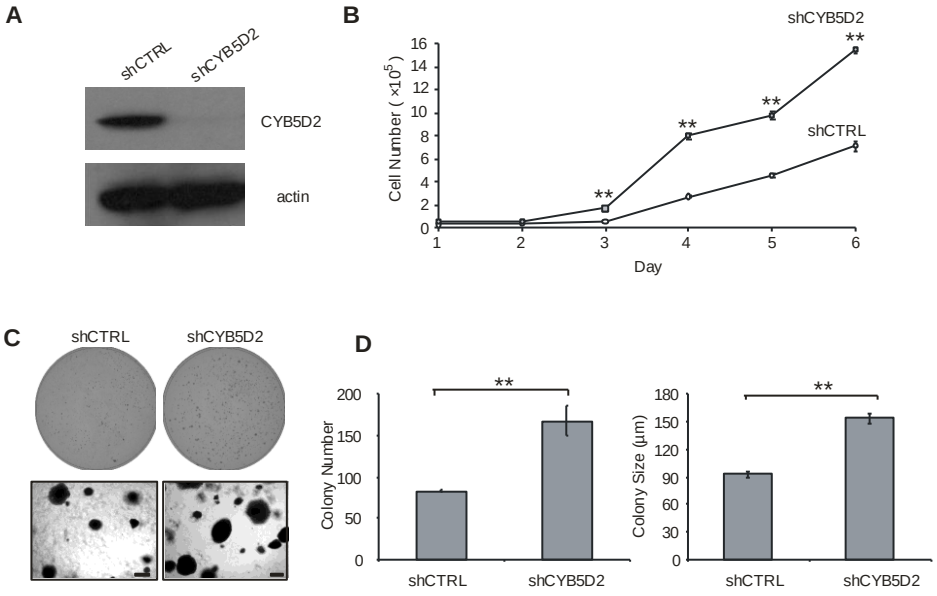

Figure 5.5 CYB5D2 knockdown promotes adherent cell proliferation and anchorage-independent growth of HeLa cells. A. Western blot analysis of HeLa cells following CYB5D2 shRNA-mediated knockdown (shCYB5D2) compared to shRNA control (shCTRL) HeLa cells. B. Cell proliferation of HeLa cells following CYB5D2 knockdown. Experiments were conducted in quadruplicate, with triplicate replicates in each experiment. Cell numbers determined at each time point are presented as mean ± SD. $^{**}P < 0.01$ (two-tailed independent Student's *t*-test). C. Anchorage-independent growth. Representative images of soft agar plates (top panels) and phase contrast images of colonies at 50x magnification (bottom panels). Scale bar is equal to 200 µm. D and E. Mean number and diameter of colonies in 10 random fields. $^{**}P < 0.01$ (two-tailed independent Student's *t*-test).

Figure 5.6 Examination of cell cycle regulators, IκB-α protein levels, AKT/PKB and ERK signal activation in CYB5D2-expressing and CYB5D2 loss-of-function HeLa cells. A. Western blot analysis of empty vector (EV), CYB5D2 and CYB5D2(D86G)-expressing HeLa cells (left panels), or shRNA control (shCTRL) and CYB5D2 shRNA-mediated knockdown (shCYB5D2) HeLa cells (right panels). Expression of cyclinD1, IkB-α, p21 and p27 proteins were examined. AKT activation was determined by examining the phosphorylation of AKT at the Serine 473 residue (AKT-P). B. ERK signalling activation was examined using a phosphorylated ERK 1/2 antibody.

Figure 5.6

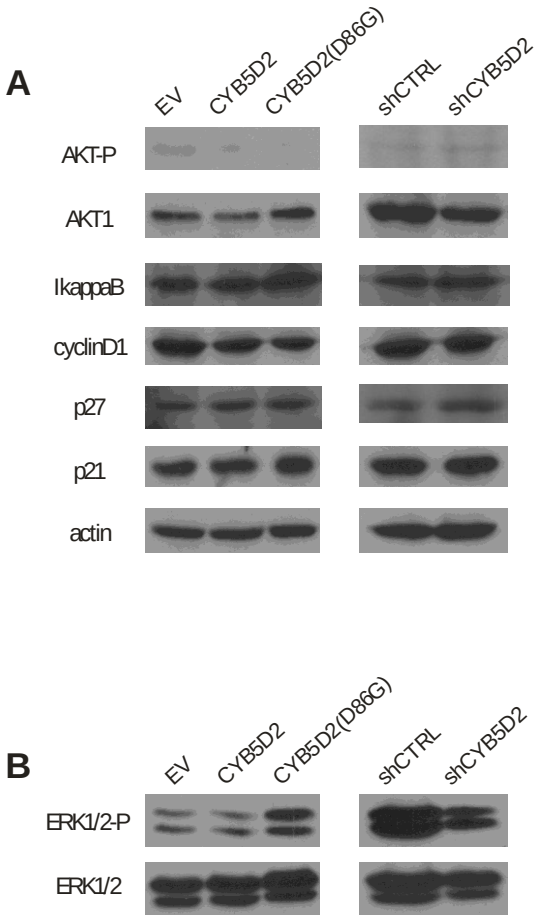
A
EV
CYB5D2
CYB5D2(D86G)
shCTRL
shCYB5D2
AKT-P
AKT1
IkappaB
cyclinD1
p27
p21
actin
B
EV
CYB5D2
CYB5D2(D86G)
shCTRL
shCYB5D2
ERK1/2-P
ERK1/2

5.4 Heme binding of CYB5D2 is required for survival from chemotherapeutic compounds

Previously, PGRMC1 has been shown to confer survival from chemotherapeutic drugs. A PGRMC1 (D120G) heme binding defective mutant was overexpressed in MCF7 cells, to asses susceptibility to the drugs doxorubicin and cisplatin (Crudden *et al*., 2006). This PGRMC1(D120G) decreased cellular viability to these drug treatments. Moreover, we have previously demonstrated CYB5D2 overexpression in HeLa cells, conferred survival from etopiside (Xie *et al*., 2011). Using deletion mutants, both the transmembrane domain and the cytochrome b5 domain were required for CYB5D2`s ability to confer survival (Xie *et al*., 2011). Initially, we sought out whether CYB5D2 could confer survival from paclitaxel and cisplatin. As seen in figure 5.6, dose curves were carried out for 24 and 48 hours, using CYB5D2 HeLa, D86G HeLa, and control EV HeLa cells.

HeLa cells expressing ectopic CYB5D2 were more resistant to increasing concentrations of paclitaxel and cisplatin treatment, using a concentration range which has previously been shown to be effective at reducing HeLa cell viability after 48 h treatment (Osmak and Eljuga 1993; Lee *et al*., 2005). Furthermore, CYB5D2(D86G) expression resulted in increased susceptibility towards paclitaxel and cisplatin treatment in a dose-dependent fashion

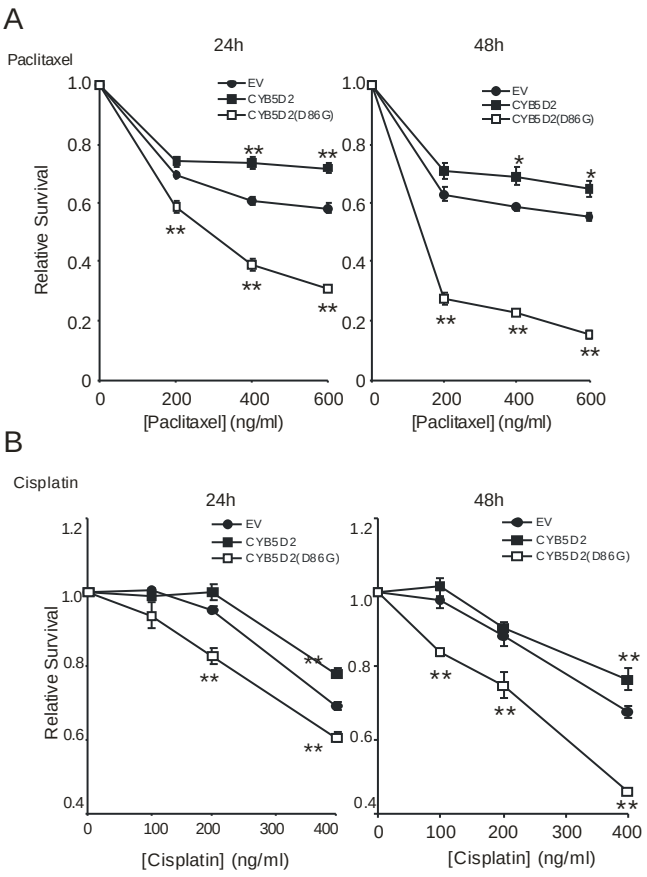

Figure 5.7 Dose-dependent response curves following treatment of HeLa cells with Paclitaxel and Cisplatin. Relative survival of paclitaxel and cisplatin-treated HeLa cells expressing ectopic CYB5D2 or CYB5D2(D86G) compared to empty vector (EV) control cells. Cells were treated with increasing concentrations of paclitaxel or cisplatin for 24 hours (h) (left panels) or 48 h (right panels). All values are mean +/- SD, (n=3), *p < 0.05; **p < 0.01 (two-tailed independent Student's t-test).

A significant difference in CYB5D2 resistance, and CYB5D2(D86G) sensitivity, was observed, following paclitaxel or cisplatin treatment (Figure 5.7). This was most noticeable at doses of 400 ng/ml following 24 h and 48 h for both drug treatments. Therefore, we evaluated the sensitivity of CYB5D2 knockdown cells following paclitaxel and cisplatin treatment at a concentration of 400 ng/ml for 24h and 48 hours.

Treatment of CYB5D2-expressing HeLa cells with both paclitaxel and cisplatin at 400 ng/ml resulted in enhanced cell survival relative to EV (control) HeLa cells (Figure 5.8). Conversely, the CYB5D2(D86G) HeLa cells demonstrated an increased susceptibility to both paclitaxel and cisplatin after 24h and 48 h, relative to control (EV) cells (Figure 5.8). Furthermore, CYB5D2 shRNA knockdown resulted in HeLa cell susceptibility following both paclitaxel and cisplatin treatments at 400 ng/ml, relative to shCTRL cells (Figure 5.8).

Lastly, treatment of these HeLa cell lines with doxorubicin (10 μM) also demonstrated that CYB5D2 expression conferred cell survival, while loss of function (CYB5D2(D86G) and CYB5D2 knockdown) reduced HeLa cell survival relative to control (Figure 5.9). This doxorubicin concentration was consistent with a ~75% reduction in HeLa cell viability after 48 hour treatments (Zhang *et al.*, 2006). Taken together, these results demonstrate that CYB5D2 confers survival from chemotherapeutic compounds, which is dependent on its ability to bind heme.

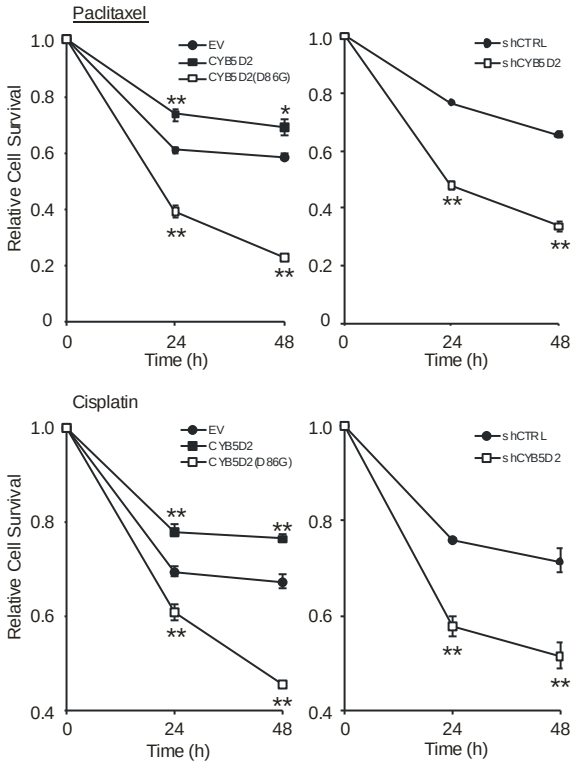

Figure 5.8 CYB5D2 confers survival from Paclitaxel and Cisplatin, while the D86G and shRNA display susceptibility. Relative survival of HeLa cells expressing ectopic CYB5D2 or CYB5D2(D86G) compared to empty vector (EV) control cells (left panels), or shRNA control (shCTRL) and CYB5D2 shRNA-mediated knockdown (shCYB5D2) HeLa cells (right panels), following treatment with either paclitaxel (400 ng/ml), cisplatin (400 ng/ml) for 24 and 48 h. All values are mean +/- SD, n=3, *$p < 0.05$; **$p < 0.01$ (two-tailed independent Student's *t*-test).

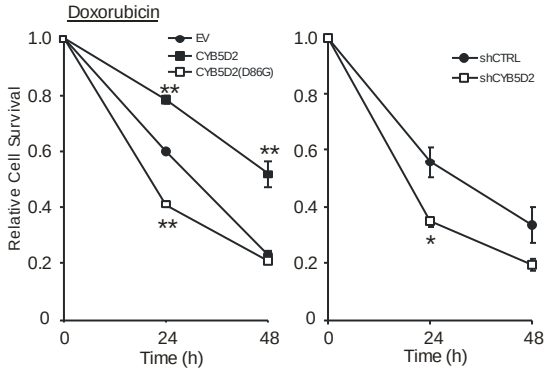

Figure 5.9 CYB5D2 confers survival from Doxorubicin. Relative survival of HeLa cells expressing ectopic CYB5D2 or CYB5D2(D86G) compared to empty vector (EV) control cells (left panels), or shRNA control (shCTRL) and CYB5D2 shRNA-mediated knockdown (shCYB5D2) HeLa cells (right panels), following treatment with either Doxorubicin (10 μM) for 24 and 48 h. All values are mean +/- SD, n=3 *p < 0.05; **p < 0.01 (two-tailed independent Student's t-test).

5.5 Generation and characterization of EV, CYB5D2, D86G, shRNA control and shRNA CYB5D2 Huh7stable cell lines: Heme binding is required for CYB5D2 to regulate proliferation in Huh7 cells.

As the previous studies on CYB5D2 were done in HeLa cells, experiments were performed to test if CYB5D2 had the same effect on a different cell line. Stable Huh7 cell lines expressing and EV (pLHCX), the wild type CYB5D2 and D86G were generated, according to our previously described methodologies. Lystaes were prepared and subsequent western blots performed using the M2-Flag antibody to confirm successful stable expression (Figure 5.10 A). Additionally, shRNA CYB5D2 stable Huh7 cell lines were also generated as well as a shRNA Huh7 stable cell line, as previously described. The carboxyl CYB5D2 antibody was used to confirm successful knockdown in the CYB5D2 shRNA Huh7 cell line, right panel (Figure 5.10 B).

These stable Huh7 cell lines were then seeded in 12 well dishes and growth curves were performed as previously described. As seen in figure 5.10 C, the CYB5D2 Huh7 proliferated slightly faster than EV Huh7 (not statistically significant), and the D86G Huh7 cells grew significantly slower. The shRNA CYB5D2 Huh7 cells also proliferated slower than shRNA control cells (Figure 5.10 D). This result is the opposite effect on proliferation that is seen in HeLa cells for the D86G and shRNA CYB5D2.

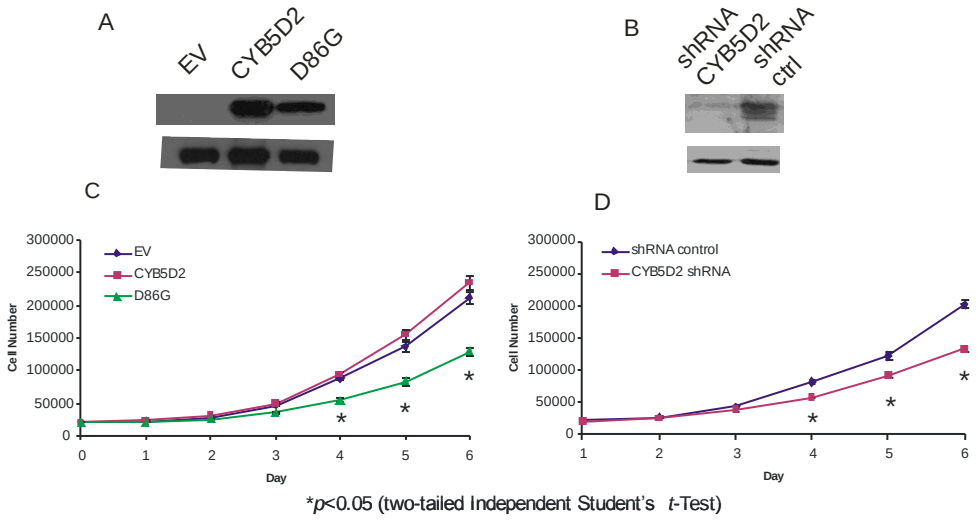

Figure 5.10 Generation of EV, CYB5D2, D86G, shRNA CYB5D2 and control shRNA Huh7 cell lines A. CYB5D2 and D86G stable Huh7 cells. 293T cells were transfected with CYB5D2 and D86G (pLHCX) retrovirus, along with GP and VSV retroviral packaging plasmids. 48 hours post-transfection, viral media from these 293T was used to infect Huh7 cells. Hygramycin was then used to select for stable EV,CYB5D2 and D86G expressing Huh7 cells. B. A Santa Cruz CYB5D2 shRNA lentiviral pool was used to package lentivirus made in 293T cells, and infect Huh7 cells. An scrambled shRNA lentivirus was used as a control. Cells were selected with Puromycin for 10 days. Lysates were prepared and western blots probed with the anti-CYB5D2 antibody. C and D. The D86G and shRNA CYB5D2 inhibit proliferation. All Huh7 cell lines were seeded into 12 well plates, $10x10^3$cells per well, and counted for 6 days. All data points represented by mean +/- standard error, n=4. *$p < 0.05$; **$p < 0.01$ (two-tailed independent Student's *t*-test).

As these shRNA CYB5D2 Huh7 cells exhibited a reduction in proliferation in adherent culture, we examined their effect on non-adherent Huh7 cells in soft agar colony formation. These shRNA CYB5D2 Huh7 cells and a shRNA control Huh7 cell line were used in soft agar assays to asses growth in an anchorage independent scenario. As seen in figure 5.11 A, the shRNA CYB5D2 Huh7 cells developed fewer colonies and smaller colonies than the shRNA control Huh7 cells, after five weeks of growth in soft agar (data not quantified).

In order to examine an *in vivo* tumorigenic scenario, immuno-comprimised NOD/SCID mice were used to assess xenograft tumor forming capacity of these Huh7 cell lines. Approximately 1 million cells of each cell line was mixed with 1 ml of matrigel. This cell and matrigel mixture was then injected into the flanks of five mice (each side), for each cell line. Tumor growth was measured every week for five weeks. As seen in figure 5.11 B the shRNA Huh7 cells were severely impaired in their ability to form tumors, relative to an shRNA Huh7 cell line that formed large tumors after five weeks (Figure 5.11 B).

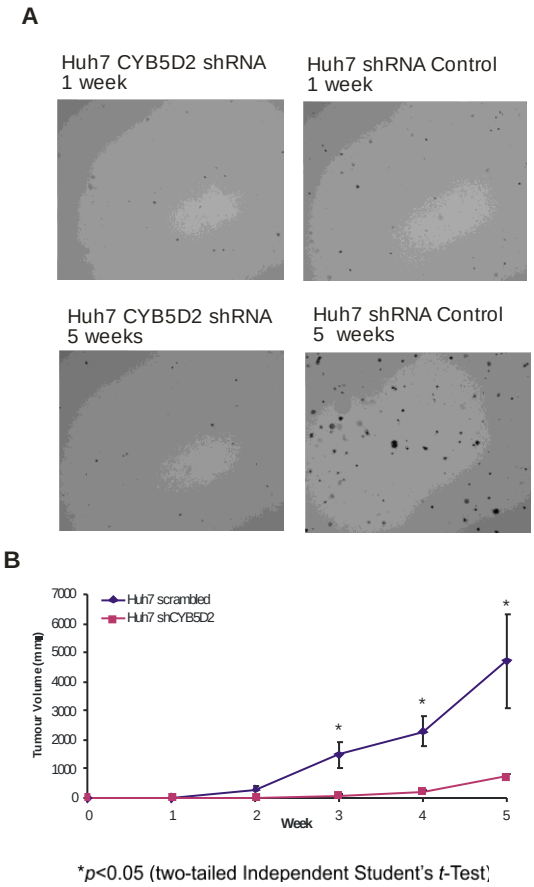

Figure 5.11 CYB5D2 is required for Huh7 tumor formation. A. Soft agar assays were performed with shRNA Huh7 and shRNA CYB5D2 Huh7 cells. After 5 weeks, the shRNA Huh7 cells formed numerous large colonies, while the shRNA CYB5D2 Huh7 cells did not (data not quantified). B. NOD/SCID mice xenografts of shRNA control Huh7 and shRNA CYB5D2 Huh7 cells. After five weeks, the shRNA control huh7 developed larger tumors. The shRNA CYB5D2 Huh7 cells had significantly smaller tumors. Date points represent mean +/- standard deviation, n=5. A two-tailed student`s T-test was used to determine significance, $p<0.05$ *.

Chapter 6. Heme binding of CYB5D2 is required for inhibition of SREBP signalling

Using a novel photo-activated cross-linking method, researchers demonstrated that PGRMC1 associated in a complex with the SCAP and Insig1 proteins (Suchanek *et al.*, 2005). This suggests a role of the MAPR family in regulating SREBP maturation/activation. In order to determine if CYB5D2 could be involved with an ER resident SREBP complex we first wanted to see if CYB5D2 localized to the ER. We started with 293T cells that were transfected with ectopic CYB5D2 via calcium phosphate method. An ER (KDEL) marker was then used in indirect immunofluorescence (Figure 6.1). When CYB5D2 was stained with an M2 Flag antibody and rhodamine red secondary, and the ER stained with a KDEL antibody and FITC Green secondary, merged images show that CYB5D2 and KDEL signals overlap, revealing CYB5D2 localized to the ER. As CYB5D2 now resides in the ER, we proceeded to examine whether CYB5D2 could affect sterol/SREBP signalling. Specifically, we tested if CYB5D2 could reduce the transcriptional activity of SREBP using 3xSREBP Responsive Element Reporters. SREBPs bind to promoter regions of sterol regulatory genes that contain non-palindromic sterol regulatory elements and palindromic sequences called E boxes (Shimomura *et al*., 1998). SREBPs bind to DNA sequences of a direct repeat of 5′-PyCAPy-3′ (Magana and Osborne 1996). In the LDL receptor the SREBP recognition site is 5`ATCACCCCAC-3′ which is designated sterol regulatory element 1 (SRE-1) (Yokoyama *et al*. 1993).

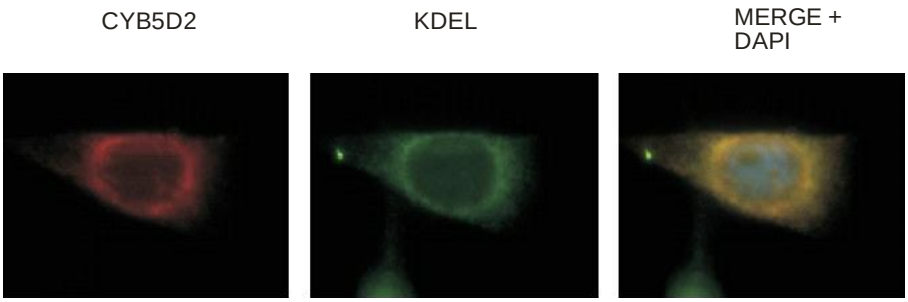

Figure 6.1 CYB5D2 localizes at the ER. 293T cells were transfected with CYB5D2 and stained for M2 Flag (rhodamine red secondary), and KDEL (FITC Green secondary). CYB5D2 (Red) co-localized with KDEL (Green) revealing an ER locale (Merge). Dapi was used to stain the nucleus (blue).

Initially, we started by using a 3xSRE-GFP (Green Fluorescent Protein) reporter. This reporter contained 3x DNA binding sites of the SREBP1/2 transcription factor, which drives the transcriptional activity of a GFP gene. Transiently, 5 μg of CYB5D2 and 5 μg Empty Vector (EV; pcDNA3) were each co-transfected with 5 μg of this 3xSRE-GFP promoter reporter into 293T cells via calcium phosphate. As the expression of SRE-GFP depends on endogenous SREBP activity, the readily detected fluorescence signal in cells transfected with SRE-GFP plus an empty vector (EV) demonstrated the existence of high levels of active SREBP activity in 293T cells (Figure 6.2A). The EV transfected samples showed a high level of 3xSRE-GFP activity in 293T cells. However when CYB5D2 was co-transfected with this reporter, a dramatic reduction of this high endogenous basal level of 3xSRE-GFP was observed. To test if CYB5D2 reduced GFP levels of the 3xSRE-GFP due to the translational inhibition of the GFP protein, a CMV-GFP was transfected with the EV (pcDNA3) and with CYB5D2 into 293T cells. CYB5D2 did not affect the CMV-GFP levels relative to the EV control. Thus CYB5D2 reduced 3xSRE-GFP activity due to a specific reduction of SREBP transcriptional activity (Figure 6.2A).

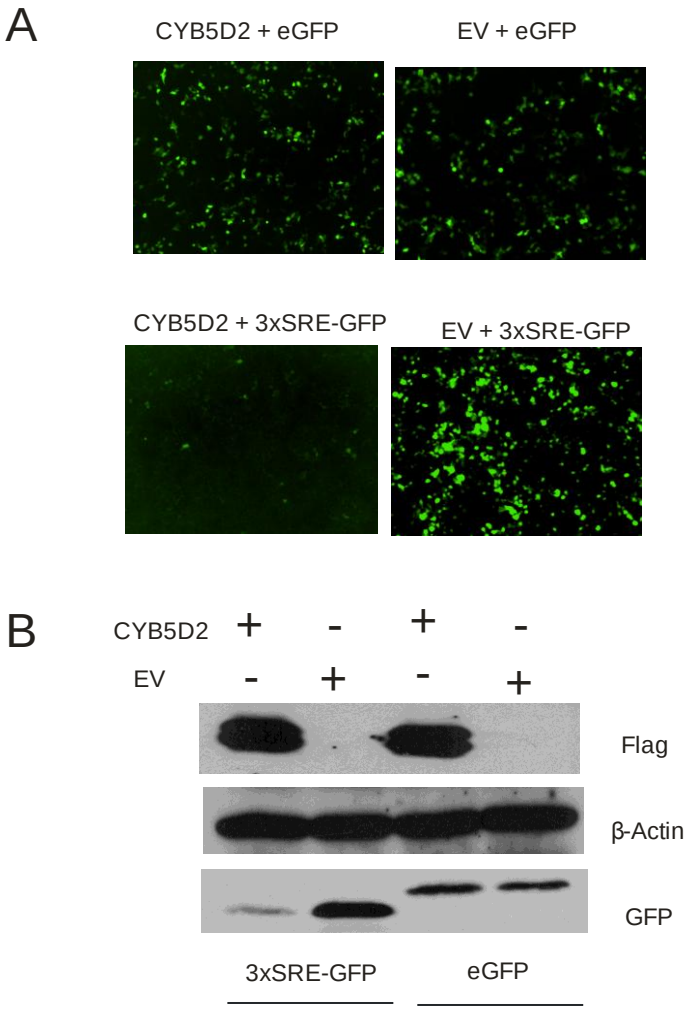

Figure 6.2 CYB5D2 inhibits a 3xSRE-GFP reporter. A 3xSRE-GFP reporter (5μg) was transfected with 5μg CYB5D2 plasmid and with 5μg Empty Vector (EV) into 293T cells, via calcium phosphate method. CYB5D2 reduced 3xSRE-GFP protein level, but did not reduce the CMV-GFP protein levels. Lysates from 293T cells from figure A were generated. Western blots confirmed that CYB5D2 reduced 3xSRE-GFP protein levels compared to the control (EV). CYB5D2 could not reduce the control CMV-GFP protein levels.

Whole cell lysates from all these samples were prepared and run on SDS-PAGE gels and subsequently transferred to nitrocellulose membranes. Western blots were probed with antibodies for GFP and M2 flag-CYB5D2 to confirm these results as seen in figure 6.2 B. CYB5D2 inhibited the 3xSRE-GFP relative to the control EV. CYB5D2 could not repress the CMV-GFP.

To quantify CYB5D2-mediated attenuation of SREBP activity, 239T cells were co-transfected with a 3xSRE-luciferase reporter, and a β-gal plasmid (as an internal control for transfection efficiency), and increasing doses of CYB5D2. Upon normalization to β-galactosidase activity, normalized luciferase assays revealed that CYB5D2 dose-dependently inhibited endogenous SREBP activity of 293T cells (Figure 6.2A). Taken together, the above observations demonstrate that CYB5D2 reduces SREBP-mediated transcriptional activity.

When full length SREBP proteins dissociate from Insig1 in the ER, they are escorted by SCAP, which brings them to the Golgi Apparatus (GA). In the Golgi, they are cleaved by two site directed proteases to generate an NH2 terminal mature fragment. This NH2 terminal fragment, now translocates to the nucleus to transcribe genes for sterol metabolism. To identify the point at which CYB5D2 inhibits SREBP-derived transcriptional activity, 293T cells were transfected with the full length SREBP2 or the NH2 terminal mature form of SREBP2 along with CYB5D2 and the SRE-luciferase reporter, in a dose dependant manner. Normalized luciferase values reveal that cells transfected with the mature active form of SREBP2 elicited higher levels of luciferase activity compared to cells transfected with the full length SREBP2 without the presence

of ectopic CYB5D2 (Figure 6.2A). When these forms of SREBP2 were co-transfected with CYB5D2 in a dose dependant manner, CYB5D2 inhibited the activation of the 3xSRE-Luciferase by this full length SREBP2 in a dose dependant manner. However, the robust activation from the N-terminal fully processed SREBP2 cDNA (nuclear only, and constitutively active), was refractory to CYB5D2 inhibition in a dose independent manner (Figure 6.3 A).

Similarly, a full length SREBP1c and an amino terminal mature SREBP1c were transfected into 293T along with CYB5D2 in a dose dependant manner. Here, the full length SREBP1c was able activate the 3xSRE-Luciferase in a dose dependant manner, and this activation was inhibited by CYB5D2. The amino terminal mature NH2-SREBP1c potently activated the 3xSRE-Luciferase reporter. Similarly, CYB5D2 was unable to inhibit this robust activation of the 3xSRE-Luciferase reporter by NH2-SERBP1c (Figure 6.3 B). Collectively, these observations reveal that CYB5D2 inhibits the maturation process of SREBP at the point in ER retention.

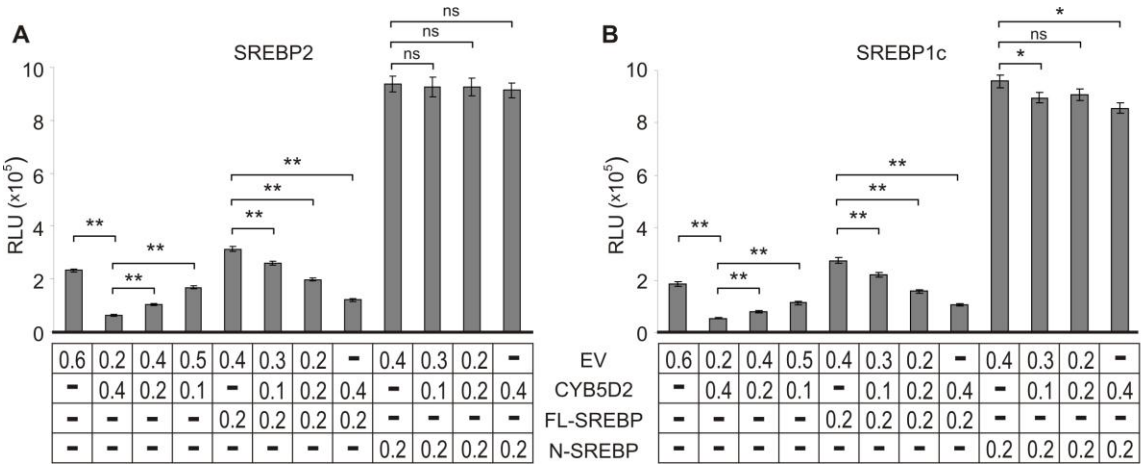

Figure 6.3 CYB5D2 inhibits 3xSRE Luciferase Activity. CYB5D2 was co-transfected in increasing amounts, along with 0.5 μg of a 3xSRE-Luciferase construct, and resulted in a dose dependent decrease of 3xSRE-Luciferase activity. A. CYB5D2 decreased the activity that a full length SREBP2 plasmid conferred on a 3xSRE-Luciferase reporter in a dose dependent manner. CYB5D2 was unable to inhibit the activity of an NH2 terminal SREBP2 mature form, which potently activated the 3xSRE-Luciferase reporter. B. CYB5D2 was transfected in increasing amounts, along with 0.5 μg of a 3xSRE-Luciferase reporter construct, and resulted in a dose dependent decrease of 3xSRE-Luciferase activity. CYB5D2 decreased the 3xSRE-Luciferase activity of a full length SREBP1c plasmid. CYB5D2 was unable to inhibit the highly potent activation of the 3xSRE-Luciferase reporter by an N-terminal SREBP1c plasmid. All relative luciferase unit (RLU) values are represented as mean +/- standard deviation (n=3). * $p < 0.05$; ** $p < 0.01$ (two-tailed Student's *t*-test). Abbreviations: full-length SREBP (FL-SREBP), N-terminal SREBP (N-SREBP), ns (not significant).

6.1 CYB5D2 Co-Immunoprecipitates with Insig1

Since an essential step governing SREBP maturation is the release of the SREBP/SCAP complex from Insig1 association, it is possible that CYB5D2 inhibits SREBP maturation via binding to Insig1. As previously mentioned, researchers used a novel photo-cross-linking method to demonstrate that PGRMC1 could be detected in a complex with SCAP and Insig1 (Suchanek *et al*., 2005). Using this information, we set out to examine if CYB5D2, like PGRMC1, could also interact with SCAP and Insig1.

In order to test for an interaction between CYB5D2 (Flag tagged) and Insig1 (myc tagged), 10 μg of each cDNA were transfected via calcium phosphate method into 293T cells. Lysates were prepared from these transfected cells, and co-immunoprecipitations were performed. These samples were subsequently run on a 12% SDS PAGE gels then transferred to western blots. As seen in figure 6.4 panel A, a Flag-CYB5D2 immunoprecipitation pulled down Insig1-myc, when both were co-transfected. When this western blot from panel A was re-probed with an M2 Flag antibody (for CYB5D2), myc-Insig1 immunoprecipitation pulls down flag-CYB5D2 (Figure 6.4 panel B). Conversely, in panel C, when both are co-transfected, a myc-Insig1 immunoprecipitation pulls down flag-CYB5D2, but not a negative control of flag-CYB5D2 alone.

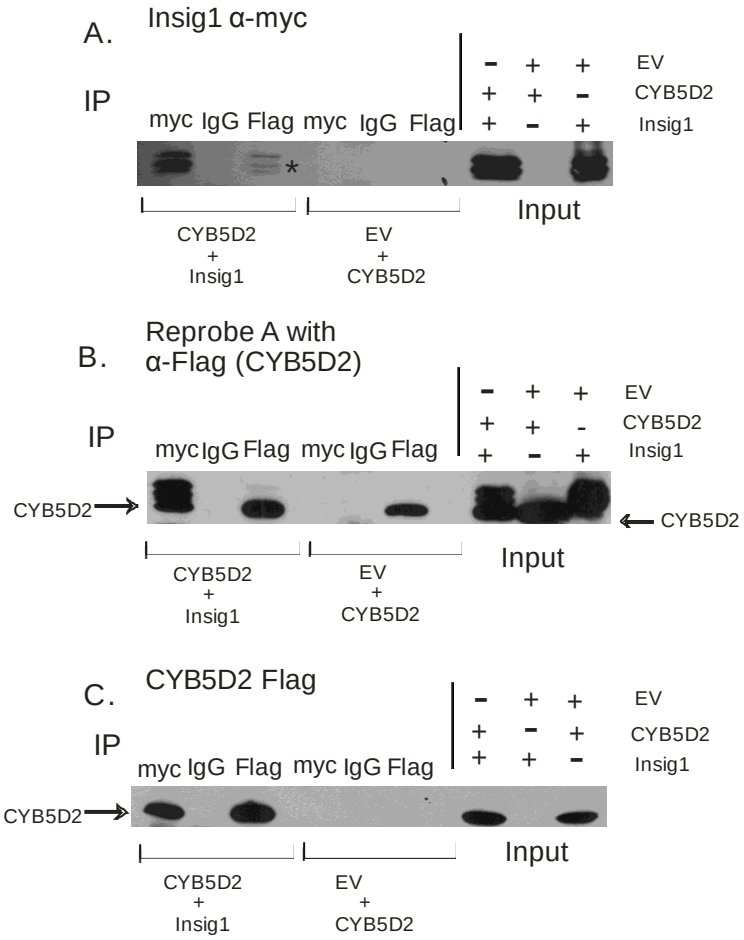

Figure 6.4 CYB5D2 co-immunoprecipitates with ectopic Insig1. Flag tagged CYB5D2 (10 μg) and myc tagged Insig1 (10 μg) were transfected seperately and together in 293T cells. Subsequently immunoprecipitations were performed. A. Flag CYB5D2 immunoprecipitation brings down Insig1(myc), asterisk (*). B The Western blot from figure A is reprobed with an M2 Flag antibody for CYB5D2, which co-immunoprecipitates with a myc (Insig1) co-immunoprecipitation. C. When Insig1-myc and CYB5D2 are co-transfected together, a myc-Insig1 immunoprecipitation pulls down an M2 flag tagged CYB5D2 (co-immunoprecipitation).

6.2 CYB5D2 Stabilizes Ectopic Insig1

The observations that CYB5D2 binds Insig1, and inhibits SREBP maturation suggest that CYB5D2 could stabilize Insig1. An increase of Insig1 protein stability could retain the SREBP/SCAP complex in the ER, whereas a decrease in the stability on Insig1 might result in the ER exit of the complex, a step that is required for SREBP maturation. Thus we wanted to see if CYB5D2 could potentiate the stability of Insig1. Here in figure 6.5 10 μg each of myc-Insig1 plasmid was co-transfected with 10 μg of CYB5D2 (pcDNA3) plasmid. This was compared to a control transfection of 10 μg EV (pcDNA3) plus 10 μg Insig-1. All plasmids were transfected into a 10 cm plate of 293T cells via calcium phosphate method, and allowed to express for 24 hours. These transfected cells were then trypsonized and then re-seeded into 6 well plates to accommodate for any transfection differences between time points. These cells were then treated with cyclohexamide (an inhibitor of protein translation) for the indicated times: 30 minutes, 60 minutes and 120 minutes. Cell lysates were prepared and 100 μg were run on an SDS-PAGE and then transferred to western blots. Western blots were probed for the indicated Ab: myc-Insig1, flag-CYB5D2 and β-Actin as an internal loading control.

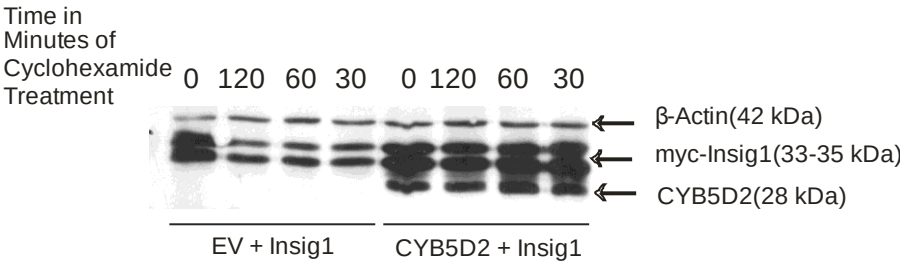

Figure 6.5 CYB5D2 stabilizes ectopic Insig1. Ectopic Insig1-myc (10 μg) was co-transfected with CYB5D2 (10 μg) and with an Empty Vector pcDNA3 (10 μg) into 293T cells in 10 cm plates. Twenty four hours after transfection, cells were trypsonized and re-seeded into 6 well plates. Cells were eventually treated with cyclohexamide for the indicated times 0, 30, 60, and 120 minutes. Subsequently lysates were prepared, SDS-PAGE gels were run and western blots performed. CYB5D2 ectopic expression resulted in higher amounts (or more stable levels) of Insig1, at all time points of cyclohexamide treatments, relative to the EV + Insig1 control samples.

CYB5D2 resulted in increased Insig1 levels throughout all times for cyclohexamide treatments, compared to lower levels of Insig1 when transfected with the EV (pcDNA3) control (Figure 6.5). CYB5D2 increased the overall stability of INSIG1.

The cyclodextran HPCD to acutely causes an efflux of cholesterol from the membranes of cells, resulting in the activation of the SREBP signalling pathway. As CYB5D2 has been demonstrated to inhibit SREBP signalling, we examined if SREBP activation stimulated by HPCD could be blocked by CYB5D2. EV and CYB5D2 HeLa cells were culutred in 5% FBS conditions, 0.5% Lipoprotein serum conditions, and 0.5% lipoprotein free serum plus 1% HPCD for one hour. In these conditions we examined the cleavage of both SREBP1 and SREBP2, and if CYB5D2 could prevent this cleavage. HPCD treatment induced the maturation of SREBP1 and SREBP2 in EV HeLa cells, based on reduction of the SREBP1 and SREBP2 full length proteins and the generation of the NH2-terminal SREBP2 fragment (Figure 6.6). This maturation process was compromised in HeLa CYB5D2 cells (Figure 6.6).

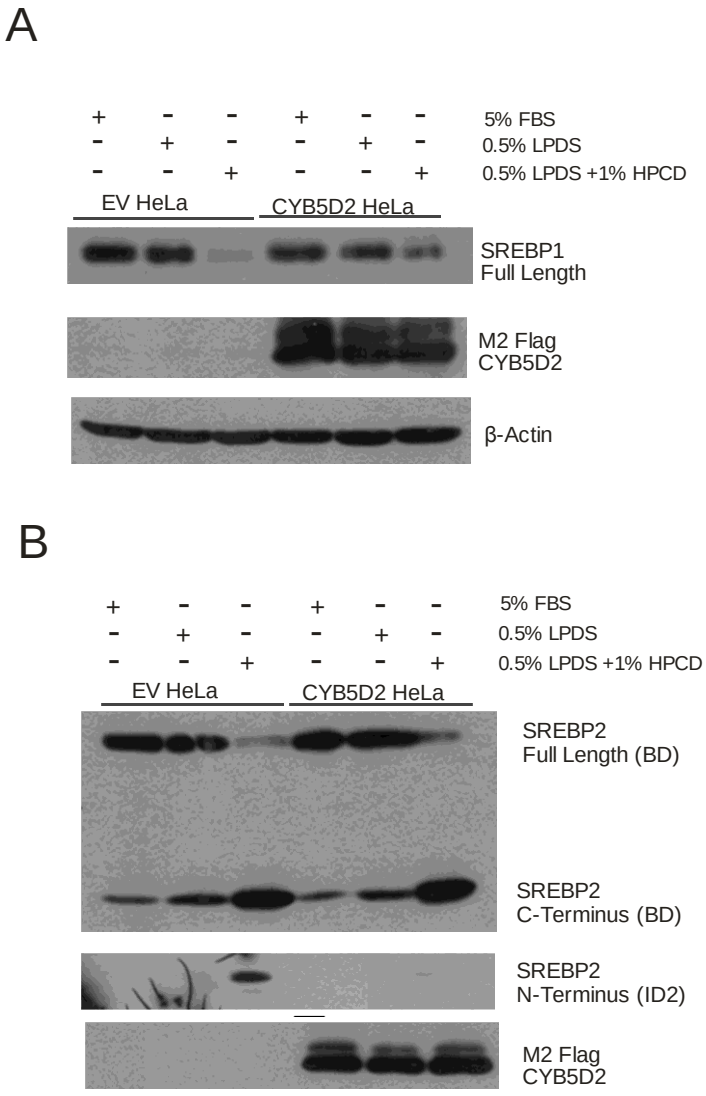

Figure 6.6 CYB5D2 impairs HPCD induced cleavage of SREBP 1 and SREBP2. EV and CYB5D2 HeLa cells were cultured in indicated conditions; 5% FBS for 24 hours, 0.5% LPDS for 24 hours, and 0.5% LPDS for 24 hours plus 1% HPCD for 1 hour. Whole cell lysates were prepared, run on SDS PAGE gels, followed by western blot analysis for the indicated proteins or protein fragments. LPDS: lipoprotein deficient serum.

6.3 The Transmembrane domain and heme binding are required for CYB5D2 to inhibit SREBP signalling

Recently, three polymorphisms of CYB5D2 were constructed by Dr. Damu Tang and Dr. YanYun Xie. Two arginine 7 mutants of CYB5D2 an R7 to proline and an R7 to glycine, were observed in Gene Ontology searches for consensus coding sequences of human colorectal cancer (Sjoblom *et al*., 2006). A third naturally occurring polymorphism was observed in further studies of the NIH full length cDNA project Mammalian Gene Collection (MGC) (Ota *et al*., 2004, Gerrard *et al*., 2004), a glutamine at 167 changed to a lysine, Q167K. Site directed mutagenesis was subsequently performed generating these CYB5D2 mutants. A schematic diagram of these mutants is shown (Figure 6.7 A). These cDNAs were then transfected into 293T cells and allowed to express for 48 hours. Lysates were prepared and run on SDS-PAGE gels, and subsequent western blots were probed with an M2 Flag antibody to confirm expression of each mutant (Figure 6.7 B).

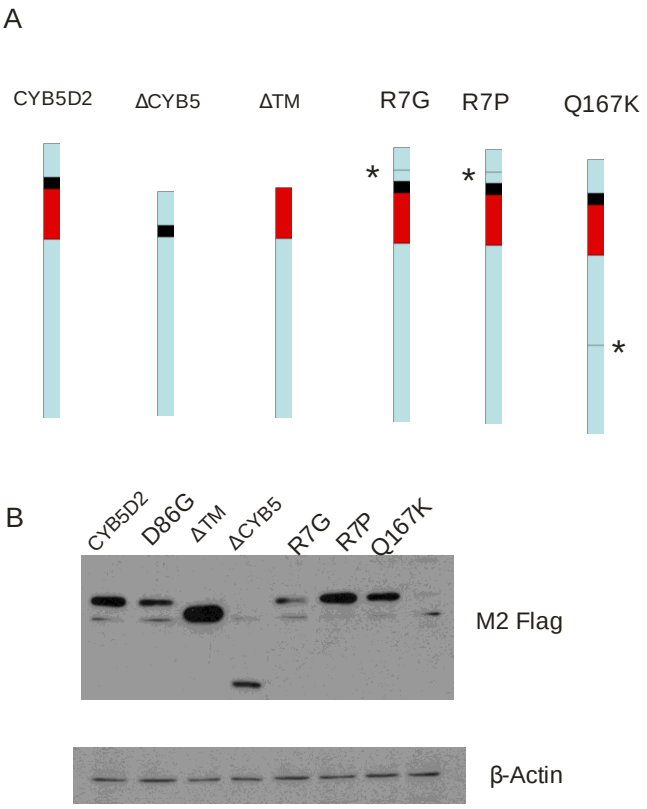

Figure 6.7 Schematic diagram and expression of two CYB5D2 deletion mutants, and three CYB5D2 polymorphism mutants. A. CYB5D2 mutants were contsructed by Dr. Damu Tang and Dr. YanYun Xie. Full Length CYB5D2 of 792 bp or 264 amino acids. A 300 bp pair region corresponding to the cytochrome heme binding region (red) was deleted (nt 103-389). The transmembrane domain at the amino terminus (black) was deleted (nt 1-87). Two Gene Ontology reported polymorphisms a R7P (*) and a R7G (*) have been reported for MGC32124/CYB5D2 in colorectal cancer. A Q167K (*) polymorphism has also been reported. B. All cDNAs were transfected into 293T cells via calcium phosphate and 48 hours later whole cell lysates were prepared. SDS-PAGE gels were run and subsequent western blots probed with an M2 Flag antibody. Beta-Actin was used as a control.

Subsequently these mutants, were tested for their capability to inhibit SREBP signalling, as wild type CYB5D2 could. These five mutants, along with a wild type CYB5D2 cDNA were co-transfected into 293T cells with a 3xSRE-Luciferase reporter, and a β-gal SV40 plasmid. Luciferase assays were performed and normalized to the internal β -gal value. As seen in figure 6.8, the ΔTM and the ΔCYB5D were unable to repress the 3xSRE-luciferase reporter like CYB5D2 could. The three polymorphisms mutants, however, were all able to repress the 3xSRE-Luciferase, similar to wild type CYB5D2. Therefore, the transmembrane domain, and the heme binding domain were required for CYB5D2 to inhibit 3xSRE reporter activity.

In order to further pinpoint the residues responsible for the requirement of heme binding in inhibiting SREBP signalling, the heme binding domain mutants Y73A, Y79A, Y127A and D86G, and EV pcDNA3 and CYB5D2 were transfected into 293T cells along with a 3xSRE-Luciferase reporter and a β-gal plasmid. Luciferase assays were performed and normalized to the internal β-gal value. The CYB5D2(D86G) Heme binding defective mutant could not repress the 3xSRE-Luciferase reporter, the way the wild type CYB5D2 and other heme domain mutants could (Figure 6.8). Collectively, these experiments establish that the transmembrane domain of CYB5D2 and heme binding of CYB5D2 are required to inhibit SREBP activation.

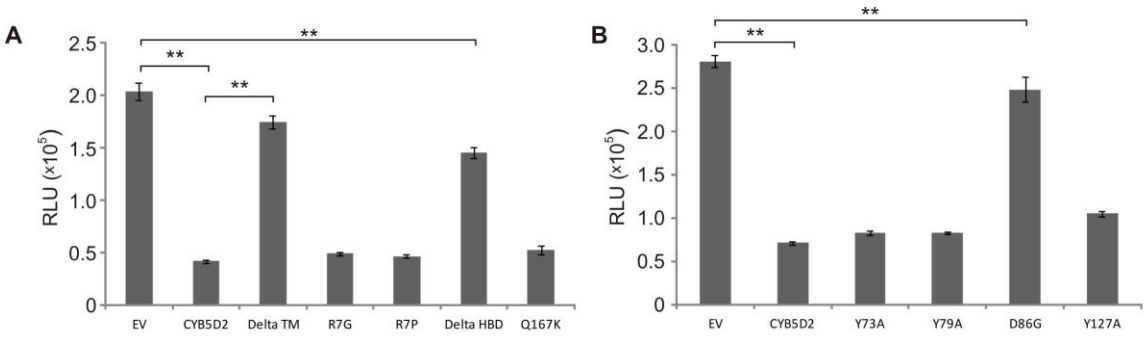

Figure 6.8 The transmembrane domain, and heme binding are required for CYB5D2 to inhibit SREBP signalling. A. Empty vector (EV; pcDNA3), wild-type CYB5D2, a deletion of the transmembrane region (Delta TM), three polymorphism mutants (R7P, R7G and Q167K), and a 300 bp deletion of the heme binding domain (Delta HBD) were co-transfected into 293T cells with a 3xSRE-Luciferase reporter. Luciferase values were normalized with β-galactosidase (β-gal) assay controls. The Delta TM plasmid and the Delta HBD mutant could not inhibit the 3xSRE-Luciferase reporter. B. Empty vector (EV; pcDNA3) and CYB5D2 constructs (CYB5D2, Y73A, Y79A, D86G, Y127A) were transfected into 293T cells along with a 3xSRE-Luciferase reporter and (β-gal) plasmid. Luciferase assays were performed and normalized to β-gal assay values. All CYB5D2 cDNAs inhibited 3xSRE-Luciferase activity except the heme binding defective mutant CYB5D2(D86G) relative to EV control. All relative luciferase unit (RLU) values are represented as mean +/- standard deviation (n=3). ** $p < 0.01$ (two-tailed Student's *t*-test).

6.4 The D86G CYB5D2 destabilizes ectopic Insig1.

As the wild type CYB5D2 could stabilize Insig1, we next examined if the CYB5D2(D86G) functioned in a similar or possibly different manner. As CYB5D2 inhibited SREBP signalling, and the D86G heme binding defective mutant could not, we sought to determine if this was through the stabilization of Insig1. Therefore, 10 μg each of myc-Insig1 was co-transfected with 10 μg D86G and compared to a control of 10 μg EV pcDNA3 plus 10 μg Insig-1. All plasmids were transfected into 293T cells via calcium phosphate method, and 24 hours post-transfection were re-seeded into 6 well plates, as described previously. These cells were then treated with cyclohexamide (an inhibitor of protein translation) for the indicated times: 30 minutes, 60 minutes and 120 minutes. Lysates were prepared then run on an SDS-PAGE gels and subsequent western blots performed. Western blots were probed for the indicated antibodies: myc-Insig1, flag-D86G and β-Actin as an internal loading control. As seen in figure 6.8, the D86G resulted in decreased Insig1 levels throughout all times for cyclohexamide treatments, compared to higher levels of Insig1 when transfected with the E V pcDNA3. Therefore CYB5D2 increased the overall stability of Inisg1, but the D86G heme binding defective mutant decreased the stability of Insig1.

While the CYB5D2(D86G) destabilized ectopic Insig1, we examined if this D86G could still co-immunoprecipitate with ectopic Insig1. To test if the D86G heme binding defective mutant could still co-immunoprecipitate with ectopic Insig1, both D86G and Insig1 were co-transfected into 293T cells, and co-immunoprecipitations were performed as described. As seen in figure 6.9, when both D86G and Insig1 were co-transfected,

M2-Flag immunoprecipitations of the D86G pulled down ectopic Insig1 as seen with a myc antibody (Figure 6.9 A). When myc-Insig1 was immunoprecipitated, we see that D86G also co-immunoprecipitates when this western blot is probed with an M2 Flag antibody (Figure 6.9 B). This reveals that CYB5D2 co-immunoprecipitating with Insig1 did not cause its stabilization. This tells us that the heme binding of CYB5D2 is required for the stabilization of Insig1 and inhibition of SREBP signalling.

In order to examine if PGRMC1 could also stabilize ectopic Insig1, both PGRMC1 and Insig1 were co-transfected into 293T cells as previously described. A control sample of EV and Insig1 was also co-transfected. Each plate was re-seeded to 6 well plates, 24 hours lates as described previously, and cyclohexamide was added for the indicated times. Lysates were prepared, run on SDS-PAGE gels and then transferred to western blots. PGRMC1 also promoted the stabilization of ectopic Insig1, relative to an EV pCDNA3.0 (Figure 6.11 A). Experiments were performed exactly as conducted for CYB5D2 and Insig1 cyclohexamide treatments (Figure 6.5). In order to see if PGRMC1 could also inhibit SREBP signalling, 3xSRE-Luciferase assays were performed as previously described. PGRMC1 was co-transfected in a dose dependant manner with a 3xSRE-Luciferase reporter, and a β-Gal plasmid into 293T cells. All values were normalized to β-gal values. As seen in figure 6.11 B, PGRMC1 decreased the 3xSRE-Luciferase reporter in a dose dependant manner.

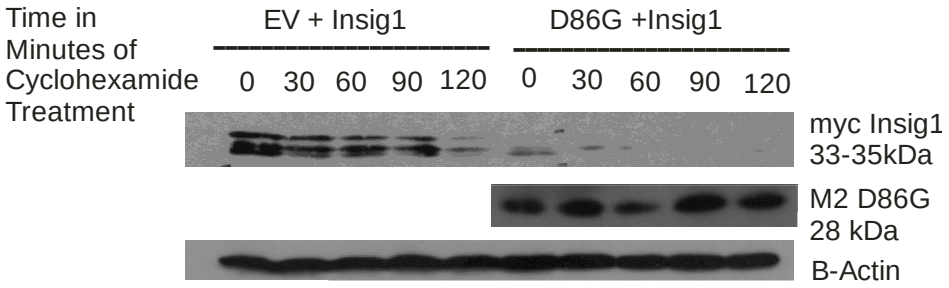

Figure 6.9 The CYB5D2(D86G) heme binding defective mutant destabilizes ectopic Insig1. A 10 cm plate of 293T cells was transfected with 10 μg of Insig1 together with EV pcDNA3, and another plate with 10 μg of CYB5D2(D86G) with 10 μg of Insig1. Twenty-four hours post-transfection, cells from each plate were re-seeded to a 6 well plate. The following day, cells were treated with cyclohexamide for the times indicated (0, 30, 60, 90, and 120 minutes). Cell lysates were generated and 100 μg from each sample was run on a 12% SDS PAGE gel. This gel was transferred to nitrocellulose and probed with the antibodies indicated. This experiment was re-produced three separate times with this same result.

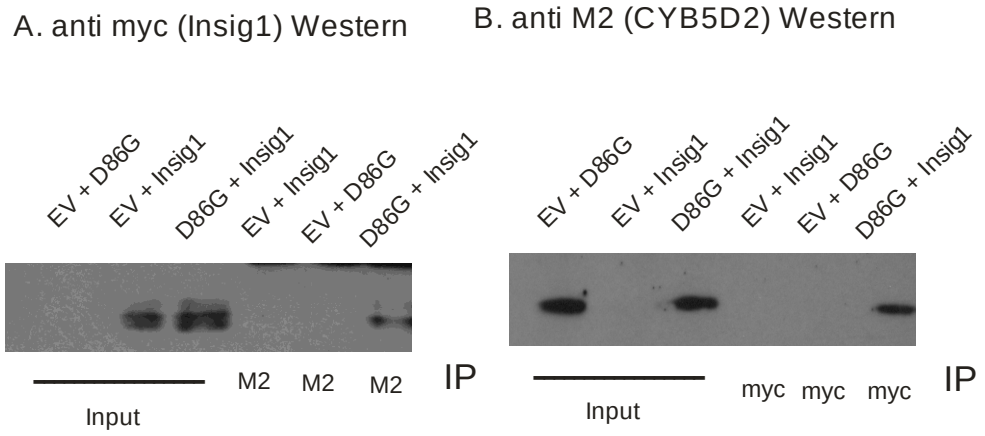

Figure 6.10 The CYB5D2(D86G) co-immunoprecipitates with ectopic Insig1. 293T cells were co-transfected with 10 μg of Insig1 and 10 μg of the CYB5D2(D86G) mutant . Immunoprecipitations (IP) were performed, with equal amounts of lysate immunoprecipitated with M2 Flag for D86G, and myc for Insig1. A. An M2-Flag immunoprecipitation can pull-down Insig1-myc, as detected on this anti-myc Western blot. B. A myc-Insig1 immunoprecipitation can pull-down the D86G, as detected on this anti-Flag (M2) co-immunoprecipitation western blot.

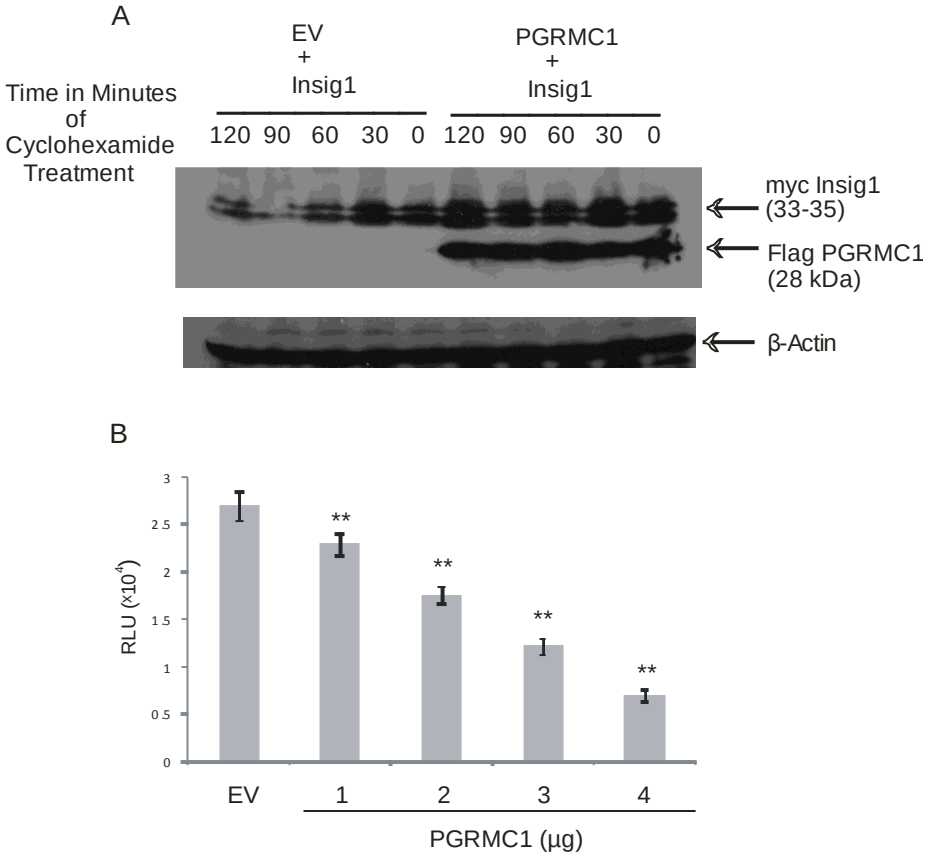

Figure 6.11 PGRMC1 stabilizes ectopic Insig1, and inhibits SREBP signalling. A. PGRMC1 and Insig1 were co-transfected into 293T cells compared with an empty vector control (EV pcDNA3) plus Insig1. Cells were treated with cyclohexamide for 30, 60, 90 and 120 minutes. Lysates were prepared, and western blots performed. β-Actin was used as a loading control. B. PCRMC1 was co-transfected in increasing amounts along with a 3xSRE Luciferase reporter and a β-galactosidase (β-gal) plasmid. PGRMC1 inhibited the 3xSRE Luciferase in a dose dependant manner. All relative luciferase unit (RLU) values were mean +/- standard deviation (n=3). ** $p < 0.01$ (two-tailed Student's *t*-test).

Chapter 7. CYB5D2 co-Immunoprecipitates with cytochrome P450 reductase, and regulates CYP51A1 lanosterol demethylase.

Previous reports have demonstrated that PGRMC1 could interact with cytochrome P450 reductase (POR) (Szczesna-Skorupa and Kemper 2011). PGRMC1 has also been shown to interact with several P450 cytochrome enzymes (Hughes *et al.*, 2007, Szczesna-Skorupa and Kemper 2011). We have observed that the heme binding of CYB5D2 is required to confer survival from chemotherapeutic drugs and to inhibit SREBP signalling. We therefore hypothesized that CYB5D2 could interact with cytochrome P450 reductase (POR), and possibly regulate the activities of certain P450 cytochromes. Furthermore, we attempted to address why heme binding of CYB5D2 was required to stabilize the ectopic Insig1 protein. In order to determine if CYB5D2 could co-immunoprecipitate with POR, 10 μg of CYB5D2 and 10 μg of YFP-POR were co-transfected into a semi-confluent 10 cm plate of 293T cells, and co-immunoprecipitations were performed. When ectopic YFP-POR was co-transfected with ectopic CYB5D2, and a GFP antibody was used to immunoprecipitate YFP-POR, ectopic CYB5D2 was co-immunoprecipitated (Figure 7.1 A). This co-immunoprecipitation was confirmed in both 10% FBS and serum free (24 hours) culture conditions. When we examined CYB5D2 expression in the input lysate, we observe that ectopic POR induced CYB5D2 into the 56 kDa dimer form, in both 10% FBS and serum free culture conditions (Figure 7.1 B).

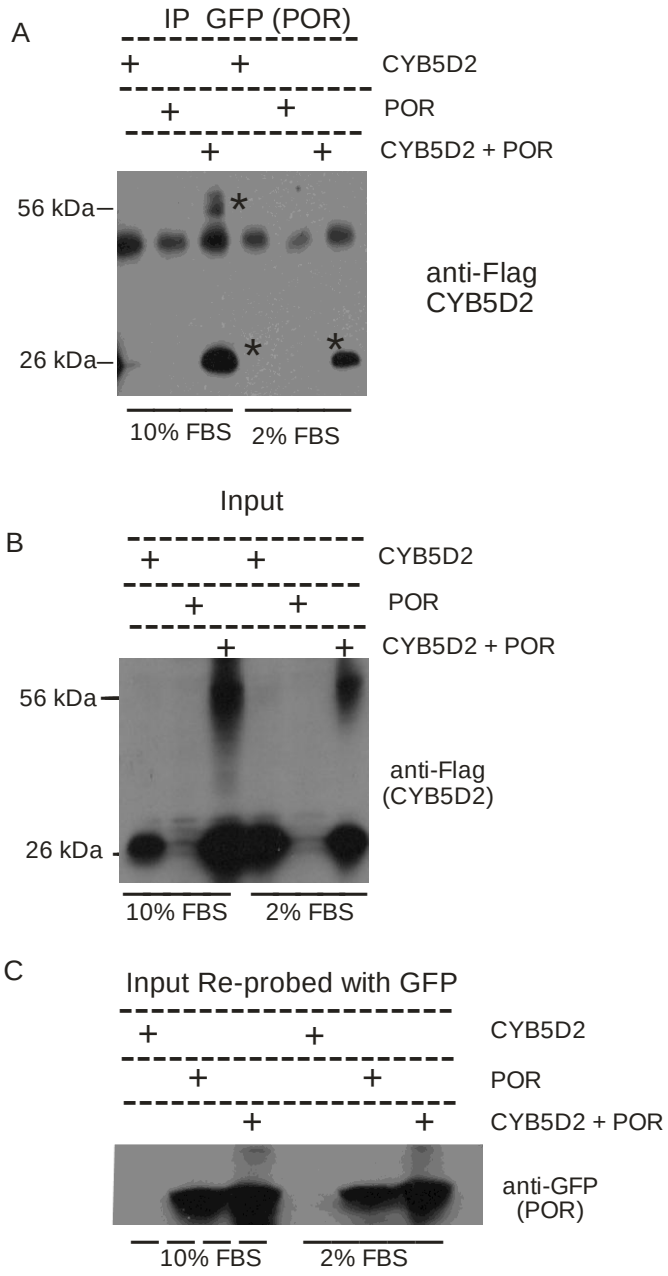

Figure 7.1 CYB5D2 co-immunoprecipitates with ectopic POR. A. Ectopic POR (YFP) and CYB5D2(Flag) co-immunoprecipitate, *asterisk. B. The Input demonstrates that ectopic POR induces CYB5D2 into the 56 kDa dimer, when both are co-transfected. C. Re-probing of panel B (input lysate) with anti GFP antibody showing expression of POR-YFP.

7.1 CYB5D2 shRNA HeLa cells have reduced CYP51A1 and Insig1 protein levels

While the previous experiments in chapter 6 examined the affect that CYB5D2 had on the stability of ectopically transfected Insig1, we wanted to determine if endogenous Insig1 protein levels were affected by CYB5D2. Therefore, the levels of endogenous Insig1 were examined in the stable HeLa EV, CYB5D2, D86G, shRNA control and shRNA CYB5D2 cell lines. Each cell line was cultured in both 10% FBS and serum free conditions for 24 hours. Whole cell lysates were prepared, run on SDS-PAGE gels and subsequent western blots performed. Endogenous Insigl protein levels were reduced in shRNA CYB5D2 knockdown HeLa cells in both 10% FBS and serum free culture conditions (Figure 7.2). A β-Actin antibody was used to monitor equal loading. These western blots were re-probed with a CYP51A1 (lanosterol demethylase) antibody. We observed that shRNA CYB5D2 cells have significantly reduced CYP51A1 protein levels, relative to the shRNA control HeLa cell line, in both 10% FBS and serum free culture conditions (Figure 7.2, middle panel). The D86G HeLa cells however still seem to display normal levels of the CYP51A1 protein.

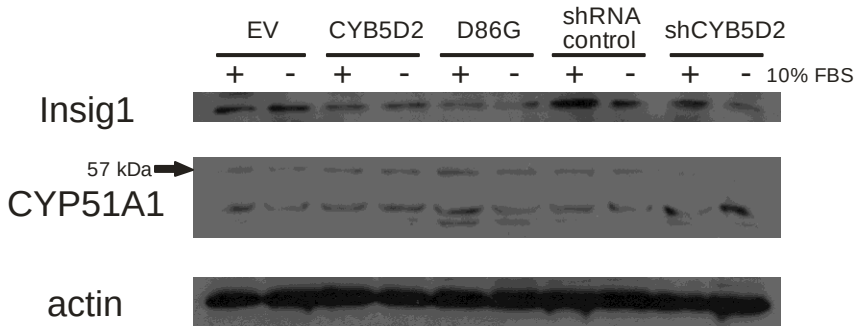

Figure 7.2 CYP51A1 and Insig1 proteins are reduced in shRNA CYB5D2 HeLa cells. EV, CYB5D2 and D86G, shRNA control and CYB5D2 shRNA (shCYB5D2) HeLa cells were cultured in 10% FBS and serum free conditions (24 hours) and probed with anti-Insig1 and anti-CYP51A1 antibodies. As seen in the shRNA control and shRNA CYB5D2 cell lines, Insig1 protein levels are reduced in the shRNA CYB5D2 cell lines in both the 10% FBS and serum free conditions. A β-actin loading control was used to measure equal loading. When these blots were re-probed with a CYP51A1 antibody, we see reduced protein levels in the shRNA CYB5D2 cells in both 10% FBS and serum free conditions.

Previously we observed that CYB5D2 could co-immunoprecipitate with ectopic Insig1. We subsequently examined if CYB5D2 could co-immunoprecipitate with endogenous Insig1 protein. These same Hela stable lines cultured in 10% FBS and serum free conditions (24 hours) were used to immunoprecipitate ectopic CYB5D2 and D86G, to look for an interaction with endogenous Insig1. Additionally, immunoprecipitations with the COOH CYB5D2 antibody were performed to detect an interaction between endogenous CYB5D2 (from shRNA control HeLa), to look for an interaction with endogenous Insig1. As seen in figure 7.3, immunoprecipitations of ectopic CYB5D2 did not pull down endogenous Insig1, in either 10% FBS or serum free cultured conditions. Immunoprecipitations of endogenous CYB5D2, with the COOH-terminus CYB5D2 antibody did not pull down endogenous Insig1 either (shRNA control HeLa) (Figure 7.3).

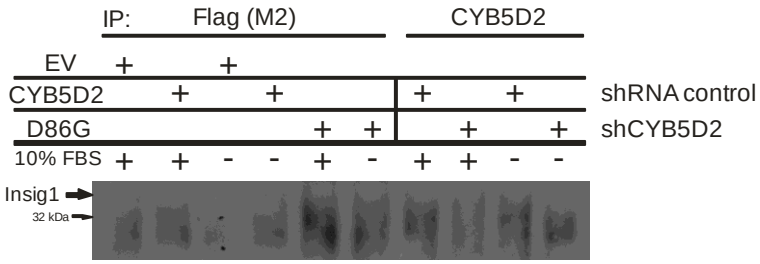

Figure 7.3 CYB5D2 does not co-immunoprecipitate with endogenous Insig1 in HeLa cells. CYB5D2, and D86G were immunoprecipitated with anti-Flag (M2) antibody. Immunoprecipitations were run on SDS-PAGE gels and transferred to western blots. Western blots were probed for endogenous Insig1. Endogenous Insig1 did not co-immunoprecipitate with ectopic CYB5D2. Endogenous CYB5D2 was immunoprecipitated with our polyclonal antibody to CYB5D2 from shRNA control HeLa and shRNA CYB5D2 HeLa (negative control) cells. Endogenous Insig1 could not co-immunoprecipitate with endogenous CYB5D2.

While ectopic CY5D2 and POR could co-immunoprecipitate in 293T cells, we wanted to confirm they co-localized in HeLa cells. Ectopic POR was transfected into CYB5D2 HeLa cells, and dual immunoflouresence performed. As seen in figure 7.4 A, CYB5D2 co-localizes with POR. As previously reported in figure 7.2, shRNA CYB5D2 HeLa cells have reduced protein levels of CYP51A1 relative to shRNA HeLa cells. This result was reproduced in figure 7.4 B, which is similar to Dap1 in yeast in regulating CYP51A1 (lanosterol demethylase) protein levels. Thus lanosterol would be accumulating in shRNA CYB5D2 HeLa cells with reduced CYP51A1 to facilitate its turnover. If the sterol synthesis pathway could be primed with excess doses of mevalonate, this accumulation of lanosterol could be evident in these shRNA CYB5D2 HeLa cells, as high lanosterol levels are toxic to the cell. Therefore shRNA CYB5D2 HeLa cells and shRNA HeLa cells were cultured in 0.5 % lipoprotein free serum for 24 hours and then treated with increasing concentrations of mevalonate. Subsequently MTT cell viability assays were performed. As seen in figure 7.4 C, the shRNA CYB5D2 HeLa cells were more susceptible to increasing mevalonate concentrations, compared to the shRNA HeLa cell line (Figure 7.4 C). CYB5D2 conferred survival from paclitaxel, cisplatin and doxorubicin and etoposide (Xie *et al*., 2011). Cytochrome P450 3A4 is the major drug metabolizing P450 cytochrome. Using a PROMEGA P450 Glo assay kit the cytochrome activity of CYP3A4 was measured in these cell lines. As seen in figure 7.4 D, shRNA CYB5D2 cells had reduced CYP3A4 activity. Ectopically transfected POR significantly increased CYP3A4 activity in the shRNA HeLa cells, but only modestly increased CYP3A4 activity in the shRNA CYB5D2 HeLa cells (Figure 7.4 D).

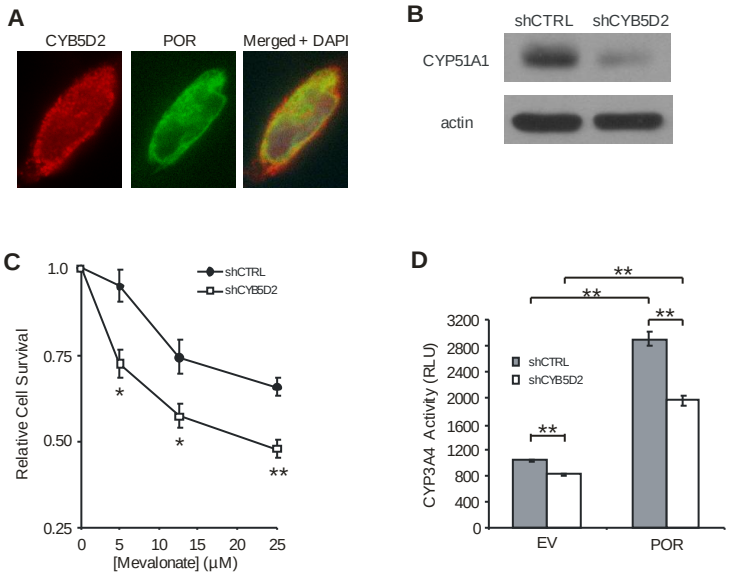

Figure 7.4 CYB5D2 shRNA HeLa cells are more susceptible to mevalonate treatment, and have reduced CYP3A4 activity. A. Ectopically transfected POR (green) co-localizes with CYB5D2 (red) in HeLa cells in dual immunoflouresence staining. B. CYP51A1 protein levels are reduced in shRNA CYB5D2 HeLa cells. Here 100 μg of lysates were run on an SDS-PAGE gel and subsequent western blots probed with a CYP51A1 antibody. C. Increasing concentrations of mevalonate decreased cell viability, however this effect was greater in the shRNA CYB5D2 HeLa cells. D. Cytochrome activity of CYP3A4 was measured using the PROMEGA P4503A4 luciferase assay. These shRNA CYB5D2 HeLa and shRNA HeLa cells were transfected with an EV pcDNA3 and POR plasmid. CYP3A4 activity was reduced in shRNA CYB5D2 HeLa cells, with and without POR. All data points represent mean +/- standard deviation (n=3), *$p < 0.05$; **$p < 0.01$ (two-tailed independent Student's T-test).

As ectopic CYB5D2 was able to co-immunoprecipitate with ectopic POR, I sought to determine if ectopic D86G could co-immunoprecipitate with ectopic POR.
Both D86G and ectopic POR were transiently co-transfected into 293T cells. When D86G was immunoprecipitated with M2-Flag, a GFP antibody could not detect ectopic POR, which was YFP tagged. When ectopic POR was immunoprecipitated with a GFP antibody, and immunoprecipitations probed with the M2-Flag antibody, the D86G could not be detected. Ectopic POR could not co-immunoprecipitate with ectopic D86G (Figure 7.5)

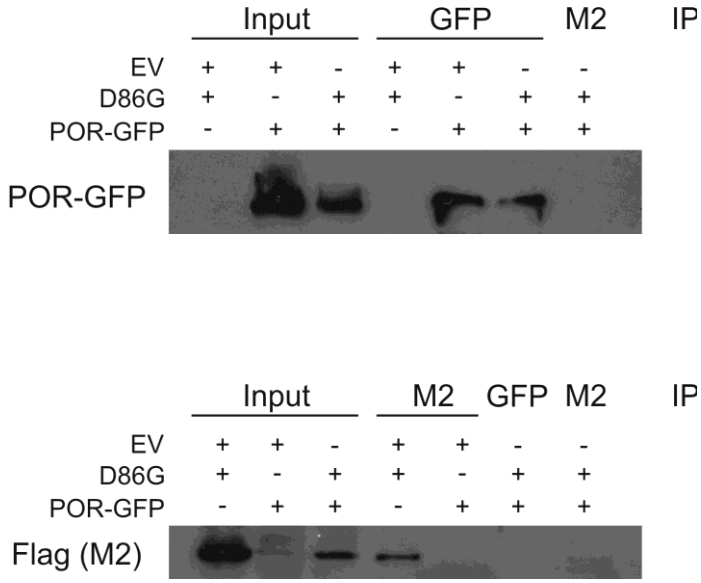

Figure 7.5 The D86G heme binding defective mutant cannot co-immunoprecipitate with ectopic cytochrome P450 reductase (POR). The D86G and POR were transfected (10 μg each) into 293T cells. Forty eight hours later, lysates were prepared, and D86G was immunoprecipitated with an M2 Flag antibody. YFP-POR was immunoprecipitated with a GFP antibody. When the D86G was immunoprecipitated with an M2 Flag antibody, POR could not be detected in a co-immunoprecipitation with D86G (top panel). Similarly, when YFP-POR was immunoprecipitated with a GFP antibody, the D86G could not be detected in a co-immunoprecipitation when western blots were probed with an M2 Flag antibody (bottom panel).

7.2 CYB5D2 co-immunoprecipitates with endogenous POR in HeLa cells in serum free conditions

Previously we demonstrated that CYB5D2 was induced into a 56 kDa dimer when PTEN is overexpressed in U87 cells cultured in reduced serum, and when NIH3T3 cells are serum starved. Moreover, CYB5D2 confers a pro-survival affect in these conditions. Therefore we examined if ectopic CYB5D2 could co- immunoprecipitate with endogenous POR in 10% FBS conditions as well as serum free (24 hours) culture conditions. Stable HeLa cell lines, EV, CYB5D2 and D86G were cultured in 10% FBS and in serum free conditions for 24 hours. Lysates were prepared and the M2 Flag antibody was used to immunoprecipitate CYB5D2, and D86G, in both 10% FBS and serum free conditions. As seen in figure 7.6, CYB5D2 co-immunoprecipitates with endogenous POR in serum free conditions, but not in 10% FBS culture conditions. The D86G could not co-immunoprecipitate with endogenous POR in either culture condition in HeLa cells (Figure 7.6). When whole cell lysates from these cells were examined by western blots probed with a POR antibody, we observe that endogenous POR protein levels do not change between these cell lines. Endogenous POR protein levels do not change from 10% FBS culture conditions to serum free conditions. Thus ectopic CYB5D2 co-immunoprecipitates with endogenous POR in serum free conditions in HeLa cells. The heme binding defective D86G does not co-immunoprecipitate with endogenous POR in HeLa cells.

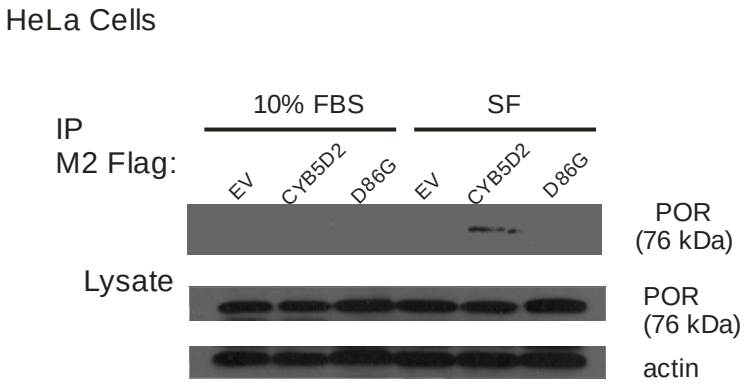

Figure 7.6 Ectopic CYB5D2 co-immunoprecipitates with endogenous POR in HeLa cells in serum free conditions. EV, CYB5D2 and D86G HeLa cells were cultured in 10% FBS and serum free conditions for 24 hours. CYB5D2 and D86G were then immunoprecipitated in both conditions with an M2 Flag antibody, and run on SDS-PAGE gels. When subsequent western blots were probed with a POR antibody, we see endogenous POR co-immunoprecipitates with ectopic CYB5D2 in serum free conditions, but not in 10% FBS culture conditions. Whole cell lysates from these cell lines show that endogenous protein levels of POR are unchanged in these cell lines, and unchanged in 10% FBS and serum free culture conditions between these cell lines.

Lanosterol has been shown to regulate the association of HMG CoA reductase with Insig1, resulting in the degradation of HMG CoA reductase by the membrane anchored ubiquitin ligase gp78 (Song *et al*., 2005). If overexpressing CYB5D2 stabilizes CYP51A1 (lanosterol demthylase), this will result in increased lanosterol turn over, and reduction of lanosterol levels. As a result, HMG CoA reductase will dissociate from Insig1, enhancing its protein stability. Therefore, HMG CoA reductase protein levels were examined in EV, CYB5D2 and D86G HeLa cells. As seen in figure 7.7, HMG CoA reductase protein levels are highest in CYB5D2 HeLa cells, relative to an EV HeLa and D86G HeLa cells. This result indirectly demonstrates that CYB5D2 overexpression is causing a reduction in lanosterol levels.

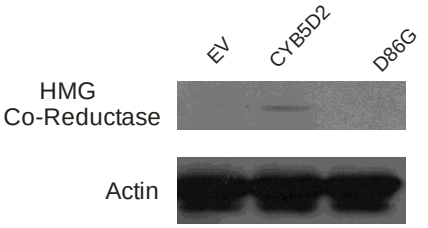

Figure 7.7 HMG CoA Reductase protein levels are increased by CYB5D2. Lysates from EV, CYB5D2 and D86G HeLa cells were prepared, and run on an SDS PAGE gel. Subsequently western blots were probed for HMG CoA reductase. CYB5D2 HeLa cells had a higher amount of HMG CoA reductase protein, relative to an EV control and the D86G HeLa cells.

7.3 CYB5D2 does not co-immunoprecpitates with endogenous Insig1 in Huh7 cells, but shRNA CYB5D2 Huh7 cells have reduced endogenous Insig1 levels

Since we were unable to detect an interaction between CYB5D2 and endogenous Insig1 in HeLa cells, co-immunoprecipitations of these proteins were performed in Huh7 cells. Using previously described stable Huh7 cell lines, EV, CYB5D2 and D86G, anti-M2 Flag immunoprecipitations were performed, for CYB5D2 and D86G. Moreover endogenous CYB5D2 was immunoprecipitated with the COOH-CYB5D2 polyclonal antibody, from the shRNA control Huh7 and shRNA CYB5D2 Huh7 cell lines. As seen in figure 7.8, endogenous Insig1 could not co-immunoprecipitate with ectopic CYB5D2 and endogenous CYB5D2 in Huh7 cells (shRNA control Huh7). Lysates from these co-immunoprecipitations were run on SDS-PAGE gels, and subsequent western blots probed for endogenous Insig1.

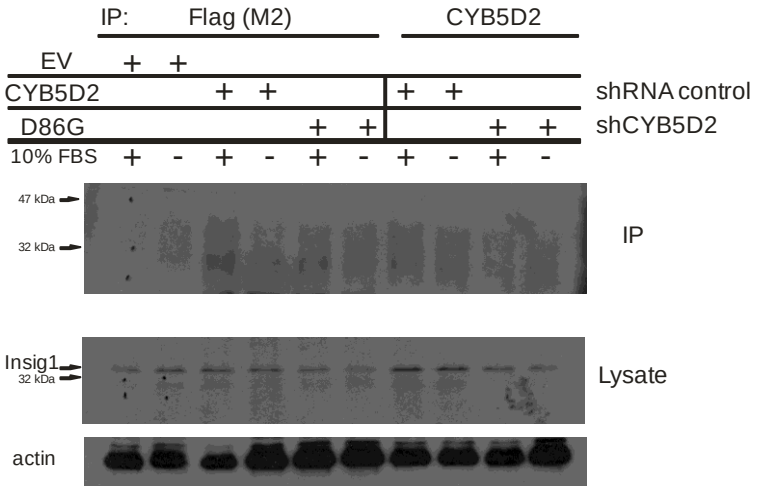

Figure 7.8 CYB5D2 does not co-immunoprecipitate with endogenous Insig1 in Huh7 cells, but shRNA CYB5D2 Huh7 cells have reduced endogenous Insig1 protein levels. Ectopic CYB5D2 and D86G were immunoprecipitated with M2 Flag from EV control, CYB5D2 and D86G stable Huh7 cells. Endogenous Insig1 did not co-immunoprecipitate with CYB5D2 or D86G in 10% or serum free (24 hours) culture conditions. Endogenous CYB5D2 was immunoprecipitated with the COOH-CYB5D2 polyclonal antibody from shRNA Huh7 control and shRNA CYB5D2 Huh7 cells. Endogenous Insig1 did not co-immunoprecipitate with endogenous CYB5D2.

Similar to shRNA CYB5D2 HeLa cells, endogenous Insig1 protein levels were reduced in shRNA CYB5D2 Huh7 cells, relative to shRNA Huh7 cells, in both 10% FBS conditions and serum free culture conditions (Figure 7.8). Collectively this demonstrates that endogenous CYB5D2 functions to stabilize endogenous Insig1 levels, in both HeLa and Huh7 cells.

7.4 CYB5D2 co-immunoprecipitates with endogenous POR in Huh7 cells in serum free conditions

As CYB5D2 could co-immunoprecipitate with endogenous POR in HeLa cells that were serum starved, we examined whether CYB5D2 in Huh7 cells could interact with endogenous POR in these conditions. The Huh7 stable cell lines, EV, CYB5D2 and D86G were cultured in 10% FBS and in serum free conditions for 24 hours. The M2 Flag antibody was used to immunoprecipitate CYB5D2 and D86G, in both 10% FBS and serum free culture conditions. As seen in figure 7.9, endogenous POR co-immunoprecipitates with CYB5D2 in serum free conditions, but not in 10% FBS culture conditions. The D86G Huh7 could not co-immunoprecipitate with endogenous POR in either 10% FBS or serum free culture conditions in Huh7 cells (Figure 7.9). Thus endogenous POR interacts with CYB5D2 in serum free conditions in Huh7 cells, similar to HeLa cells.

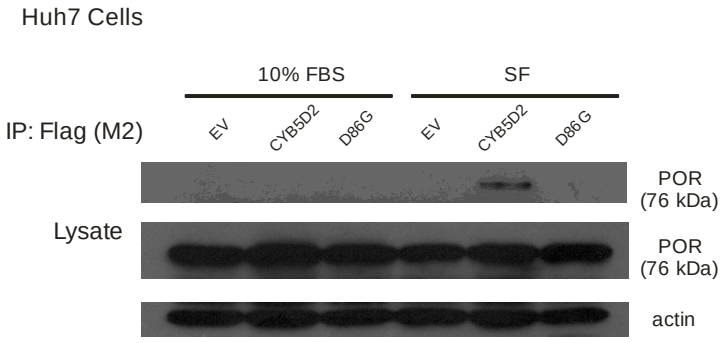

Figure 7.9 CYB5D2 co-immunoprecipitates with endogenous POR in serum free conditions in Huh7 cells. EV, CYB5D2 and D86G Huh7 cells were cultured in 10% FBS and serum free conditions for 24 hours. CYB5D2 and D86G were immunoprecipitated in these two conditions, and these immunoprecipitates run on SDS-PAGE gels and subsequent western blots probed with a POR antibody. CYB5D2 co-immunoprecipitates with endogenous POR in serum free conditions, but not in 10% FBS culture conditions. This result is consistent with CYB5D2 in HeLa cells, despite having different proliferative affects in these two cell types. Endogenous POR protein levels did not change in 10% FBS culture conditions compared to serum free conditions. Endogenous POR protein levels did not change between these various Huh7 stable cell lines.

Chapter 8. Discussion

8.1 Discussion (Chapter 3)

CYB5D2 was identified in a screen in LNCAP cells as a gene that conferred survival from ectopic PTEN death. Additionally, CYB5D2 confers protection from PTEN induced cell death in U87 cells. In CYB5D2 U87 cells that sustained PTEN expression, we observed reduced phosphorylated serine 473 AKT/PKB levels, indicating that ectopic PTEN is still functioning, sufficient to reduce activation of PI3Kinase signalling and subsequent AKT/PKB signalling. CYB5D2 was not detected in an interaction with PTEN, as seen in these co-immunoprecipitations. From this information it is possible, though unknown, if CYB5D2 attenuates some lipid phosphatase independent PTEN function. Alternatively, it is also possible that CYB5D2 confers survival downstream of reduced AKT/PKB signalling.

CYB5D2 conferred survival from serum starvation in NIH3T3 cells, relative to EV NIH3T3. In these serum reduced culture conditions, CYB5D2 dramatically reduces the proliferative capacity of these cells. Moreover CYB5D2 NIH3T3 cells were observed to be more viable, when recovering from serum starvation. This implicates CYB5D2 as having a pro-survival function in nutrient deprived conditions. Since overexpressing PTEN and serum starving cells can inactivate the PI3Kinase signalling pathway, CYB5D2 could well function in a pro-survival role when PI3Kinase signalling is downregulated. This pro-survival function of CYB5D2 could also be induced by these conditions (inhibition of PI3Kinase signalling), as CYB5D2 appears in a 56 kDa dimer in these conditions.

Discussion (Chapter 4)

By generating a polyclonal antibody to CYB5D2, the existence of the endogenous protein in numerous human cell types is verified. CYB5D2 protein was expressed (in varying degrees) in all cell types, with the exception of liver HEPG2 cells. It is unclear why CYB5D2 was expressed in the Huh7 liver cancer cell line, but not the HEPG2 liver cancer cell line. As CYB5D2 was highly expressed in neural cancer cell lines, its high expression in these cell lines could indicate a requirement for a role in survival or maintenance of neural cancer. A similar rationale for prostate cancer could be made due to its moderate expression levels in these cancer cell lines.

Moreover, these results indicate that endogenous CYB5D2 exists as a 56 kDa dimer (doublet) in lysates from these various cell lines. By increasing the denaturing conditions of the sample buffer used to prepare lysates from these cells, we can resolve CYB5D2 into a protein band at 28 kDa, indicative of a monomer of 28 kDa. Therefore, CYB5D2 only really exists *in vivo* as a 56 kDa dimer, and it is the denaturing conditions of the sample buffer and SDS PAGE gel that resolve the endogenous protein into a 28 kDa monomer.

Discussion (Chapter 5)

CYB5D2/ Neuferricin has previously been shown to bind heme, a process that requires the cyt-b5 domain (Kimura *et al*., 2010). However, the critical residue(s) responsible for this association remains unknown. While several residues, including Y73, Y79, D86, and Y127, have been implicated to play a role in heme binding based on the roles of their

conserved counterparts in heme association in other MAPR members, the systematic investigation of these residues individually, clearly demonstrates that D86 plays an essential role in CYB5D2-mediated heme association. This conclusion was based on the loss of heme binding, when D86 was substituted with G86 (D86G). The recombinant CYB5D2(D86G) was demonstrated to be heme binding defective by heme agarose precipitations, "in gel" peroxidase assays, UV visible absorbption spectra data, and through the inability to be oxidized and reduced. Overall, the recombinant D86G protein was incapable of heme association in comparison to recombinant CYB5D2, demonstrating that the mutant is defective in directly binding to heme. This recombinant protein data shows that CYB5D2 alone binds to heme, and that the D86G is defective in this, meaning that no accessory protein is responsible for this.

An shRNA CYB5D2 knockdown was also generated, and this was used in tandem with D86G stable cell lines to compare both of these loss of function tools against the wild type CYB5D2. The CYB5D2(D86G) behaved in an opposite fashion to CYB5D2, and in a similar fashion to the shRNA CYB5D2 cell lines, in proliferation and growth in HeLa cells and Huh7 cells. Furthermore, the heme binding of CYB5D2 was required for CYB5D2 to confer survival from chemotherapeutic compounds. These experiments shows that lack of heme binding results in a loss of function for CYB5D2.

Overall the different effects that CYB5D2 conferred on HeLa and Huh7 cell proliferation was related to its ability to bind heme. Exactly how heme binding of CYB5D2 is affecting the different proliferative functions of CYB5D2 in different cell lines is unknown here.

Discussion (Chapter 6)

The CYB5D2 protein co-localizes to the Endoplasmic Reticulum (ER). This location places CYB5D2 in an area where sterol metabolism, and cytochrome P450 microsomal proteins reside. CYB5D2 inhibits SREBP signalling, in transient transfection assays in 293T cells. We show that only the full length unprocessed form of SREBP1c and SREBP2 are inhibited by CYB5D2, indicating that CYB5D2 only inhibits these transcription factors when they are retained in the ER.

Structurally, the transmembrane domain and the heme binding domain are required for CYB5D2 to inhibit SREBP signalling. This transmembrane domain deletion mutant (ΔTM) has been shown to ablate the peri-nuclear localization of CYB5D2 (Xie *et al*., 2011). Thus the ER localization of CYB5D2 is required for its inhibition of SREBP signalling. Specifically the D86G heme binding defective mutant cannot inhibit SREBP signalling. This indicates that CYB5D2 needs to bind to heme to inhibit SREBP signalling. While CYB5D2 can bind to and stabilize ectopic Insig1, the D86G promoted the destabilization of Insig1, but still co-immunoprecipitated with Insig1. Therefore it is not the binding of CYB5D2 to Insig1 that promotes its stabilization, but rather its ability to bind to heme that confers its stabilization affect on Insig1. PGRMC1 can also stabilize Insig1 and inhibit the 3xSRE Luciferase reporter in dose dependant manner. It could therefore be possible that CYB5D2, like PGRMC1, might affect the CYP51A1 protein stability, and ultimately lanosterol levels, resulting in more stable Insig1 protein.

Discussion (Chapter 7)

Microsomal P450 cytochromes require cytochrome P450 reductase (POR) for their activation. Yeast Dap1, has been shown to be involved in regulating ERG11p (lanosterol demethylase) (Hand *et al*., 2003; Mallory *et al*., 2005). PGRMC1 has been shown to bind to P450 cytochromes and to cytochrome P450 reductase (Hughes *et al* 2007; Sczesna and Kemper 2010). Furthermore, these groups have shown that Dap1 is required to stabilize the ERG11p lanosterol demethylase protein, and knockdown of PGRMC1 has been shown to result in an increase of lanosterol levels (Mallory *et al*., 2005; Hughes *et al*., 2007; Szczesna-Skorupa and Kemper, 2010). CYB5D2 can interact with POR when both were co-transfected into 293T cells. Moreover, this ectopic co-expression of POR induced CYB5D2 into the 56 kDa dimer form. This 56 kDa dimer was oberved when CYB5D2 NIH3T3 cells are serum starved, and when CYB5D2 + PTEN U87 cells are cultured in reduced serum (chapter 3). CYB5D2 also co-localizes with POR in dual immunoflouresence staining. CYP51A1 protein levels are reduced in shRNA CYB5D2 HeLa cells, indicating that CYB5D2 protein functions to stabilize the CYP51A1 protein, similar to Dap1. In these shRNA CYB5D2 HeLa, reduced CYP51A1 would result in a defect in sterol synthesis, which is evident in their increased susceptibility to mevalonate treatment. Priming sterol synthesis with excess mevalonate results in a greater flux through the sterol synthesis pathway. Without sufficient CYP51A1 to modify lanosterol it would accumulate, resulting in cellular toxicity. This block in lanosterol turnover in the sterol synthesis pathway in the shRNA CYB5D2 HeLa cells, is exposed by their increase in susceptibility to mevalonate treatment. Additionally, by regulating lanosterol levels,

CYB5D2 would affect stability of HMG CoA reductase. This is observed as CYB5D2 HeLa cells have higher levels of HMG CoA reductase, relative to EV HeLa and D86G HeLa. Since CYB5D2 functions to stabilize CYP51A1, which results in lower lanosterol and more stable HMG CoA reductase, this promotes an increase in the sterol synthesis pathway at these two major steps. This overall increase in sterol synthesis production would result in higher levels of cholesterol, which would be detected by SCAP. When this excess cholesterol and SCAP bind to Insig1, Insig1 becomes more stable. This suggests that CYB5D2 and PGRMC1 can initiate an increase in sterol synthesis by affecting CYP51A1 stability/activity and lanosterol levels, and this excess cholesterol is detected by increased Insig1 stability. Since endogenous Insig1 protein levels were reduced in shRNA CYB5D2 HeLa and Huh7 cells, this indicates that sterol synthesis and overall cholesterol levels were reduced by the loss of CYB5D2. While CYB5D2 stabilized ectopic Insig1, the D86G heme binding defective mutant destabilized ectopic Insig1. CYB5D2 can interact with POR but the D86G cannot. It is likely that CYP51A1 (a P450 cytochrome) requires activation from POR, and by CYB5D2 to some degree. It is important to note, that CYP51A1 protein levels were not reduced in the D86G HeLa cell line. This result implies that it is the expression of CYB5D2 protein that would cause the stabilization of CYP51A1, and not the heme binding. It seems plausible that these cytochrome b5 heme binding proteins like PGRMC1 and CYB5D2 keep Insig1 in close proximity, to be receptive to regulated lanosterol levels.

CYB5D2 interacted with endogenous POR in serum free conditions. This happens when CYB5D2 is overexpressed in HeLa cells and Huh7cells, despite CYB5D2 having

different proliferative affects on these cell lines. It is likely that the signalling pathways that regulate the interaction of CYB5D2 with POR are similar between these two cell types, even though the affect of CY5D2 on proliferation and growth is different in these cell types. The D86G could not interact with endogenous POR in any serum culture conditions. This explains the mechanism of why the D86G acts in a dominant negative fashion compared to wild type CYB5D2 in the functions studied here ie proliferation, survival from chemotherapeutic drugs, and Insig1 stabilization. This data further demonstrates that CYP51A1 protein levels and CYP3A4 activity are reduced in shRNA CYB5D2 HeLa cells. These are both cytochrome P450 enzymes, which require POR for their activity.

8.2 Conclusion

CYB5D2 was identified from a screen in LNCAP prostate cancer cells for its ability to confer survival from the PTEN tumor suppressor gene. CYB5D2 also conferred survival from PTEN overexpression in U87 cells, and from serum starvation in NIH3T3 cells. CYB5D2 likely confers survival from the inhibition of PI3Kinase signalling in these cells. These conditions also induce ectopic CYB5D2 into a 56 kDa dimer when CYB5D2 is immunoprecipitated, where it would function in a pro-survival capacity.

The endogenous CYB5D2 56 kDa dimer is resolved into a 28 kDa monomer by increasing the denaturing capacity of the lysis buffer. The endogenous CYB5D2 protein is expressed in neural, breast, prostate, kidney, and liver cells.

CYB5D2 inhibits SREBP signalling in transient expression assays. This inhibition requires the transmembrane domain and the heme binding domain of CYB5D2. While SREBP signalling was affected following transient transfections of CYB5D2 with SRE reporters in 293T cells, in our stable HeLa and Huh7 cell lines, we did not detect any differences between EV, CYB5D2, D86G, shRNA CYB5D2 or shRNA control HeLa and Huh7 cells using a 3xSRE-GFP reporter. One possibility for the lack of effect on the 3xSRE-GFP reporter could be that Insig1 itself is an SREBP target, which would be now downregulated when the Insig1 protein is stabilized and SREBP signalling is inhibited.

This work characterizes the generation and characterization of a heme binding defective mutant of CYB5D2 (D86G) that acts in a dominant negative fashion for CYB5D2. Using this mutant in tandem with CYB5D2 shRNA we show that heme binding of CYB5D2 is required to confer survival from chemotherapeutic compounds. Moreover heme binding of CYB5D2 is required to regulate proliferation in HeLa and Huh7 cells. Heme binding of CYB5D2 is also required to stabilize Insig1, and to inhibit SREBP signalling. Similar to Dap1`s function to stabilize the (CYP51A1) protein in yeast (Craven *et al*., 2007), CYB5D2 regulated CYP51A1 protein levels. PGRMC1 reportedly bound to CYP51A1, and consequently regulates lanosterol levels as well (Hughes *et al*., 2007; Szczesna-Skorupa and Kemper. 2011). An interaction between CYB5D2 and CYP51A1 was not detected in co-immunoprecipitations (data not shown). These results demonstrate that CYB5D2 shRNA HeLa cells have reduced CYP51A1 protein levels, reduced CYP3A4 activity and reduced Insig1 protein levels. This suggests that CYB5D2 functions to regulate CYP51A1 protein levels (and subsequently regulating lanosterol levels), results

in increased sterol synthesis which ultimately modulates Insig1 stability. This thesis is the first demonstration that PGRMC1 could stabilize ectopic Insig1 and inhibit the 3xSRE-Luciferase reporter. PGRMC1 and CYB5D2 likely keep Insig1 in close physical proximity, where it can be readily available to fluctuating lanosterol levels (DeBose-Boyd, 2007). Stabilizing CYP51A1 would result in lower lanosterol levels, averting an interaction between Insig1 and HMG CoA-reductase, resulting in more stable HMG CoA-reductase levels. This would also leave more Insig1 available for SCAP binding, and increase the rate of sterol synthesis at the 3-hydroxy-3-methylglutary-CoA/mevalonate step by HMG CoA reductase. Excess levels of sterols would be sensed by SCAP and induce its interaction with Insig1, which would now stabilize Insig1. The stabilization of Insig1 by CYB5D2 is a direct measure of increased cholesterol production. However, stabilizing Insig1 would inhibit SREBP signalling, and decrease transcription of Insig1. CYB5D2 would inhibit this model of "convergent feedback". How this would affect the overall cholesterol picture and feedback mechanisms remains unclear. Further investigation of how these processes are affected by these proteins is required.

More directly, heme binding of CYB5D2 is required to interact with cytochrome P450 reductase (POR). CYB5D2 interacted with endogenous POR in serum free culture conditions in HeLa and Huh7 cells, while the D86G could not. Overall, this represents a primary direct function of CYB5D2, and explains the dominant negative functions of D86G. As CYP51A1 is the major cytochrome P450 associated with POR and its associated roles and phenotypes, it seems both PGRMC1 and CYB5D2 have evolved to regulate this POR dependant enzyme and this step of lanosterol breakdown. Additionally,

lanosterol is an important molecule in regulating HMG CoA reductase association with Insig1 and subsequent degradation (Song *et al*., 2005). Therefore by regulating lanosterol levels, both PGRMC1 and CYB5D2 can indirectly regulate Insig1 stability, and inhibit SREBP activation.

It remains to be seen what other cytochrome P450 enzymes are also regulated by CYB5D2. It is possible, that these cytochrome P450 substrates regulated by CYB5D2-POR could vary from one cell type to another. Further investigation to identify CYB5D2 interacting proteins and POR P450 cytochrome substrates will be required. Because CYB5D2 interacted with endogenous POR in HeLa cells and Huh7 cells that were serum starved (despite having different proliferative affects in these cell lines), CYB5D2 might function to promote cell survival in these conditions by interacting with POR and regulating specific P450 cytochrome enzymes in these conditions.

Whether a process like autophagy becomes induced by CYB5D2 (POR associated) in this serum starved scenario remains to be seen. Further definitive examination of the role of CYP51A1, lanosterol demethylase, could be performed by inhibiting this protein with itraconazole and fluconazole. Inhibition of this protein could determine its role in CYB5D2 and PGRMC1 mediated Insig1 stability. One overall picture of these MAPR proteins PGRMC1 and CYB5D2 could be to increase sterol synthesis to increase the cholesterol needed for the processes that these P450 cytochrome enzymes are involved in.

We were unable to detect ectopic CYB5D2 expressed in the media from stable CYBD2 HeLa cells. Therefore the secretion of CYB5D2 is likely cell type specific, and all the functions described here refer to the intracellular protein and its subsequent functions.

While most papers published on PGRMC1 describe its function as a progesterone receptor, we do not know if CYB5D2 functions as some kind of hormone receptor. Moreover, it is unclear if any cytochrome P450 enzymes involved in steroid biosynthesis or bile acid synthesis are regulated by this CYB5D2 POR interaction in serum starved conditions. Furthermore, while PGRMC1 has been shown to be a sigma 2 receptor, we have yet to determine if CYB5D2 is also a sigma receptor. Future experiments will be needed to address this.

Experiments and data implicating CYB5D2 in an ER stress response were omitted from this thesis. Further experiments characterizing this connection need to be explored, as this story is only partially characterized. Moreover, examining the signalling pathways regulating the association of CYB5D2 and POR were not permitted in this thesis. Future work elucidating the signalling regulating CYB5D2 functions would be required.

8.3 Future Directions

In this study, we identify two P450 cytochromes affected by CYB5D2, CYP51A1 and CYP3A4. Whether additional P450 cytochromes are affected by CYB5D2 would need further investigation. In order to show that CYP51A1 activity was affected directly, mass spec analysis to measure lanosterol levels would need to be performed. While CYB5D2 conferred survival from serum starvation, the exact mechanism was not determined. Further investigation on CYB5D2`s pro-survival function would be required, along with indentifying the cytochrome P450 enzymes that could be underlying this CYB5D2-POR mediated pro-survival response. Furthermore, the exact mechanistic explanation of why

the heme binding of CYB5D2 affected proliferation and survival from chemotherapeutic drugs is not answered. Whether CYP3A4 or CYP51A1 are responsible for survival from chemotherapeutic drugs is uncertain.

Experiments examining a PI3Kinase signalling pathway regulating CYB5D2 functions should be addressed. The output for examining this signalling pathway could be an interaction with POR, survival from serum starvation, or an affect on 3xSRE-reporter activity.

While the initial reports of CYB5D2/Neuferricin claimed it functioned as a secreted protein, the authors failed to acknowledge the existence of the intracellular protein. Ectopic CYB5D2 in HeLa cells was not detected as secreted in these cells, therefore all work performed here is on the intracellular function. Whether any function of the secreted protein exists is unknown.

Further experiments to examine the type of cholesterol that is affected by CYB5D2 could also be conducted. Specifically, the role of CYB5D2 in the liver could be explored, and whether or not CYB5D2 participates with POR P450 cytochromes involved in converting cholesterol to bile acids. CYB5D2`s role could vary from cell type to cell type, as liver conversion of cholesterol to bile acids by P450 cytochromes could be different than CYB5D2`s neural function with P450 cytochromes involved in processing and exporting bile acids. As CYP7A1 has been implicated and studied in colorectal cancer, examining the CYB5D2 R7P and CYB5D2 R7G mutants found in colorectal cancer, could implicate CYB5D2`s role in affecting this cytochrome involved in bile acid synthesis, and the role of CYB5D2 in colorectal cancer. It is also possible that CYB5D2

could function to modulate some of the POR affected cytochrome P450 substrates observed in Antley Bixler Syndrome.

An examination of the promoter and transcriptional regulation of the CYB5D2 gene was not performed here. Future work could examine the regulatory elements in the promoter region of the CYB5D2 gene.

A more extensive analysis of interacting proteins that could interact with CYB5D2 could be performed, using mass spec analysis. This could be performed in serum free culture conditions as well as complete 10% FBS culture conditions.

Lastly, an examination of CYB5D2 functions with hormones could be performed. While PGRMC1 is a progesterone receptor, experiments could be conducted with both PGRMC1 and CYB5D2 in tandem, to determine if CYB5D2 is also a progesterone receptor. If CYB5D2 is not a progesterone receptor, identifying which (if any) hormone ligand it could be a receptor for, would need to be addressed. Moreover, experiments addressing whether or not CYB5D2 affects the synthesis of various cytochrome P450 enzymes in hormone synthesis could also be determined.

References

Acosta-Alvear D, Zhou Y, Blais A, Tsikitis M, Lents NH, Arias C, Lennon CJ, Kluger Y & Dynlacht BD 2007 XBP1 controls diverse cell type- and condition-specific transcriptional regulatory networks. *Mol Cell* **27** 53-66.

Ahmed IS, Chamberlain C & Craven RJ 2012 S2R(Pgrmc1): the cytochrome-related sigma-2 receptor that regulates lipid and drug metabolism and hormone signaling. *Expert Opin Drug Metab Toxicol* **8** 361-370.

Ahmed IS, Rohe HJ, Twist KE & Craven RJ 2010 Pgrmc1 (progesterone receptor membrane component 1) associates with epidermal growth factor receptor and regulates erlotinib sensitivity. *J Biol Chem* **285** 24775-24782.

Ahmed IS, Rohe HJ, Twist KE, Mattingly MN & Craven RJ 2010 Progesterone receptor membrane component 1 (Pgrmc1): a heme-1 domain protein that promotes tumorigenesis and is inhibited by a small molecule. *J Pharmacol Exp Ther* **333** 564-573.

Aleck KA & Bartley DL 1997 Multiple malformation syndrome following fluconazole use in pregnancy: report of an additional patient. *Am J Med Genet* **72** 253-256.

Amemiya-Kudo M, Shimano H, Hasty AH, Yahagi N, Yoshikawa T, Matsuzaka T, Okazaki H, Tamura Y, Iizuka Y, Ohashi K, Osuga J, Harada K, Gotoda T, Sato R, Kimura S, Ishibashi S & Yamada N 2002 Transcriptional activities of nuclear SREBP-1a, -1c, and -2 to different target promoters of lipogenic and cholesterogenic genes. *J Lipid Res* **43** 1220-1235.

Arlt W, Walker EA, Draper N, Ivison HE, Ride JP, Hammer F, Chalder SM, Borucka-Mankiewicz M, Hauffa BP, Malunowicz EM, Stewart PM & Shackleton CH 2004 Congenital adrenal hyperplasia caused by mutant P450 oxidoreductase and human androgen synthesis: analytical study. *Lancet* **363** 2128-2135.

Athanikar JN, Sanchez HB & Osborne TF 1997 Promoter selective transcriptional synergy mediated by sterol regulatory element binding protein and Sp1: a critical role for the Btd domain of Sp1. *Mol Cell Biol* **17** 5193-5200.

Backes WL & Kelley RW 2003 Organization of multiple cytochrome P450s with NADPH-cytochrome P450 reductase in membranes. *Pharmacol Ther* **98** 221-233.

Beckner ME, Gobbel GT, Abounader R, Burovic F, Agostino NR, Laterra J & Pollack IF 2005 Glycolytic glioma cells with active glycogen synthase are sensitive to PTEN and inhibitors of PI3K and gluconeogenesis. *Lab Invest* **85** 1457-1470.

Bennett CB, Lewis LK, Karthikeyan G, Lobachev KS, Jin YH, Sterling JF, Snipe JR & Resnick MA 2001 Genes required for ionizing radiation resistance in yeast. *Nat Genet* **29** 426-434.

Bernauer S, Wehling M, Gerdes D & Falkenstein E 2001 The human membrane progesterone receptor gene: genomic structure and promoter analysis. *DNA Seq* **12** 13-25.

Berry EA & Trumpower BL 1987 Simultaneous determination of hemes a, b, and c from pyridine hemochrome spectra. *Anal Biochem* **161** 1-15.

Black SD & Coon MJ 1987 P-450 cytochromes: structure and function. *Adv Enzymol Relat Areas Mol Biol* **60** 35-87.

Bodin K, Lindbom U & Diczfalusy U 2005 Novel pathways of bile acid metabolism involving CYP3A4. *Biochim Biophys Acta* **1687** 84-93.

Briggs MR, Yokoyama C, Wang X, Brown MS & Goldstein JL 1993 Nuclear protein that binds sterol regulatory element of low density lipoprotein receptor promoter. I. Identification of the protein and delineation of its target nucleotide sequence. *J Biol Chem* **268** 14490-14496.

Brown AJ, Sun L, Feramisco JD, Brown MS & Goldstein JL 2002 Cholesterol addition to ER membranes alters conformation of SCAP, the SREBP escort protein that regulates cholesterol metabolism. *Mol Cell* **10** 237-245.

Brown DA & London E 1998 Functions of lipid rafts in biological membranes. *Annu Rev Cell Dev Biol* **14** 111-136.

Brown MS & Goldstein JL 1980 Multivalent feedback regulation of HMG CoA reductase, a control mechanism coordinating isoprenoid synthesis and cell growth. *J Lipid Res* **21** 505-517.

Brown MS & Goldstein JL 1997 The SREBP pathway: regulation of cholesterol metabolism by proteolysis of a membrane-bound transcription factor. *Cell* **89** 331-340.

Brown MS & Goldstein JL 1999 A proteolytic pathway that controls the cholesterol content of membranes, cells, and blood. *Proc Natl Acad Sci U S A* **96** 11041-11048.

Bulun SE, Lin Z, Imir G, Amin S, Demura M, Yilmaz B, Martin R, Utsunomiya H, Thung S, Gurates B, Tamura M, Langoi D & Deb S 2005 Regulation of aromatase expression in estrogen-responsive breast and uterine disease: from bench to treatment. *Pharmacol Rev* **57** 359-383.

Burg JS & Espenshade PJ 2011 Regulation of HMG-CoA reductase in mammals and yeast. *Prog Lipid Res* **50** 403-410.

Cahill MA 2007 Progesterone receptor membrane component 1: an integrative review. *J Steroid Biochem Mol Biol* **105** 16-36.

Cantley LC & Baselga J 2011 The era of cancer discovery. *Cancer Discov* **1** 1.

Cantley LC & Neel BG 1999 New insights into tumor suppression: PTEN suppresses tumor formation by restraining the phosphoinositide 3-kinase/AKT pathway. *Proc Natl Acad Sci U S A* **96** 4240-4245.

Charvat KA, Hornstein L & Oestreich AE 1991 Radio-ulnar synostosis in Williams syndrome. A frequently associated anomaly. *Pediatr Radiol* **21** 508-510.

Chen HW, Leonard DA, Fischer RT & Trzaskos JM 1988 A mammalian mutant cell lacking detectable lanosterol 14 alpha-methyl demethylase activity. *J Biol Chem* **263** 1248-1254.

Chen TC, Sakaki T, Yamamoto K & Kittaka A 2012 The roles of cytochrome P450 enzymes in prostate cancer development and treatment. *Anticancer Res* **32** 291-298.

Chun K, Siegel-Bartelt J, Chitayat D, Phillips J & Ray PN 1998 FGFR2 mutation associated with clinical manifestations consistent with Antley-Bixler syndrome. *Am J Med Genet* **77** 219-224.

Clarke PR & Hardie DG 1990 Regulation of HMG-CoA reductase: identification of the site phosphorylated by the AMP-activated protein kinase in vitro and in intact rat liver. *Embo J* **9** 2439-2446.

Colburn NH, Bruegge WF, Bates JR, Gray RH, Rossen JD, Kelsey WH & Shimada T 1978 Correlation of anchorage-independent growth with tumorigenicity of chemically transformed mouse epidermal cells. *Cancer Res* **38** 624-634.

Cooper MK, Wassif CA, Krakowiak PA, Taipale J, Gong R, Kelley RI, Porter FD & Beachy PA 2003 A defective response to Hedgehog signaling in disorders of cholesterol biosynthesis. *Nat Genet* **33** 508-513.

Cox JS, Shamu CE & Walter P 1993 Transcriptional induction of genes encoding endoplasmic reticulum resident proteins requires a transmembrane protein kinase. *Cell* **73** 1197-1206.

Craven RJ, Mallory JC & Hand RA 2007 Regulation of iron homeostasis mediated by the heme-binding protein Dap1 (damage resistance protein 1) via the P450 protein Erg11/Cyp51. *J Biol Chem* **282** 36543-36551.

Crosignani A, Zuin M, Allocca M & Del Puppo M 2011Oxysterols in bile acid metabolism. *Clin Chim Acta* **412** 2037-2045.

Crudden G, Chitti RE & Craven RJ 2006 Hpr6 (heme-1 domain protein) regulates the susceptibility of cancer cells to chemotherapeutic drugs. *J Pharmacol Exp Ther* **316** 448-455.

Crudden G, Loesel R & Craven RJ 2005 Overexpression of the cytochrome p450 activator hpr6 (heme-1 domain protein/human progesterone receptor) in tumors. *Tumour Biol* **26** 142-146.

Daum G, Lees ND, Bard M & Dickson R 1998 Biochemistry, cell biology and molecular biology of lipids of Saccharomyces cerevisiae. *Yeast* **14** 1471-1510.

Debeljak N, Fink M & Rozman D 2003 Many facets of mammalian lanosterol 14alpha-demethylase from the evolutionarily conserved cytochrome P450 family CYP51. *Arch Biochem Biophys* **409** 159-171.

Debose-Boyd RA 2007 A helping hand for cytochrome p450 enzymes. *Cell Metab* **5** 81-83.

DeBose-Boyd RA 2008 Feedback regulation of cholesterol synthesis: sterol-accelerated ubiquitination and degradation of HMG CoA reductase. *Cell Res* **18** 609-621.

Demoulin JB, Ericsson J, Kallin A, Rorsman C, Ronnstrand L & Heldin CH 2004 Platelet-derived growth factor stimulates membrane lipid synthesis through activation of phosphatidylinositol 3-kinase and sterol regulatory element-binding proteins. *J Biol Chem* **279** 35392-35402.

Doolman R, Leichner GS, Avner R & Roitelman J 2004 Ubiquitin is conjugated by membrane ubiquitin ligase to three sites, including the N terminus, in transmembrane region of mammalian 3-hydroxy-3-methylglutaryl coenzyme A reductase: implications for sterol-regulated enzyme degradation. *J Biol Chem* **279** 38184-38193.

Du X, Kristiana I, Wong J & Brown AJ 2006 Involvement of Akt in ER-to-Golgi transport of SCAP/SREBP: a link between a key cell proliferative pathway and membrane synthesis. *Mol Biol Cell* **17** 2735-2745.

Dull T, Zufferey R, Kelly M, Mandel RJ, Nguyen M, Trono D & Naldini L 1998 A third-generation lentivirus vector with a conditional packaging system. *J Virol* **72** 8463-8471.

Eberle D, Hegarty B, Bossard P, Ferre P & Foufelle F 2004 SREBP transcription factors: master regulators of lipid homeostasis. *Biochimie* **86** 839-848.

Engelking LJ, Liang G, Hammer RE, Takaishi K, Kuriyama H, Evers BM, Li WP, Horton JD, Goldstein JL & Brown MS 2005 Schoenheimer effect explained--feedback regulation of cholesterol synthesis in mice mediated by Insig proteins. *J Clin Invest* **115** 2489-2498.

Engelman JA, Luo J & Cantley LC 2006 The evolution of phosphatidylinositol 3-kinases as regulators of growth and metabolism. *Nat Rev Genet* **7** 606-619.

Espenshade PJ, Cheng D, Goldstein JL & Brown MS 1999 Autocatalytic processing of site-1 protease removes propeptide and permits cleavage of sterol regulatory element-binding proteins. *J Biol Chem* **274** 22795-22804.

Espenshade PJ & Hughes AL 2007 Regulation of sterol synthesis in eukaryotes. *Annu Rev Genet* **41** 401-427.

Estabrook RW, Franklin MR, Cohen B, Shigamatzu A & Hildebrandt AG 1971 Biochemical and genetic factors influencing drug metabolism. Influence of hepatic microsomal mixed function oxidation reactions on cellular metabolic control. *Metabolism* **20** 187-199.

Falkenstein E, Eisen C, Schmieding K, Krautkramer M, Stein C, Losel R & Wehling M 2001 Chemical modification and structural analysis of the progesterone membrane binding protein from porcine liver membranes. *Mol Cell Biochem* **218** 71-79.

Falkenstein E, Meyer C, Eisen C, Scriba PC & Wehling M 1996 Full-length cDNA sequence of a progesterone membrane-binding protein from porcine vascular smooth muscle cells. *Biochem Biophys Res Commun* **229** 86-89.

Falkenstein E, Schmieding K, Lange A, Meyer C, Gerdes D, Welsch U & Wehling M 1998 Localization of a putative progesterone membrane binding protein in porcine hepatocytes. *Cell Mol Biol (Noisy-le-grand)* **44** 571-578.

Fang DL, Wan Y, Shen W, Cao J, Sun ZX, Yu HH, Zhang Q, Cheng WH, Chen J & Ning B 2013 Endoplasmic reticulum stress leads to lipid accumulation through upregulation of SREBP-1c in normal hepatic and hepatoma cells. *Mol Cell Biochem*.

Finn RD, Henderson CJ, Scott CL & Wolf CR 2009 Unsaturated fatty acid regulation of cytochrome P450 expression via a CAR-dependent pathway. *Biochem J* **417** 43-54.

Fischer RT, Stam SH, Johnson PR, Ko SS, Magolda RL, Gaylor JL & Trzaskos JM 1989 Mechanistic studies of lanosterol 14 alpha-methyl demethylase: substrate requirements for the component reactions catalyzed by a single cytochrome P-450 isozyme. *J Lipid Res* **30** 1621-1632.

Flanagan JN, Young MV, Persons KS, Wang L, Mathieu JS, Whitlatch LW, Holick MF & Chen TC 2006 Vitamin D metabolism in human prostate cells: implications for prostate cancer chemoprevention by vitamin D. *Anticancer Res* **26** 2567-2572.

Fleischmann M & Iynedjian PB 2000 Regulation of sterol regulatory-element binding protein 1 gene expression in liver: role of insulin and protein kinase B/cAkt. *Biochem J* **349** 13-17.

Fluck CE & Miller WL 2006 P450 oxidoreductase deficiency: a new form of congenital adrenal hyperplasia. *Curr Opin Pediatr* **18** 435-441.

Fluck CE, Mullis PE & Pandey AV 2010 Reduction in hepatic drug metabolizing CYP3A4 activities caused by P450 oxidoreductase mutations identified in patients with disordered steroid metabolism. *Biochem Biophys Res Commun* **401** 149-153.

Fluck CE & Pandey AV 2011 Clinical and biochemical consequences of p450 oxidoreductase deficiency. *Endocr Dev* **20** 63-79.

Fluck CE, Tajima T, Pandey AV, Arlt W, Okuhara K, Verge CF, Jabs EW, Mendonca BB, Fujieda K & Miller WL 2004 Mutant P450 oxidoreductase causes disordered steroidogenesis with and without Antley-Bixler syndrome. *Nat Genet* **36** 228-230.

Franke TF, Kaplan DR, Cantley LC & Toker A 1997 Direct regulation of the Akt proto-oncogene product by phosphatidylinositol-3,4-bisphosphate. *Science* **275** 665-668.

Freedman VH & Shin SI 1974 Cellular tumorigenicity in nude mice: correlation with cell growth in semi-solid medium. *Cell* **3** 355-359.

Frye LL, Cusack KP, Leonard DA & Anderson JA 1994 Oxolanosterol oximes: dual-action inhibitors of cholesterol biosynthesis. *J Lipid Res* **35** 1333-1344.

Fukami M, Horikawa R, Nagai T, Tanaka T, Naiki Y, Sato N, Okuyama T, Nakai H, Soneda S, Tachibana K, Matsuo N, Sato S, Homma K, Nishimura G, Hasegawa T & Ogata T 2005 Cytochrome P450 oxidoreductase gene mutations and Antley-Bixler syndrome with abnormal genitalia and/or impaired steroidogenesis: molecular and clinical studies in 10 patients. *J Clin Endocrinol Metab* **90** 414-426.

Fukami M, Nishimura G, Homma K, Nagai T, Hanaki K, Uematsu A, Ishii T, Numakura C, Sawada H, Nakacho M, Kowase T, Motomura K, Haruna H, Nakamura M, Ohishi A,

Adachi M, Tajima T, Hasegawa Y, Hasegawa T, Horikawa R, Fujieda K & Ogata T 2009 Cytochrome P450 oxidoreductase deficiency: identification and characterization of biallelic mutations and genotype-phenotype correlations in 35 Japanese patients. *J Clin Endocrinol Metab* **94** 1723-1731.

Gerdes D, Wehling M, Leube B & Falkenstein E 1998 Cloning and tissue expression of two putative steroid membrane receptors. *Biol Chem* **379** 907-911.

Gerhard DS, Wagner L, Feingold EA, Shenmen CM, Grouse LH, Schuler G, Klein SL, Old S, Rasooly R, Good P, *et al.*, 2004 The status, quality, and expansion of the NIH full-length cDNA project: the Mammalian Gene Collection (MGC). *Genome Res* **14** 2121-2127.

Gething MJ & Sambrook J 1992 Protein folding in the cell. *Nature* **355** 33-45.

Ghosh K, Thompson AM, Goldbeck RA, Shi X, Whitman S, Oh E, Zhiwu Z, Vulpe C & Holman TR 2005 Spectroscopic and biochemical characterization of heme binding to yeast Dap1p and mouse PGRMC1p. *Biochemistry* **44** 16729-16736.

Gilles-Gonzalez MA, and Gonzalez G. 2004 Signal transduction by heme-containing PAS-domain proteins. *J Appl Physiol*. **96(2**) 774-783
Gilles-Gonzalez MA, and Gonzalez G. 2005. Heme-based sensors: defining characteristics, recent developments, and regulatory hypothesis. *J Inorg Biochem*. **99(1)** 1-22

Goldstein JL & Brown MS 1990 Regulation of the mevalonate pathway. *Nature* **343** 425-430.

Goldstein JL, DeBose-Boyd RA, Brown MS 2006 Protein sensors for membrane sterols. *Cell* **124** 35-46.

Gong Y, Lee JN, Lee PC, Goldstein JL, Brown MS & Ye J 2006 Sterol-regulated ubiquitination and degradation of Insig-1 creates a convergent mechanism for feedback control of cholesterol synthesis and uptake. *Cell Metab* **3** 15-24.

Gu J, Weng Y, Zhang QY, Cui H, Behr M, Wu L, Yang W, Zhang L & Ding X 2003 Liver-specific deletion of the NADPH-cytochrome P450 reductase gene: impact on plasma cholesterol homeostasis and the function and regulation of microsomal cytochrome P450 and heme oxygenase. *J Biol Chem* **278** 25895-25901.

Hand RA & Craven RJ 2003 Hpr6.6 protein mediates cell death from oxidative damage in MCF-7 human breast cancer cells. *J Cell Biochem* **90** 534-547.

Hand RA, Jia N, Bard M & Craven RJ 2003 Saccharomyces cerevisiae Dap1p, a novel DNA damage response protein related to the mammalian membrane-associated progesterone receptor. *Eukaryot Cell* **2** 306-317.

Harding HP, Novoa I, Zhang Y, Zeng H, Wek R, Schapira M & Ron D 2000 Regulated translation initiation controls stress-induced gene expression in mammalian cells. *Mol Cell* **6** 1099-1108.

Harding HP, Zhang Y, Bertolotti A, Zeng H & Ron D 2000 Perk is essential for translational regulation and cell survival during the unfolded protein response. *Mol Cell* **5** 897-904.

Harding HP, Zhang Y & Ron D 1999 Protein translation and folding are coupled by an endoplasmic-reticulum-resident kinase. *Nature* **397** 271-274.

Hegarty BD, Bobard A, Hainault I, Ferre P, Bossard P & Foufelle F 2005 Distinct roles of insulin and liver X receptor in the induction and cleavage of sterol regulatory element-binding protein-1c. *Proc Natl Acad Sci U S A* **102** 791-796.

Henderson CJ, Otto DM, Carrie D, Magnuson MA, McLaren AW, Rosewell I & Wolf CR 2003 Inactivation of the hepatic cytochrome P450 system by conditional deletion of hepatic cytochrome P450 reductase. *J Biol Chem* **278** 13480-13486.

High S, Gorlich D, Wiedmann M, Rapoport TA & Dobberstein B 1991 The identification of proteins in the proximity of signal-anchor sequences during their targeting to and insertion into the membrane of the ER. *J Cell Biol* **113** 35-44.

Horton JD, Goldstein JL & Brown MS 2002 SREBPs: activators of the complete program of cholesterol and fatty acid synthesis in the liver. *J Clin Invest* **109** 1125-1131.

Horton JD & Shimomura I 1999 Sterol regulatory element-binding proteins: activators of cholesterol and fatty acid biosynthesis. *Curr Opin Lipidol* **10** 143-150.

Hua X, Yokoyama C, Wu J, Briggs MR, Brown MS, Goldstein JL & Wang X 1993 SREBP-2, a second basic-helix-loop-helix-leucine zipper protein that stimulates transcription by binding to a sterol regulatory element. *Proc Natl Acad Sci U S A* **90** 11603-11607.

Huang N, Pandey AV, Agrawal V, Reardon W, Lapunzina PD, Mowat D, Jabs EW, Van Vliet G, Sack J, Fluck CE & Miller WL 2005 Diversity and function of mutations in p450 oxidoreductase in patients with Antley-Bixler syndrome and disordered steroidogenesis. *Am J Hum Genet* **76** 729-749.

Hughes AL, Powell DW, Bard M, Eckstein J, Barbuch R, Link AJ & Espenshade PJ 2007 Dap1/PGRMC1 binds and regulates cytochrome P450 enzymes. *Cell Metab* **5** 143-149.

Hylemon PB, Zhou H, Pandak WM, Ren S, Gil G & Dent P 2009 Bile acids as regulatory molecules. *J Lipid Res* **50** 1509-1520.

Idkowiak J, Randell T, Dhir V, Patel P, Shackleton CH, Taylor NF, Krone N & Arlt W 2012 A missense mutation in the human cytochrome b5 gene causes 46,XY disorder of sex development due to true isolated 17,20 lyase deficiency. *J Clin Endocrinol Metab* **97** E465-475.

Ingelman-Sundberg M 2005 The human genome project and novel aspects of cytochrome P450 research. *Toxicol Appl Pharmacol* **207** 52-56.

Istvan ES & Deisenhofer J 2000 The structure of the catalytic portion of human HMG-CoA reductase. *Biochim Biophys Acta* **1529** 9-18.

Iwakoshi NN, Lee AH & Glimcher LH 2003 The X-box binding protein-1 transcription factor is required for plasma cell differentiation and the unfolded protein response. *Immunol Rev* **194** 29-38.

Jo Y, Lee PC, Sguigna PV & DeBose-Boyd RA 2011 Sterol-induced degradation of HMG CoA reductase depends on interplay of two Insigs and two ubiquitin ligases, gp78 and Trc8. *Proc Natl Acad Sci U S A* **108** 20503-20508.

Johannessen M, Fontanilla D, Mavlyutov T, Ruoho AE & Jackson MB 2011 Antagonist action of progesterone at sigma-receptors in the modulation of voltage-gated sodium channels. *Am J Physiol Cell Physiol* **300** C328-337.

Kahn A and Quigley J. 2011. Control of intracellular heme levels: Heme transporters and hemeoxygenases. *Biochimica et Biophysica Acta*. **1813** 668-682

Kammoun HL, Chabanon H, Hainault I, Luquet S, Magnan C, Koike T, Ferre P & Foufelle F 2009 GRP78 expression inhibits insulin and ER stress-induced SREBP-1c activation and reduces hepatic steatosis in mice. *J Clin Invest* **119** 1201-1215.

Kaplan BH. 1977. Synthesis of heme. In Williams WJ, Beutler E., Erslev AJ, and Wayne R. *Hematology* (2^{nd} ed.) 287-294.

Keber R, Motaln H, Wagner KD, Debeljak N, Rassoulzadegan M, Acimovic J, Rozman D & Horvat S 2011 Mouse knockout of the cholesterogenic cytochrome P450 lanosterol 14alpha-demethylase (Cyp51) resembles Antley-Bixler syndrome. *J Biol Chem* **286** 29086-29097.

Kelley RI, Kratz LE, Glaser RL, Netzloff ML, Wolf LM & Jabs EW 2002 Abnormal sterol metabolism in a patient with Antley-Bixler syndrome and ambiguous genitalia. *Am J Med Genet* **110** 95-102.

Khan AA & Quigley JG 2011 Control of intracellular heme levels: heme transporters and heme oxygenases. *Biochim Biophys Acta* **1813** 668-682.

Kilsdonk EP, Morel DW, Johnson WJ & Rothblat GH 1995 Inhibition of cellular cholesterol efflux by 25-hydroxycholesterol. *J Lipid Res* **36** 505-516.

Kilsdonk EP, Yancey PG, Stoudt GW, Bangerter FW, Johnson WJ, Phillips MC & Rothblat GH 1995 Cellular cholesterol efflux mediated by cyclodextrins. *J Biol Chem* **270** 17250-17256.

Kim YK, Kim KS & Lee AS 1987 Regulation of the glucose-regulated protein genes by beta-mercaptoethanol requires de novo protein synthesis and correlates with inhibition of protein glycosylation. *J Cell Physiol* **133** 553-559.

Kimura I, Nakayama Y, Konishi M, Kobayashi T, Mori M, Ito M, Hirasawa A, Tsujimoto G, Ohta M, Itoh N & Fujimoto M 2010 Neuferricin, a novel extracellular heme-binding protein, promotes neurogenesis. *J Neurochem* **112** 1156-1167.

Kimura I, Nakayama Y, Konishi M, Terasawa K, Ohta M, Itoh N & Fujimoto M 2012 Functions of MAPR (membrane-associated progesterone receptor) family members as heme/steroid-binding proteins. *Curr Protein Pept Sci* **13** 687-696.

Kimura I, Nakayama Y, Yamauchi H, Konishi M, Miyake A, Mori M, Ohta M, Itoh N & Fujimoto M 2008 Neurotrophic activity of neudesin, a novel extracellular heme-binding protein, is dependent on the binding of heme to its cytochrome b5-like heme/steroid-binding domain. *J Biol Chem* **283** 4323-4331.

Klein K & Zanger UM 2013 Pharmacogenomics of Cytochrome P450 3A4: Recent Progress Toward the "Missing Heritability" Problem. *Front Genet* **4** 12.

Kumar S & Bandyopadhyay U 2005 Free heme toxicity and its detoxification systems in human. *Toxicol Lett* **157** 175-188.

Lajoie P & Nabi IR 2010 Lipid rafts, caveolae, and their endocytosis. *Int Rev Cell Mol Biol* **282** 135-163.

Lee AH & Glimcher LH 2009 Intersection of the unfolded protein response and hepatic lipid metabolism. *Cell Mol Life Sci* **66** 2835-2850.

Lee AH, Heidtman K, Hotamisligil GS & Glimcher LH 2011 Dual and opposing roles of the unfolded protein response regulated by IRE1alpha and XBP1 in proinsulin processing and insulin secretion. *Proc Natl Acad Sci U S A* **108** 8885-8890.

Lee AH, Iwakoshi NN & Glimcher LH 2003 XBP-1 regulates a subset of endoplasmic reticulum resident chaperone genes in the unfolded protein response. *Mol Cell Biol* **23** 7448-7459.

Lee AH, Scapa EF, Cohen DE & Glimcher LH 2008 Regulation of hepatic lipogenesis by the transcription factor XBP1. *Science* **320** 1492-1496.

Lee BE, Feinberg M, Abraham JJ & Murthy AR 1992 Congenital malformations in an infant born to a woman treated with fluconazole. *Pediatr Infect Dis J* **11** 1062-1064.

Lee JN & Ye J 2004 Proteolytic activation of sterol regulatory element-binding protein induced by cellular stress through depletion of Insig-1. *J Biol Chem* **279** 45257-45265.

Lee KH, Yim EK, Kim CJ, Namkoong SE, Um SJ & Park JS 2005 Proteomic analysis of anti-cancer effects by paclitaxel treatment in cervical cancer cells. *Gynecol Oncol* **98** 45-53.

Leonard DA, Kotarski MA, Tessiatore JE, Favata MF & Trzaskos JM 1994 Post-transcriptional regulation of 3-hydroxy-3-methylglutaryl coenzyme A reductase by 3 beta-hydroxy-lanost-8-en-32-al, an intermediate in the conversion of lanosterol to cholesterol. *Arch Biochem Biophys* **310** 152-157.

Lepesheva GI & Waterman MR 2007 Sterol 14alpha-demethylase cytochrome P450 (CYP51), a P450 in all biological kingdoms. *Biochim Biophys Acta* **1770** 467-477.

Li S, Brown MS & Goldstein JL 2010 Bifurcation of insulin signaling pathway in rat liver: mTORC1 required for stimulation of lipogenesis, but not inhibition of gluconeogenesis. *Proc Natl Acad Sci U S A* **107** 3441-3446.

Lindh JD, Holm L, Andersson ML & Rane A 2009 Influence of CYP2C9 genotype on warfarin dose requirements--a systematic review and meta-analysis. *Eur J Clin Pharmacol* **65** 365-375.

Liscum L, Finer-Moore J, Stroud RM, Luskey KL, Brown MS & Goldstein JL 1985 Domain structure of 3-hydroxy-3-methylglutaryl coenzyme A reductase, a glycoprotein of the endoplasmic reticulum. *J Biol Chem* **260** 522-530.

Losel RM, Besong D, Peluso JJ & Wehling M 2008 Progesterone receptor membrane component 1--many tasks for a versatile protein. *Steroids* **73** 929-934.

Luo HR, Hattori H, Hossain MA, Hester L, Huang Y, Lee-Kwon W, Donowitz M, Nagata E & Snyder SH 2003 Akt as a mediator of cell death. *Proc Natl Acad Sci U S A* **100** 11712-11717.

Maehama T & Dixon JE 1998 The tumor suppressor, PTEN/MMAC1, dephosphorylates the lipid second messenger, phosphatidylinositol 3,4,5-trisphosphate. *J Biol Chem* **273** 13375-13378.
Maehama T & Dixon JE 1999 PTEN: a tumour suppressor that functions as a phospholipid phosphatase. *Trends Cell Biol* **9** 125-128.

Makishima M, Okamoto AY, Repa JJ, Tu H, Learned RM, Luk A, Hull MV, Lustig KD, Mangelsdorf DJ & Shan B 1999 Identification of a nuclear receptor for bile acids. *Science* **284** 1362-1365.

Mallory JC, Crudden G, Johnson BL, Mo C, Pierson CA, Bard M & Craven RJ 2005 Dap1p, a heme-binding protein that regulates the cytochrome P450 protein Erg11p/Cyp51p in Saccharomyces cerevisiae. *Mol Cell Biol* **25** 1669-1679.

Manning BD & Cantley LC 2003 United at last: the tuberous sclerosis complex gene products connect the phosphoinositide 3-kinase/Akt pathway to mammalian target of rapamycin (mTOR) signalling. *Biochem Soc Trans* **31** 573-578.

Mansouri MR, Schuster J, Badhai J, Stattin EL, Losel R, Wehling M, Carlsson B, Hovatta O, Karlstrom PO, Golovleva I, Toniolo D, Bione S, Peluso J & Dahl N 2008 Alterations in the expression, structure and function of progesterone receptor membrane component-1 (PGRMC1) in premature ovarian failure. *Hum Mol Genet* **17** 3776-3783.

Martinez-Botas J, Suarez Y, Ferruelo AJ, Gomez-Coronado D, Lasuncion MA 1999 Cholesterol starvation decreases p34(cdc2) kinase activity and arrests the cell cycle at G2, *Faseb J* **13** 1359-1370

Martinez-Botas J, Ferruelo AJ, Suarez Y, Fernandez C, Gomez-Coronado D, Lasuncion MA 2001 Dose-dependent effects of lovastatin on cell cycle progression. Distinct requirement of cholesterol and non-sterol mevalonate derivatives *Biochimica et Biophysica Acta* **1532** 185-194.

Mast N, Charvet C, Pikuleva IA & Stout CD 2010 Structural basis of drug binding to CYP46A1, an enzyme that controls cholesterol turnover in the brain. *J Biol Chem* **285** 31783-31795.

McClain MR, Palomaki GE, Piper M & Haddow JE 2008 A rapid-ACCE review of CYP2C9 and VKORC1 alleles testing to inform warfarin dosing in adults at elevated risk for thrombotic events to avoid serious bleeding. *Genet Med* **10** 89-98.

McCubrey JA, Steelman LS, Abrams SL, Lee JT, Chang F, Bertrand FE, Navolanic PM, Terrian DM, Franklin RA, D'Assoro AB, Salisbury JL, Mazzarino MC, Stivala F & Libra M 2006 Roles of the RAF/MEK/ERK and PI3K/PTEN/AKT pathways in malignant transformation and drug resistance. *Adv Enzyme Regul* **46** 249-279.

McCubrey JA, Steelman LS, Chappell WH, Abrams SL, Wong EW, Chang F, Lehmann B, Terrian DM, Milella M, Tafuri A, Stivala F, Libra M, Basecke J, Evangelisti C, Martelli AM & Franklin RA 2007 Roles of the Raf/MEK/ERK pathway in cell growth, malignant transformation and drug resistance. *Biochim Biophys Acta* **1773** 1263-1284.

McLean KJ, Hans M & Munro AW 2012 Cholesterol, an essential molecule: diverse roles involving cytochrome P450 enzymes. *Biochem Soc Trans* **40** 587-593.

McPherson R & Gauthier A 2004 Molecular regulation of SREBP function: the Insig-SCAP connection and isoform-specific modulation of lipid synthesis. *Biochem Cell Biol* **82** 201-211.

Merla G, Howald C, Henrichsen CN, Lyle R, Wyss C, Zabot MT, Antonarakis SE & Reymond A 2006 Submicroscopic deletion in patients with Williams-Beuren syndrome influences expression levels of the nonhemizygous flanking genes. *Am J Hum Genet* **79** 332-341.

Meyer C, Schmid R, Schmieding K, Falkenstein E & Wehling M 1998 Characterization of high affinity progesterone-binding membrane proteins by anti-peptide antiserum. *Steroids* **63** 111-116.

Meyer C, Schmid R, Scriba PC & Wehling M 1996 Purification and partial sequencing of high-affinity progesterone-binding site(s) from porcine liver membranes. *Eur J Biochem* **239** 726-731.

Meyer RP, Podvinec M & Meyer UA 2002 Cytochrome P450 CYP1A1 accumulates in the cytosol of kidney and brain and is activated by heme. *Mol Pharmacol* **62** 1061-1067.

Miki Y, Suzuki T & Sasano H 2007 Aromatase inhibitor and bone. *Biomed Pharmacother* **61** 540-542.

Miller WL 2012 P450 oxidoreductase deficiency: a disorder of steroidogenesis with multiple clinical manifestations. *Sci Signal* **5** pt11.

Miller WL 1986 Congenital adrenal hyperplasia. *N Engl J Med* **314** 1321-1322.

Miller WL, Agrawal V, Sandee D, Tee MK, Huang N, Choi JH, Morrissey K & Giacomini KM 2011 Consequences of POR mutations and polymorphisms. *Mol Cell Endocrinol* **336** 174-179.

Miller WL & Bose HS 2011 Early steps in steroidogenesis: intracellular cholesterol trafficking. *J Lipid Res* **52** 2111-2135.

Miller WL, Huang N, Fluck CE & Pandey AV 2004 P450 oxidoreductase deficiency. *Lancet* **364** 1663.

Miller WL, Huang N, Pandey AV, Fluck CE & Agrawal V 2005 P450 oxidoreductase deficiency: a new disorder of steroidogenesis. *Ann N Y Acad Sci* **1061** 100-108.

Min L, Strushkevich NV, Harnastai IN, Iwamoto H, Gilep AA, Takemori H, Usanov SA, Nonaka Y, Hori H, Vinson GP & Okamoto M 2005 Molecular identification of adrenal inner zone antigen as a heme-binding protein. *Febs J* **272** 5832-5843.

Mori K, Ma W, Gething MJ & Sambrook J 1993 A transmembrane protein with a cdc2+/CDC28-related kinase activity is required for signaling from the ER to the nucleus. *Cell* **74** 743-756.

Mutch DM, Klocke B, Morrison P, Murray CA, Henderson CJ, Seifert M & Williamson G 2007 The disruption of hepatic cytochrome p450 reductase alters mouse lipid metabolism. *J Proteome Res* **6** 3976-3984.

Nakamoto SS, Hamel P & Merchant S 2000 Assembly of chloroplast cytochromes b and c. *Biochimie* **82** 603-614.

Nebert DW & Russell DW 2002 Clinical importance of the cytochromes P450. *Lancet* **360** 1155-1162.

Nohturfft A, Brown MS & Goldstein JL 1998 Sterols regulate processing of carbohydrate chains of wild-type SREBP cleavage-activating protein (SCAP), but not sterol-resistant mutants Y298C or D443N. *Proc Natl Acad Sci U S A* **95** 12848-12853.

Nohturfft A, Brown MS & Goldstein JL 1998 Topology of SREBP cleavage-activating protein, a polytopic membrane protein with a sterol-sensing domain. *J Biol Chem* **273** 17243-17250.

Norlin M & Wikvall K 2007 Enzymes in the conversion of cholesterol into bile acids. *Curr Mol Med* **7** 199-218.

Normington K, Kohno K, Kozutsumi Y, Gething MJ & Sambrook J 1989 S. cerevisiae encodes an essential protein homologous in sequence and function to mammalian BiP. *Cell* **57** 1223-1236.

Oda S, Nakajima M, Toyoda Y, Fukami T & Yokoi 2011 T Progesterone receptor membrane component 1 modulates human cytochrome p450 activities in an isoform-dependent manner. *Drug Metab Dispos* **39** 2057-2065.

Oliver J, Jungnickel B, Gorlich D, Rapoport T & High S 1995 The Sec61 complex is essential for the insertion of proteins into the membrane of the endoplasmic reticulum. *FEBS Lett* **362** 126-130.

Omura T 2013 Contribution of cytochrome P450 to the diversification of eukaryotic organisms. *Biotechnol Appl Biochem* **60** 4-8.

Ono T 1980 [Possible role of cytosol factors on the enzymatic conversion of squalene to cholesterol (author's transl)]. *Seikagaku* **52** 1280-1283.

Ono T & Bloch K 1975 Solubilization and partial characterization of rat liver squalene epoxidase. *J Biol Chem* **250** 1571-1579.

Osborne TF & Espenshade PJ 2009 Evolutionary conservation and adaptation in the mechanism that regulates SREBP action: what a long, strange tRIP it's been. *Genes Dev* **23** 2578-2591.

Osmak M & Eljuga D 1993 The characterization of two human cervical carcinoma HeLa sublines resistant to cisplatin. *Res Exp Med (Berl)* **193** 389-396.

Ota T, Suzuki Y, Nishikawa T, Otsuki T, Sugiyama T, Irie R, Wakamatsu A, Hayashi K, Sato H, Nagai K, *et al*. 2004 Complete sequencing and characterization of 21,243 full-length human cDNAs. *Nat Genet* **36** 40-45.

Otto DM, Henderson CJ, Carrie D, Davey M, Gundersen TE, Blomhoff R, Adams RH, Tickle C & Wolf CR 2003 Identification of novel roles of the cytochrome p450 system in early embryogenesis: effects on vasculogenesis and retinoic Acid homeostasis. *Mol Cell Biol* **23** 6103-6116.

Pandey AV & Fluck CE 2013 NADPH P450 oxidoreductase: Structure, function, and pathology of diseases. *Pharmacol Ther*.

Pandey AV, Fluck CE, Huang N, Tajima T, Fujieda K & Miller WL 2004 P450 oxidoreductase deficiency: a new disorder of steroidogenesis affecting all microsomal P450 enzymes. *Endocr Res* **30** 881-888.

Pantopoulos K, Porwal SK, Tartkoff A, Devireddy L. 2012. Mechanisms of mammalian iron homeotstasis. *Biochemistry*. **51(29)** 5705-5724

Partsch CJ, Pankau R, Blum WF, Gosch A & Wessel A 1994 Hormonal regulation in children and adults with Williams-Beuren syndrome. *Am J Med Genet* **51** 251-257.

Patki KC, Von Moltke LL & Greenblatt DJ 2003 In vitro metabolism of midazolam, triazolam, nifedipine, and testosterone by human liver microsomes and recombinant cytochromes p450: role of cyp3a4 and cyp3a5. *Drug Metab Dispos* **31** 938-944.

Peluso JJ 2003 Progesterone as a regulator of granulosa cell viability. *J Steroid Biochem Mol Biol* **85** 167-173.

Peluso JJ, Liu X, Saunders MM, Claffey KP & Phoenix K 2008 Regulation of ovarian cancer cell viability and sensitivity to cisplatin by progesterone receptor membrane component-1. *J Clin Endocrinol Metab* **93** 1592-1599.

Pinto N & Dolan ME 2011 Clinically relevant genetic variations in drug metabolizing enzymes. *Curr Drug Metab* **12** 487-497.

Porstmann T, Griffiths B, Chung YL, Delpuech O, Griffiths JR, Downward J & Schulze A 2005 PKB/Akt induces transcription of enzymes involved in cholesterol and fatty acid biosynthesis via activation of SREBP. *Oncogene* **24** 6465-6481.

Porstmann T, Santos CR, Lewis C, Griffiths B & Schulze A 2009 A new player in the orchestra of cell growth: SREBP activity is regulated by mTORC1 and contributes to the regulation of cell and organ size. *Biochem Soc Trans* **37** 278-283.

Porter TD, Banerjee S, Stolarczyk EI & Zou L 2011 Suppression of cytochrome P450 reductase (POR) expression in hepatoma cells replicates the hepatic lipidosis observed in hepatic POR-null mice. *Drug Metab Dispos* **39** 966-973.

Pursley TJ, Blomquist IK, Abraham J, Andersen HF & Bartley JA 1996 Fluconazole-induced congenital anomalies in three infants. *Clin Infect Dis* **22** 336-340.

Ravid T, Doolman R, Avner R, Harats D & Roitelman J 2000 The ubiquitin-proteasome pathway mediates the regulated degradation of mammalian 3-hydroxy-3-methylglutaryl-coenzyme A reductase. *J Biol Chem* **275** 35840-35847.

Rawson RB 2003 The SREBP pathway--insights from Insigs and insects. *Nat Rev Mol Cell Biol* **4** 631-640.

Rezen T, Rozman D, Pascussi JM & Monostory K 2011 Interplay between cholesterol and drug metabolism. *Biochim Biophys Acta*.

Rohe HJ, Ahmed IS, Twist KE & Craven RJ 2009 PGRMC1 (progesterone receptor membrane component 1): a targetable protein with multiple functions in steroid signaling, P450 activation and drug binding. *Pharmacol Ther* **121** 14-19.

Roitelman J & Simoni RD 1992 Distinct sterol and nonsterol signals for the regulated degradation of 3-hydroxy-3-methylglutaryl-CoA reductase. *J Biol Chem* **267** 25264-25273.

Ron D & Walter P 2007 Signal integration in the endoplasmic reticulum unfolded protein response. *Nat Rev Mol Cell Biol* **8** 519-529.

Russell DW 2003 The enzymes, regulation, and genetics of bile acid synthesis. *Annu Rev Biochem* **72** 137-174.

Rybak AP, He L, Kapoor A, Cutz JC & Tang D 2011 Characterization of sphere-propagating cells with stem-like properties from DU145 prostate cancer cells. *Biochim Biophys Acta* **1813** 683-694.

Sakai J, Nohturfft A, Goldstein JL & Brown MS 1998 Cleavage of sterol regulatory element-binding proteins (SREBPs) at site-1 requires interaction with SREBP cleavage-activating protein. Evidence from in vivo competition studies. *J Biol Chem* **273** 5785-5793.

Schroeder F, Gallegos AM, Atshaves BP, Storey SM, McIntosh AL, Petrescu AD, Huang H, Starodub O, Chao H, Yang H, Frolov A & Kier AB 2001 Recent advances in membrane microdomains: rafts, caveolae, and intracellular cholesterol trafficking. *Exp Biol Med (Maywood)* **226** 873-890.

Selmin O, Lucier GW, Clark GC, Tritscher AM, Vanden Heuvel JP, Gastel JA, Walker NJ, Sutter TR & Bell DA 1996 Isolation and characterization of a novel gene induced by 2,3,7,8-tetrachlorodibenzo-p-dioxin in rat liver. *Carcinogenesis* **17** 2609-2615.

Sever N, Lee PC, Song BL, Rawson RB & Debose-Boyd RA 2004 Isolation of mutant cells lacking Insig-1 through selection with SR-12813, an agent that stimulates degradation of 3-hydroxy-3-methylglutaryl-coenzyme A reductase. *J Biol Chem* **279** 43136-43147.

Sever N, Song BL, Yabe D, Goldstein JL, Brown MS & DeBose-Boyd RA 2003 Insig-dependent ubiquitination and degradation of mammalian 3-hydroxy-3-methylglutaryl-CoA reductase stimulated by sterols and geranylgeraniol. *J Biol Chem* **278** 52479-52490.

Sever N, Yang T, Brown MS, Goldstein JL & DeBose-Boyd RA 2003 Accelerated degradation of HMG CoA reductase mediated by binding of insig-1 to its sterol-sensing domain. *Mol Cell* **11** 25-33.

Shaffer AL, Shapiro-Shelef M, Iwakoshi NN, Lee AH, Qian SB, Zhao H, Yu X, Yang L, Tan BK, Rosenwald A, Hurt EM, Petroulakis E, Sonenberg N, Yewdell JW, Calame K, Glimcher LH & Staudt LM 2004 XBP1, downstream of Blimp-1, expands the secretory apparatus and other organelles, and increases protein synthesis in plasma cell differentiation. *Immunity* **21** 81-93.

Shen AL, O'Leary KA & Kasper CB 2002 Association of multiple developmental defects and embryonic lethality with loss of microsomal NADPH-cytochrome P450 oxidoreductase. *J Biol Chem* **277** 6536-6541.

Shimano H 2001 Sterol regulatory element-binding proteins (SREBPs): transcriptional regulators of lipid synthetic genes. *Prog Lipid Res* **40** 439-452.

Shin SI, Freedman VH, Risser R & Pollack R 1975 Tumorigenicity of virus-transformed cells in nude mice is correlated specifically with anchorage independent growth in vitro. *Proc Natl Acad Sci U S A* **72** 4435-4439.

Sidrauski C, Chapman R & Walter P 1998 The unfolded protein response: an intracellular signalling pathway with many surprising features. *Trends Cell Biol* **8** 245-249.

Sim SC & Ingelman-Sundberg M 2010 The Human Cytochrome P450 (CYP) Allele Nomenclature website: a peer-reviewed database of CYP variants and their associated effects. *Hum Genomics* **4** 278-281.

Singh D, Kashyap A, Pandey RV & Saini KS 2011 Novel advances in cytochrome P450 research. *Drug Discov Today* **16** 793-799.

Sjoblom T, Jones S, Wood LD, Parsons DW, Lin J, Barber TD, Mandelker D, Leary RJ, Ptak J, Silliman N, Szabo S, Buckhaults P, Farrell C, Meeh P, Markowitz SD, Willis J, Dawson D, Willson JK, Gazdar AF, Hartigan J, Wu L, Liu C, Parmigiani G, Park BH, Bachman KE, Papadopoulos N, Vogelstein B, Kinzler KW & Velculescu VE 2006 The consensus coding sequences of human breast and colorectal cancers. *Science* **314** 268-274.

Skalnik DG, Brown DA, Brown PC, Friedman RL, Hardeman EC, Schimke RT & Simoni RD 1985 Mechanisms of 3-hydroxy-3-methylglutaryl coenzyme A reductase overaccumulation in three compactin-resistant cell lines. *J Biol Chem* **260** 1991-1994.

Skalnik DG, Narita H, Kent C & Simoni RD 1988 The membrane domain of 3-hydroxy-3-methylglutaryl-coenzyme A reductase confers endoplasmic reticulum localization and sterol-regulated degradation onto beta-galactosidase. *J Biol Chem* **263** 6836-6841.

Song BL & DeBose-Boyd RA 2004 Ubiquitination of 3-hydroxy-3-methylglutaryl-CoA reductase in permeabilized cells mediated by cytosolic E1 and a putative membrane-bound ubiquitin ligase. *J Biol Chem* **279** 28798-28806.

Song BL, Javitt NB & DeBose-Boyd RA 2005 Insig-mediated degradation of HMG CoA reductase stimulated by lanosterol, an intermediate in the synthesis of cholesterol. *Cell Metab* **1** 179-189.

Song BL, Sever N & DeBose-Boyd RA 2005 Gp78, a membrane-anchored ubiquitin ligase, associates with Insig-1 and couples sterol-regulated ubiquitination to degradation of HMG CoA reductase. *Mol Cell* **19** 829-840.

Song J, Vinarov D, Tyler EM, Shahan MN, Tyler RC & Markley JL 2004 Hypothetical protein At2g24940.1 from Arabidopsis thaliana has a cytochrome b5 like fold. *J Biomol NMR* **30** 215-218.

Staubach S & Hanisch FG 2011 Lipid rafts: signaling and sorting platforms of cells and their roles in cancer. *Expert Rev Proteomics* **8** 263-277.

Stephens L, Anderson K, Stokoe D, Erdjument-Bromage H, Painter GF, Holmes AB, Gaffney PR, Reese CB, McCormick F, Tempst P, Coadwell J & Hawkins PT 1998 Protein kinase B kinases that mediate phosphatidylinositol 3,4,5-trisphosphate-dependent activation of protein kinase B. *Science* **279** 710-714.

Stokoe D, Stephens LR, Copeland T, Gaffney PR, Reese CB, Painter GF, Holmes AB, McCormick F & Hawkins PT 1997 Dual role of phosphatidylinositol-3,4,5-trisphosphate in the activation of protein kinase B. *Science* **277** 567-570.

Strobel HW, Kawashima H, Geng J, Sequeira D, Bergh A, Hodgson AV, Wang H & Shen S 1995 Expression of multiple forms of brain cytochrome P450. *Toxicol Lett* **82-83** 639-643.

Stromstedt M, Rozman D & Waterman MR 1996 The ubiquitously expressed human CYP51 encodes lanosterol 14 alpha-demethylase, a cytochrome P450 whose expression is regulated by oxysterols. *Arch Biochem Biophys* **329** 73-81.

Su TP 1991 Sigma receptors. Putative links between nervous, endocrine and immune systems. *Eur J Biochem* **200** 633-642.

Su TP, London ED & Jaffe JH 1988 Steroid binding at sigma receptors suggests a link between endocrine, nervous, and immune systems. *Science* **240** 219-221.

Suchanek M, Radzikowska A & Thiele C 2005 Photo-leucine and photo-methionine allow identification of protein-protein interactions in living cells. *Nat Methods* **2** 261-267.

Szczesna-Skorupa E & Kemper B 2008 Influence of protein-protein interactions on the cellular localization of cytochrome P450. *Expert Opin Drug Metab Toxicol* **4** 123-136.

Szczesna-Skorupa E & Kemper B 2011 Progesterone receptor membrane component 1 inhibits the activity of drug-metabolizing cytochromes P450 and binds to cytochrome P450 reductase. *Mol Pharmacol* **79** 340-350.

Tang D, Chun AC, Zhang M & Wang JH 1997 Cyclin-dependent kinase 5 (Cdk5) activation domain of neuronal Cdk5 activator. Evidence of the existence of cyclin fold in neuronal Cdk5a activator. *J Biol Chem* **272** 12318-12327.

Thomas PE, Ryan D & Levin W 1976 An improved staining procedure for the detection of the peroxidase activity of cytochrome P-450 on sodium dodecyl sulfate polyacrylamide gels. *Anal Biochem* **75** 168-176.

Toker A & Cantley LC 1997 Signalling through the lipid products of phosphoinositide-3-OH kinase. *Nature* **387** 673-676.

Tolias KF & Cantley LC 1999 Pathways for phosphoinositide synthesis. *Chem Phys Lipids* **98** 69-77.

Tomalik-Scharte D, Maiter D, Kirchheiner J, Ivison HE, Fuhr U & Arlt W 2010 Impaired hepatic drug and steroid metabolism in congenital adrenal hyperplasia due to P450 oxidoreductase deficiency. *Eur J Endocrinol* **163** 919-924.

Trzaskos JM 1995 Oxylanosterols as modifiers of cholesterol biosynthesis. *Prog Lipid Res* **34** 99-116.

Trzaskos JM, Bowen WD, Shafiee A, Fischer RT & Gaylor JL 1984 Cytochrome P-450-dependent oxidation of lanosterol in cholesterol biosynthesis. Microsomal electron transport and C-32 demethylation. *J Biol Chem* **259** 13402-13412.

Trzaskos JM & Henry MJ 1989 Comparative effects of the azole-based fungicide flusilazole on yeast and mammalian lanosterol 14 alpha-methyl demethylase. *Antimicrob Agents Chemother* **33** 1228-1231.

Trzaskos JM, Ko SS, Magolda RL, Favata MF, Fischer RT, Stam SH, Johnson PR & Gaylor JL 1995 Substrate-based inhibitors of lanosterol 14 alpha-methyl demethylase: I. Assessment of inhibitor structure-activity relationship and cholesterol biosynthesis inhibition properties. *Biochemistry* **34** 9670-9676.

Tsiftsoglou A, Tsamadou A, Papadopoulou. 2006. Heme as key regulator of major mammalian cellular functions: Molecular, cellular, and pharmacological aspects. *Pharmacology and Therapeutics.* **111** 327-345.

Vaya J, Szuchman A, Tavori H & Aluf Y 2011 Oxysterols formation as a reflection of biochemical pathways: summary of in vitro and in vivo studies. *Chem Phys Lipids* **164** 438-442.

Wang X, Briggs MR, Hua X, Yokoyama C, Goldstein JL & Brown MS 1993 Nuclear protein that binds sterol regulatory element of low density lipoprotein receptor promoter. II. Purification and characterization. *J Biol Chem* **268** 14497-14504.

Weng Y, DiRusso CC, Reilly AA, Black PN & Ding X 2005 Hepatic gene expression changes in mouse models with liver-specific deletion or global suppression of the NADPH-cytochrome P450 reductase gene. Mechanistic implications for the regulation of microsomal cytochrome P450 and the fatty liver phenotype. *J Biol Chem* **280** 31686-31698.

Williamson L, Arlt W, Shackleton C, Kelley RI & Braddock SR 2006 Linking Antley-Bixler syndrome and congenital adrenal hyperplasia: a novel case of P450 oxidoreductase deficiency. *Am J Med Genet A* **140A** 1797-1803.

Woodard SI and Dailey HA. 2000. Multiple regulatory steps in erythroid heme biosynthesis. *Arch Biochem Biopphys* **384(2)** 375-378

Wu L, Gu J, Cui H, Zhang QY, Behr M, Fang C, Weng Y, Kluetzman K, Swiatek PJ, Yang W, Kaminsky L & Ding X 2005 Transgenic mice with a hypomorphic NADPH-cytochrome P450 reductase gene: effects on development, reproduction, and microsomal cytochrome P450. *J Pharmacol Exp Ther* **312** 35-43.

Xie Y, Bruce A, He L, Wei F, Tao L & Tang D 2011 CYB5D2 enhances HeLa cells survival of etoposide-induced cytotoxicity. *Biochem Cell Biol* **89** 341-350.

Yabe D, Xia ZP, Adams CM & Rawson RB 2002 Three mutations in sterol-sensing domain of SCAP block interaction with insig and render SREBP cleavage insensitive to sterols. *Proc Natl Acad Sci U S A* **99** 16672-16677.

Yang T, Espenshade PJ, Wright ME, Yabe D, Gong Y, Aebersold R, Goldstein JL & Brown MS 2002 Crucial step in cholesterol homeostasis: sterols promote binding of SCAP to INSIG-1, a membrane protein that facilitates retention of SREBPs in ER. *Cell* **110** 489-500.

Ye J & DeBose-Boyd RA 2011 Regulation of cholesterol and fatty acid synthesis. *Cold Spring Harb Perspect Biol* **3**.

Yellaturu CR, Deng X, Cagen LM, Wilcox HG, Mansbach CM, 2nd, Siddiqi SA, Park EA, Raghow R & Elam MB 2009 Insulin enhances post-translational processing of nascent SREBP-1c by promoting its phosphorylation and association with COPII vesicles. *J Biol Chem* **284** 7518-7532.

Yokoyama C, Wang X, Briggs MR, Admon A, Wu J, Hua X, Goldstein JL & Brown MS 1993 SREBP-1, a basic-helix-loop-helix-leucine zipper protein that controls transcription of the low density lipoprotein receptor gene. *Cell* **75** 187-197.

Yoshitani N, Satou K, Saito K, Suzuki S, Hatanaka H, Seki M, Shinozaki K, Hirota H & Yokoyama S 2005 A structure-based strategy for discovery of small ligands binding to functionally unknown proteins: combination of in silico screening and surface plasmon resonance measurements. *Proteomics* **5** 1472-1480.

Zanger UM, Turpeinen M, Klein K & Schwab M 2008 Functional pharmacogenetics/genomics of human cytochromes P450 involved in drug biotransformation. *Anal Bioanal Chem* **392** 1093-1108.

Zhang Q, Xiang G, Zhang Y, Yang K, Fan W, Lin J, Zeng F & Wu J 2006 Increase of doxorubicin sensitivity for folate receptor positive cells when given as the prodrug N-(phenylacetyl) doxorubicin in combination with folate-conjugated PGA. *J Pharm Sci* **95** 2266-2275.

Zhou RH, Yao M, Lee TS, Zhu Y, Martins-Green M & Shyy JY 2004 Vascular endothelial growth factor activation of sterol regulatory element binding protein: a potential role in angiogenesis. *Circ Res* **95** 471-478.